Chapter 2

Formation and Evolution of the Lower Magdalena Valley Basin and San Jacinto Fold Belt of Northwestern Colombia: Insights from Upper Cretaceous to Recent Tectono–Stratigraphy

https://doi.org/10.32685/pub.esp.37.2019.02
Published online 26 November 2020

Josué Alejandro MORA–BOHÓRQUEZ[1*], Onno ONCKEN[2], Eline LE BRETON[3], Mauricio IBAÑEZ–MEJIA[4], Gabriel VELOZA[5], Andrés MORA[6], Vickye VÉLEZ[7], and Mario DE FREITAS[8]

1 alejandro.mora@hocol.com.co
Hocol S.A.
Vicepresidencia de Exploración
Carrera 7 n.° 113–46, piso 16
Bogotá, Colombia

2 onno.oncken@gfz-potsdam.de
Deutsches GeoForschungsZentrum GFZ
Telegrafenberg 14473
Potsdam, Germany

3 eline.lebreton@fu-berlin.de
Freie Universität Berlin
Institute of Geological Sciences
Malteserstraβe 74–100, D–12249
Berlin, Germany

4 ibanezm@arizona.edu
Department of Geosciences
University of Arizona
Tucson, Arizona, 85721, USA

5 gabriel.veloza@hocol.com.co
Hocol S.A.
Vicepresidencia de Exploración
Carrera 7 n.° 113–46, piso 16
Bogotá, Colombia

6 andres.mora@ecopetrol.com.co
Ecopetrol S.A.
Vicepresidencia de Exploración
Bogotá, Colombia

7 vickye.velez@hocol.com.co
Hocol S.A.
Vicepresidencia de Exploración
Carrera 7 n.° 113–46, piso 16
Bogotá, Colombia

8 defreitas.mario@gmail.com
Caravela Energy
Bogotá, Colombia

* Corresponding author

Abstract Using a regional geological and geophysical dataset, we reconstructed the stratigraphic evolution of the Lower Magdalena Valley Basin and San Jacinto fold belt of northwestern Colombia. Detailed interpretations of reflection seismic data and new geochronology analyses reveal that the basement of the Lower Magdalena Basin is the northward continuation of the basement terranes of the northern Central Cordillera and consists of Permian – Triassic metasedimentary rocks intruded by Upper Cretaceous granitoids. Structural analyses suggest that the NE–SW strike of faults in basement rocks underlying the northeastern Lower Magdalena is inherited from a Jurassic rifting event, while the ESE–WNW striking faults in the western part originated from a Late Cretaceous to Eocene strike–slip and extensional episode. The Upper Cretaceous to lower Eocene sedimentary rocks preserved in the present–day San Jacinto fold belt were deposited in a submarine, forearc basin formed during the coeval oblique convergence between the Caribbean and South American Plates. A lower to middle Eocene angular unconformity at the top of the upper Paleocene to lower Eocene San Cayetano Sequence, the termination of the activity of the Romeral Fault System, and the cessation of arc magmatism are all interpreted to indicate the onset of low–angle orthogonal subduction of the Caribbean Plateau beneath South America between 56 and 43 Ma. Flat subduction of the plateau has continued to the present and would be the main cause of amagmatic post–Eocene deposition and formation of the Lower Magdalena Valley forearc basin. Extensional reactivation of inherited, pre–Oligocene basement faults was crucial for the tectonic segmentation of the basin and the formation of its two depocenters (Plato and San Jorge). Late Oligocene to early Miocene fault–controlled subsidence allowed initial infill of the Lower Magdalena, while uplift of Andean terranes made possible the connection of the Lower and Middle Magdalena Valleys, and the formation of the largest Colombian drainage system (Magdalena River system). This drainage system started delivering enormous amounts of sediments in middle Miocene times, as fault–controlled subsidence was gradually replaced by sedimentary

Supplementary Information:
S: https://www2.sgc.gov.co/LibroGeologiaColombia/tgc/sgcpubesp37201902s.pdf

Citation: Mora–Bohórquez, J.A., Oncken, O., Le Breton, E., Ibañez–Mejia, M., Veloza, G., Mora, A., Vélez, V. & De Freitas, M. 2020. Formation and evolution of the Lower Magdalena Valley Basin and San Jacinto fold belt of northwestern Colombia: Insights from Upper Cretaceous to recent tectono–stratigraphy. In: Gómez, J. & Mateus–Zabala, D. (editors), The Geology of Colombia, Volume 3 Paleogene – Neogene. Servicio Geológico Colombiano, Publicaciones Geológicas Especiales 37, p. 21–66. Bogotá. https://doi.org/10.32685/pub.esp.37.2019.02

loading. Such dramatic increase in sedimentation and the huge volume of sediment being delivered to the trench caused the formation of forearc highs in San Jacinto and of an accretionary prism farther to the west. Our results highlight the fundamental role of plate kinematics, inherited basement structure, and sediment flux on the evolution of forearc basins such as the Lower Magdalena and San Jacinto.
Keywords: *forearc basin, basement, flat–slab subduction, tectono–stratigraphy, Lower Magdalena, San Jacinto fold belt, Caribbean, subsidence, sedimentation.*

Resumen Utilizando una base de datos regional de geología y geofísica reconstruimos la evolución estratigráfica de la Cuenca del Valle Inferior del Magdalena y del cinturón plegado de San Jacinto al noroeste de Colombia. Interpretaciones detalladas de sísmica de reflexión y nuevos análisis geocronológicos revelan que el basamento de la Cuenca del Magdalena Inferior es la continuación hacia el norte de terrenos de basamento del norte de la cordillera Central y consiste en rocas metasedimentarias del Pérmico–Triásico intruidas por granitoides del Cretácico Superior. Análisis estructurales sugieren que el patrón NE–SW de fallas de basamento en el noreste del Magdalena Inferior es heredado de un evento de *rifting* jurásico, mientras que el patrón ESE–WNW de la parte oeste es heredado de un episodio Cretácico Tardío a Eoceno caracterizado por deformación de rumbo y extensión. Los sedimentos del Cretácico Superior a Eoceno inferior que se encuentran preservados en el actual cinturón de San Jacinto fueron depositados en una cuenca marina de antearco formada durante la convergencia oblicua entre las placas del Caribe y de Suramérica. Una discordancia angular del Eoceno inferior a medio al tope de la secuencia San Cayetano del Paleoceno–Eoceno inferior, la terminación de la actividad del Sistema de Fallas de Romeral y el cese del magmatismo de arco se interpretan como indicativos del comienzo de la subducción ortogonal y de bajo ángulo del *Plateau* del Caribe bajo Suramérica entre 56 y 43 Ma. La subducción plana del *plateau* ha continuado hasta el presente y sería la causa del depósito pos–Eoceno y la formación del Valle Inferior del Magdalena con ausencia de magmatismo. La reactivación extensional de fallas heredadas de basamento preoligocenas fue crucial para la segmentación tectónica de la cuenca y la formación de sus dos depocentros (Plato y San Jorge). La subsidencia controlada por fallas entre el Oligoceno Tardío y el Mioceno temprano permitió el llenado inicial del Magdalena Inferior, mientras que pulsos de levantamiento coetáneos en terrenos andinos posibilitaron la conexión de los valles Inferior y Medio del Magdalena, y la formación del sistema de drenaje más grande de Colombia (sistema del río Magdalena). Este sistema de drenaje comenzó a aportar grandes cantidades de sedimento en el Mioceno medio, a medida que la subsidencia controlada por fallas fue reemplazada por subsidencia debido a la carga sedimentaria incremental. Este dramático incremento en sedimentación y los grandes volúmenes de sedimento a la fosa causaron la formación de altos de antearco en San Jacinto y de un prisma de acreción más al oeste. Nuestros resultados resaltan el papel fundamental de la cinemática de placas, de la estructura heredada del basamento y del aporte de sedimentos en la evolución de cuencas de antearco como el Magdalena Inferior y San Jacinto.
Palabras clave: *cuenca de antearco, basamento, subducción plana, tectonoestratigrafía, Magdalena Inferior, cinturón de San Jacinto, Caribe, subsidencia, sedimentación.*

1. Introduction

The formation and evolution of the Lower Magdalena Valley Basin (LMV) and San Jacinto fold belt (SJFB) of northwestern Colombia (Figure 1) have not only been influenced by the interaction between the Caribbean and South American Plates and the Chocó–Panamá Block, but also by the uplift of different provinces within the northern Andes and the evolution of related drainage systems. Though these provinces have been the focus of several previous, important research studies (Duque–Caro, 1979, 1984, 1991; Reyes–Harker et al., 2000; Cerón et al., 2007; Mantilla–Pimiento, 2007; Mantilla–Pimiento et al., 2009; Bernal–Olaya et al., 2015a, 2015b, 2015c), there continues to be an active debate in certain fundamental aspects, such as the origin and classification of the basins (Cerón et al., 2007; Bernal–Olaya et al., 2015c). Hydrocarbon exploration, reflection–seismic, borehole drilling, and earthquake seismology and tomography in the LMV has led to a better understanding of its formation and evolution, whereas the San Jacinto fold belt has remained less understood due to intense deformation and scarcity of data. Several litho–tectonic provinces and terranes have been proposed in northern Colombia based on outcrop studies (Etayo–Serna et al., 1983; Toussaint & Restrepo, 1994; Cediel et al., 2003), but their extension and geometry beneath sedimentary basins such as the LMV and SJFB has remained speculative. Concerning the sedimentary succession, previous studies have described in some detail the stratigraphy and paleogeography of San Jacinto (e.g., Duque–Caro, 1979, 1991; Guzmán, 2007; Guzmán et al., 2004) and the LMV (e.g., Reyes–Harker et al., 2000; Bernal–Olaya et al., 2015c), and though they discuss their possible origin, they do not link their stratigraphic and paleo–geographic models with plate tectonic kinematics and Andean uplift events in NW South America.

The main goal of this contribution is to characterize the LMV and San Jacinto Basins in terms of their mechanisms of formation, evolution, and present configuration, through the integration of a regional geological and geophysical database provided by Hocol S.A. (Figure 2). The basement underneath the LMV was characterized, based on the integration of a regional subsurface database, which included geochronologic analyses of borehole samples in combination with outcrop data from the literature (Figure 3; Mora et al., 2017a). Then, the tectono–stratigraphy of Upper Cretaceous to Eocene sequences in the forearc basin that today corresponds to the SJFB was studied, linking them with the plate tectonic kinematics (Mora et al., 2017b). Finally, the Oligocene to recent tectono–stratigraphic sequences in the LMV were studied, and the subsidence, extension, sedimentation, and paleo–geographic history of the basin was reconstructed, proposing possible mechanisms controlling its evolution (Mora et al., 2018). It will be shown here that while Late Cretaceous to Eocene kinematics of the Caribbean and South American Plates controlled the evolution of the San Jacinto Forearc Basin and left a clear imprint on its stratigraphy, Oligocene to recent stratigraphy and evolution of the Lower Magdalena forearc were apparently more influenced by changes in the hinterland, such as the uplift of the Andes and the formation of the proto–Magdalena and Cauca River systems. The influence of inherited basement faults, sediment flux, flat subduction, and underplating processes in forearc basin evolution will be discussed.

2. Geological Framework

The LMV and SJFB of northwestern Colombia are located in an area in which the Caribbean oceanic plate, including the Chocó–Panamá Block, and the South American continental plate have been interacting throughout the Cenozoic (Figure 1). Though there has been some debate about the occurrence of flat–subduction of the Caribbean Plate under South America, beneath the LMV and SJFB (e.g., Rosello & Cossey, 2012), GPS data have shown (e.g., Müller et al., 1999; Trenkamp et al., 2002; Boschman et al., 2014; Matthews et al., 2016) that NW South America and the Caribbean are converging in a nearly orthogonal fashion (Symithe et al., 2015). Furthermore, seismicity data indicates the existence of a Benioff zone in the eastern LMV (Bernal–Olaya et al., 2015a; Syracuse et al., 2016; Mora et al., 2017a, 2017b), while geophysical studies including tomography data (Mantilla–Pimiento, 2007; Mantilla–Pimiento et al., 2009; Bernal–Olaya et al., 2015a), have provided new and more robust evidence supporting a flat–subduction geometry. Hence, there is agreement between the results and interpretations of this study and previous proposals (e.g., Mantilla–Pimiento et al., 2009), which consider the LMV as a forearc basin within a convergent margin where flat–slab subduction is operational (Bernal–Olaya et al., 2015a, 2015b, 2015c).

The present–day SJFB is a NNE–SSW–trending and WNW–verging fold and thrust belt located between the LMV to the E and the Sinú accretionary prism to the W. The SJFB covers an area of 17 500 km^2, it is ca. 370 km long, 40 to 57 km wide, and it is limited by the Romeral Fault System (RFS) to the E and by the Sinú Fault to the W. The LMV is a lozenge–shaped basin, covering an area of 42 000 km^2, located between two major basement terranes, the northern Central Cordillera (CC) in the S and SE and the Sierra Nevada de Santa Marta (SNSM) in the NE (Figures 1–3). The Santa Marta left–lateral, strike–slip fault is separating the northeastern part of the basin from the SNSM, while the northern extension of the Romeral Fault System (RFS) is separating the Lower Magdalena from the SJFB to the west. Pre–Oligocene sedimentary units are exposed in the SJFB, which has been considered the northward extension of the Western Cordillera of Colombia (Barrero et al., 1969; Duque–Caro, 1979, 1984; Cediel et al., 2003) and has been related to an oceanic to transitional–type basement. The RFS, which is also considered to continue from the south to form the western boundary of the LMV, separates the oceanic to transitional basement under the belt from the felsic continental basement of the South American crust, which floors the LMV in the east (Duque–Caro, 1979, 1984; Flinch, 2003; Mora et al., 2017a). In the SJFB, located west of the RFS, there are Upper Cretaceous to Eocene sedimentary units that are not preserved in the LMV to the east (Duque–Caro, 1979, 1984; Mora et al., 2017b). By contrast, Oligocene to recent units have been mostly eroded in the SJFB and are well preserved in the LMV (Figures 4 and 5).

3. Materials and Methods

This chapter summarizes the main results of previous work presented in recent publications (Mora et al., 2017a, 2017b, 2018).

→

Figure 1. (a) Tectonic map of northwestern South America with topography and bathymetry, showing the location of the Lower Magdalena Valley Basin (LMV) and the Sinú–San Jacinto fold belt (SSJFB). Present–day tectonic plate motions are shown in yellow (after Trenkamp et al., 2002). **(b)** Geological map of the Lower Magdalena Valley Basin and San Jacinto fold belt (Gómez et al., 2015), showing major structural and morphologic features. (OF) Oca Fault; (SNSM) Sierra Nevada de Santa Marta; (SMF) Santa Marta Fault; (BoF) Boconó Fault; (PFS) Palestina Fault System; (WC) Western Cordillera; (CC) Central Cordillera; (MMV) Middle Magdalena Valley; (BF) Bucaramanga Fault; (EC) Eastern Cordillera; (RFS) Romeral Fault System; (CF) Cuisa Fault; (SiF) Sinú Fault; (UF) Uramita Fault.

Hocol S.A. provided the regional database that was used in this study, with reflection–seismic and drillhole data, for the interpretation of the structure of the basement in the LMV and for the construction of the tectono–stratigraphic framework of the SJFB and LMV (Figures 2–5). Regional data of potential methods (Bouguer gravity and magnetics; Figure 6) was also used to constrain the basement depth and configuration, as well as publicly available seismicity data from the Red Sismológica Nacional (RSNC) of the Servicio Geológico Colombiano (https://www.datos.gov.co/Minas-y-Energ-a/Estaciones-Red-Sismol-gica-Nacional-de-Colombia-Se/sefu-3xqc/data), to study the lithospheric configuration of NW Colombia. More than 30 000 km of 2D and more than 2000 km^2 of 3D–reflection–seismic data were interpreted in two–way–time (TWT), all of which were tied to most of the ca. 400 wells that have been drilled in the basin. New zircon U–Pb geochronology and Hf isotope geochemistry results from basement and sedimentary borehole samples were integrated and analyzed. We have based our interpretations in the biostratigraphic data and charts that Duque–Caro (1979, 1984, 1991, 2000, 2001, 2010, 2014) has constructed for the LMV and SJFB (Figures 4 and 5), based on previous planktonic foraminiferal zonations (Blow, 1969; Petters & Sarmiento, 1956).

Interpretation in TWT of the top of the acoustic basement, the main unconformities, and the tops of the main sequences in the LMV and SJFB, was done using Schlumberger's Petrel seismic interpretation package, provided by Hocol S.A. After performing well–seismic ties, these horizons were mapped in TWT and depth–converted. In order to reconstruct the basin paleo–geography, seismic–stratigraphic analyses were carried out to define stratal stacking patterns, terminations, and contacts (Catuneanu et al., 2009), and integrate the well data (electrical logs, cores, and reports). Paleo–tectonic reconstructions from Late Cretaceous to recent were done using the open access software package GPlates (version 2.0.0, www.gplates.org; Boyden et al., 2011) and two paleo–tectonic models available for this area (Boschman et al., 2014; Matthews et al., 2016 from the GPlates database). Based on such reconstructions, convergence velocities and obliquities were calculated at different time windows, in order to correlate them with plate kinematics, subsidence patterns, sedimentation rates, and the main regional Andean tectonic events.

In the LMV, 1D geohistory and subsidence analyses (Allen & Allen, 2005; Steckler & Watts, 1978; Watts & Ryan, 1976) were carried out with data from 32 representative wells in different parts of the basin, including the San Jacinto fold belt, and from 12 wells drilled in the Sinú onshore and offshore accretionary prism (Mora et al., 2018). Three different approaches were followed in order to obtain well–supported extension estimates for the crust beneath the LMV (Mora et al., 2018). The first approach was to do a simple line–length calculation using a NNE–SSW–trending, depth–converted structural cross–section, which we built in the Move software of Midland Valley. The second approach was a backstripping technique assuming an Airy isostasy model and using sediment thickness data from the drill holes, in order to construct the total versus tectonic subsidence curves and to obtain the stretching factor (β factor, McKenzie, 1978). The third approach was to compile crustal thickness and Moho depth data from NW Colombia (e.g., Bernal–Olaya et al., 2015a; Poveda et al., 2015) and use our basin floor (basement) depth map to obtain the crustal thickness beneath the LMV, after removing the sedimentary infill. Of the three approaches, the third one implies less error, while the line–length balancing method considerably underestimates the amounts of extension. The calculation of the amount of stretching (β factor, McKenzie, 1978) is used in basins with a fast initial fault–related "synrift" subsidence, followed by a slower thermal "post–rift" subsidence. Therefore, the application of this methodology to basins that show different subsidence curves, such as the LMV as will be discussed farther on, can lead to an overestimation of the amount of stretching.

4. Results

4.1. Potential Methods and Reflection Seismic

Initial analyses of the LMV and SJFB basement configuration involved potential methods and the comparison with the depth–converted basement map obtained from regional reflection seismic data (Figures 2 and 3; Mora et al., 2017a). In the Total Bouguer gravity anomaly map (Figure 6a), the most notorious basement lows are marked by negative gravity anomalies, while the most prominent positive gravity anomaly occurs in the SNSM, a very high (>5000 m) basement massif that is not in isostatic equilibrium (Case & MacDonald, 1973). While the gravity data provided a much broader image of the basement morphology, the data from the total magnetic intensity reduced to the pole (TMIRP; Figure 6b) shows more localized concentrations of highly–magnetic rocks which correspond to

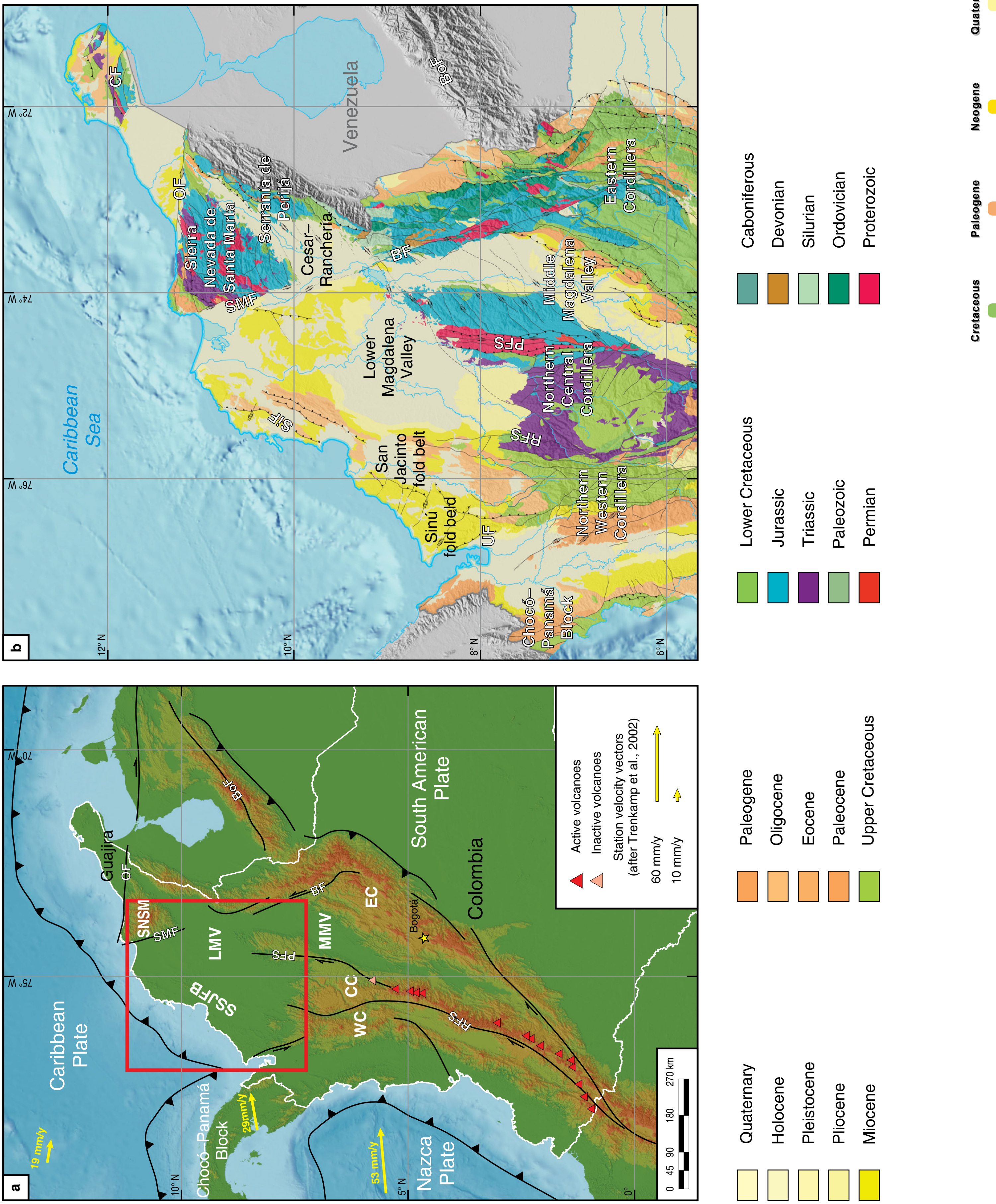
a
Caribbean Plate
Chocó–Panamá Block
Nazca Plate
South American Plate
Colombia
Guajira
SNSM
SMF
OF
LMV
SSJFB
PFS
MMV
EC
CC
WC
RFS
BF
BoF
Bogotá
19 mm/y
29mm/y
53 mm/y
Active volcanoes
Inactive volcanoes
Station velocity vectors (after Trenkamp et al., 2002)
60 mm/y
10 mm/y
0 45 90 180 270 km
10° N
5° N
0°
75° W
70° W
b
Caribbean Sea
Venezuela
Sierra Nevada de Santa Marta
Serranía de Perijá
Cesar–Ranchería
Lower Magdalena Valley
San Jacinto fold belt
Sinu fold beld
Middle Magdalena Valley
Eastern Cordillera
Northern Central Cordillera
Northern Western Cordillera
Chocó–Panamá Block
CF
OF
SMF
BF
BoF
SJF
PFS
RFS
UF
12° N
10° N
8° N
6° N
76° W
74° W
72° W
Quaternary
Holocene
Pleistocene
Pliocene
Miocene
Paleogene
Oligocene
Eocene
Paleocene
Upper Cretaceous
Lower Cretaceous
Jurassic
Triassic
Paleozoic
Permian
Caboniferous
Devonian
Silurian
Ordovician
Proterozoic
Quaternary
Neogene
Paleogene
Cretaceous

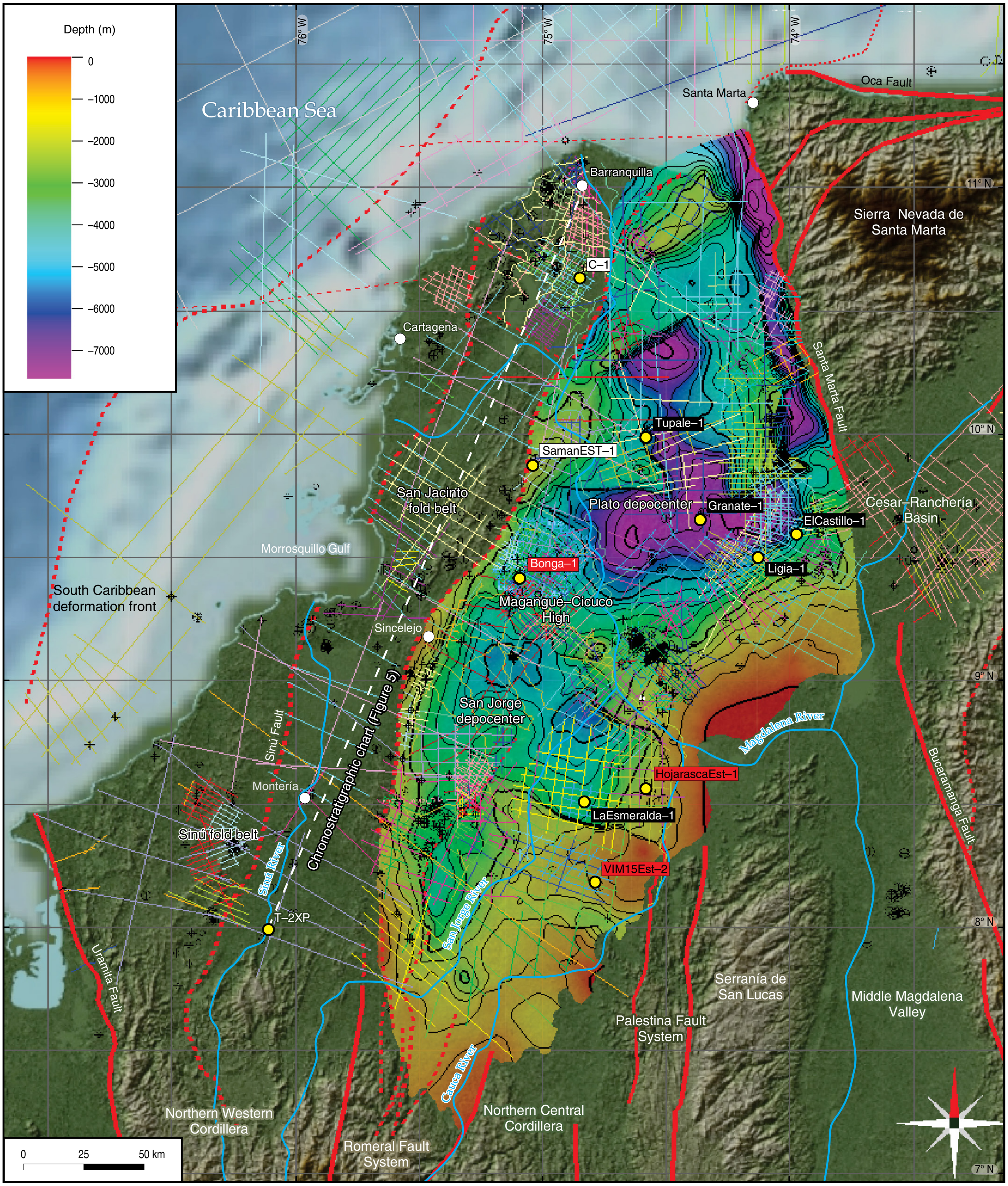

Figure 2. Reflection seismic and well database used for this study and provided by Hocol S.A. All wells are shown as small black crosses or circles with crosses, and relevant wells are highlighted: wells with red labels have basement U–Pb geochronological analyses, the two wells with white labels have detrital zircon U–Pb geochronological analyses, and wells with black labels have subsidence analyses (note Bonga–1 well has basement geochronology and subsidence analysis). Colors of seismic lines represent different seismic surveys. Topography and main drainages are also shown, as well as the structural map in depth of the basement under the LMV, after Mora et al. (2017a).

basement highs or to elongated features related to major fault zones. When comparing the Bouguer anomaly map with the depth–converted top basement map of the LMV (Figure 6a), a very good match can be seen in terms of basement configuration. The southeastern boundaries of the LMV are the Palestina Fault System (PFS) and the basement outcrops of the northernmost CC, while the boundaries in the northeast are the Santa Marta Fault (SMF) and the SNSM. The western limit of the LMV has been considered the northward extension of the RFS (Duque–Caro, 1979, 1984), which would be separating the basin from the San Jacinto deformed belt to the west. However, based on reflection seismic data, an east–verging fault splay was interpreted in the southwestern LMV (Mora et al., 2017a), which correlates at surface with the San Jerónimo Fault (SJF; Figures 3 and 6) and appears to correspond to the southwestern limit of the continental affinity basement of the LMV. The main morphological features of the basement underneath the LMV are the Plato depocenter in the north, with depths in excess of 7 km (23 000 feet), the Magangué–Cicuco High (MCH) in the center, and the San Jorge depocenter in the south, with depths of more than 5 km (17 000 feet).

4.2. Basement Fault Families

Detailed seismic mapping of the basement underneath the LMV showed that the fault pattern is much more complex than previously considered (Figure 7; Mora et al., 2017a). The basement faults were divided into four fault families according mainly to their trend and to their age, and found that these families define two structural regions in the LMV: a western region with a dominant ESE–WNW–trending fault family and a northeastern region with a dominant NE–SW–trending family (Figure 7). The oldest fault family (family 1, green traces in Figure 7) comprises normal faults trending NE–SW (40–60°) and includes the southern El Difícil Fault, the Pivijay Fault, and the fault that limits the Remolino–Ciénaga High to the south. The second fault family (family 2, red traces in Figure 7) comprises extensional faults which exhibit subtle strike–slip and inversion deformation affecting the sedimentary infill and which have an WNW–ESE–trend (265–320°). The third fault family (orange traces in Figure 7) trends NNW–SSE (330–360°) and corresponds to the Algarrobo Fault, a trans–tensional strike–slip fault, and to the northern Apure Fault. The fourth family in the LMV (blue traces in Figure 7) comprises normal faults with subtle inversion and a NNE–SSW–orientation (0–30°), hence implying an ESE–WNW–oriented extensional component. Neogene to recent, E–W and SE–NW contraction has obscured the original Cretaceous to Paleogene structural fabric in most of the San Jacinto fold belt, except for the northernmost area, where NW–SE–trending Eocene extensional features that influenced sedimentation have been recently interpreted (Figure 7; Mora et al., 2013a).

4.3. Basement Zircon U–Pb Geochronology and Hf Isotope Geochemistry

Mora et al. (2017a) selected eight samples from deep exploratory and stratigraphic wells that drilled through the basement to be processed for zircon U–Pb geochronology and Hf isotope geochemistry. Three core samples were analyzed from the metamorphic basement drilled in the VIM15Est–2 stratigraphic well in the southeastern part of the basin (Figures 2 and 3). Five ditch cutting samples were analyzed from the basement in the HojarascaEst–1 stratigraphic well in the eastern part of the San Jorge depocenter, and from the Bonga–1 exploratory well, located in the western MCH. Detrital zircon U–Pb dates from low–grade metasedimentary rocks indicated a Middle to Late Triassic maximum depositional age for their sedimentary protoliths, estimated to 234 ± 5 Ma (n = 4, MSWD = 0.7) for Hojarasca and 233 ± 4 Ma for VIM15 (n= 4, MSWD= 0.7) based on the youngest group of at least three zircons that define an equivalent population within 2σ uncertainties (e.g., Dickinson & Gehrels, 2009). The age spectra retrieved for both localities was dominated by zircons with early Permian to Middle Triassic crystallization ages, with subdued older populations in the early Paleozoic (Cambrian – Ordovician) and the Meso– and Neoproterozoic. A comparison with the known age distributions of pre–Jurassic basement domains in NW South America revealed that these DZ age populations are most similar to the igneous and detrital zircon U–Pb ages found in the basement of the CC and the SNSM (Mora et al., 2017a), thus suggesting a close paleo–geographic connection.

In the Bonga–1 well, located in the western part of the MCH (Figures 2 and 3), samples of a granitic basement were recovered, yielding zircon U–Pb ages in the range of 76 to 89 Ma (Coniacian – Campanian). The results from the Bonga–1 well clearly indicated that magmatism in this portion of the LMV basement was ongoing for this time interval in the Late Cretaceous, as has been observed in other parts of the basin; for instance, a granite sample from the Cicuco Field in the MCH was dated as Santonian (Aleman, 1983 in Reyes–Harker et al., 2000), while a recent study by Silva–Arias et al. (2016), provided a similar age (84.5 Ma, U–Pb in zircon) for the granodioritic basement in the Cicuco–22 well in the eastern MCH. Another Late Cretaceous age was reported in the Coral–9 well (74.5 Ma, Silva–Arias et al., 2016). In addition to the new U–Pb results for the Bonga–1 well, the Hf isotopic compositions of the dated zircons also indicated a rather juvenile affinity for this portion of the LMV basement (Mora et al., 2017a). Several analyses conducted in two of the Bonga samples yielded εHf(t) values in excess of +10 and up to +15, exceeding the values typical for arc–related crust (Dhuime et al., 2011) and overlapping with a depleted mantle–like composition (Vervoort & Blichert–Toft, 1999). In contrast, samples from the VIM15 and Hojarasca wells discussed above yielded much lower

→

Figure 3. Geological map of the NW Colombia (modified after Gómez et al., 2007), highlighting basement terranes and pre–Tertiary sedimentary units, and integrating a subsurface basement map in depth (meters) of the LMV. Colored circles are wells that drilled into the basement and have basic rock descriptions; previous and new geochronological data from the basement is depicted. (OF) Oca Fault; (RFS) Romeral Fault System; (SL) Sevilla Lineament; (LMV) Lower Magdalena Valley; (CRB) Cesar–Ranchería Basin; (SP) serranía de Perijá; (MCH) Magangué–Cicuco High; (SJF) San Jerónimo Fault; (SM) Santander Massif; (CAF) Cauca–Almaguer Fault; (ESF) Espíritu Santo Fault; (PFS) Palestina Fault System; (CC) Central Cordillera; (WC) Western Cordillera; (MMV) Middle Magdalena Valley; (EC) Eastern Cordillera. Modified from Mora et al. (2017a).

εHf(t) values, mostly ranging between +4 and –8, thus indicating a much older crustal source for the preceding magmas from which these detrital zircons crystalized.

4.4. Detrital Zircon U–Pb Geochronology and Hf Isotope Geochemistry of Pre–Oligocene Units

Samples (cuttings) for petrography and detrital zircon U–Pb and Hf isotope analyses were recovered from two wells located in the northern half of the SJFB (Figure 2; Mora et al., 2017b). Six samples from upper Paleocene to upper Eocene units (San Cayetano and Chengue) were collected in the C–1 well, located in the northern San Jacinto fold belt, while two more samples from an upper Eocene to lower Oligocene unit (San Jacinto) were collected in the SamanEST–1 well, located farther south, close to the boundary between the SJFB and the LMV (Figure 2). U–Pb dates of detrital zircon from samples of upper Paleocene to Eocene strata (Sequences 2 to 4) showed three clear provenance peaks, namely a main Late Cretaceous (70–88 Ma, Coniacian – Maastrichtian) peak, a secondary peak of Permian – Triassic age (230–250 Ma) which is less evident in the SamanEST–1 well, and a minor Albian – Cenomanian peak (ca. 100 Ma; Mora et al., 2017b). However, the Paleocene to middle Eocene samples also evidenced both early Paleozoic and Proterozoic provenance. Therefore, detrital zircon U–Pb geochronology indicated that the upper Paleocene to lower Oligocene sediments of Sequences 2 to 4 were mostly sourced from Upper Cretaceous and Permian – Triassic basement blocks.

Hf isotopic data showed that the three dated detrital zircon populations (Coniacian – Maastrichtian, Albian – Cenomanian, and Permian – Triassic) are related to different magmatic sources. While the Coniacian – Maastrichtian zircons would be related to a juvenile mantle source (i.e., positive εHf), the older Albian – Cenomanian and Permian – Triassic zircons have much lower εHf(t) values, indicating a much older crustal source. Furthermore, in the SamanEST–1 well there were two sub–populations within the Late Cretaceous Coniacian – Maastrichtian population, and both overlapped quite well with the compositions of the Bonga Pluton (Mora et al., 2017a), located 50 km to the south (Figures 2 and 3). The Permian – Triassic Hf isotopic compositions from the C–1 well also showed a good match with the Hf compositions of the Permian – Triassic basement in the HojarascaEST–1 and VIM15Est–2 wells (Mora et al., 2017a) and with data from previous studies (Cardona et al., 2012; Cochrane et al., 2014).

4.5. Upper Cretaceous to Eocene Tectono–Stratigraphy in the SJFB

Though this tectono–stratigraphic framework is mostly based on previous research, it was built after incorporating a great deal of recent regional drill hole, seismic, and outcrop data and interpretations (Figures 4 and 5). The same sequence definition and numbering proposed by Mora et al. (2017b) is used here. Upper Cretaceous to Eocene deposits are better preserved and exposed in the SJFB, while they are only locally preserved in the western portion of the LMV. The general characteristics of the identified and studied Upper Cretaceous to Eocene tectono–stratigraphic sequences are presented in Table 1 of the Supplementary Information.

The oldest, 2nd–order sequence is of Coniacian to Maastrichtian age (Mora et al., 2017b) and comprises the bituminous shales, cherts, and limestones of the Cansona unit (Sequence 1 in Figures 4 and 5). Biostratigraphic data compiled by Duque–Caro (2000, 2001) and Guzmán (2007) showed an absence of lower Paleocene planktonic foraminiferal zones (P.0 to P.2) in the SJFB, indicating the existence of a regional unconformity which marks the upper limit of this sequence. Sequence 2, called San Cayetano, is also a 2nd–order sequence which has been dated as late Paleocene to early Eocene (planktonic foraminiferal zones P.3 to P.9). The late Paleocene was characterized by a high global sea level (eustatic curves in Figure 4; Haq et al., 1987), which could have influenced the onset and extension of San Cayetano sedimentation. Biostratigraphic data showed that there is a big hiatus in the center of the SJFB, where the lower Eocene is missing, while to the north the section is more complete and the contact with the overlying sequence appears to be a disconformity (Figures 4 and 5; Table 1 of the Supplementary Information). A middle to upper Eocene, 2nd–order sequence (Sequence 3) corresponds to the Chengue Group, defined by the P.10 to P.14 planktonic foraminiferal zones of middle to late Eocene age. Biostratigraphy indicated that the unconformity between Sequences 2 (San Cayetano) and 3 (Chengue) corresponds to the P.9 to P.10 foraminiferal zones, implying a time interval of 46 to 51 Ma which includes the limit between the early and middle Eocene. This syn–tectonic sequence has

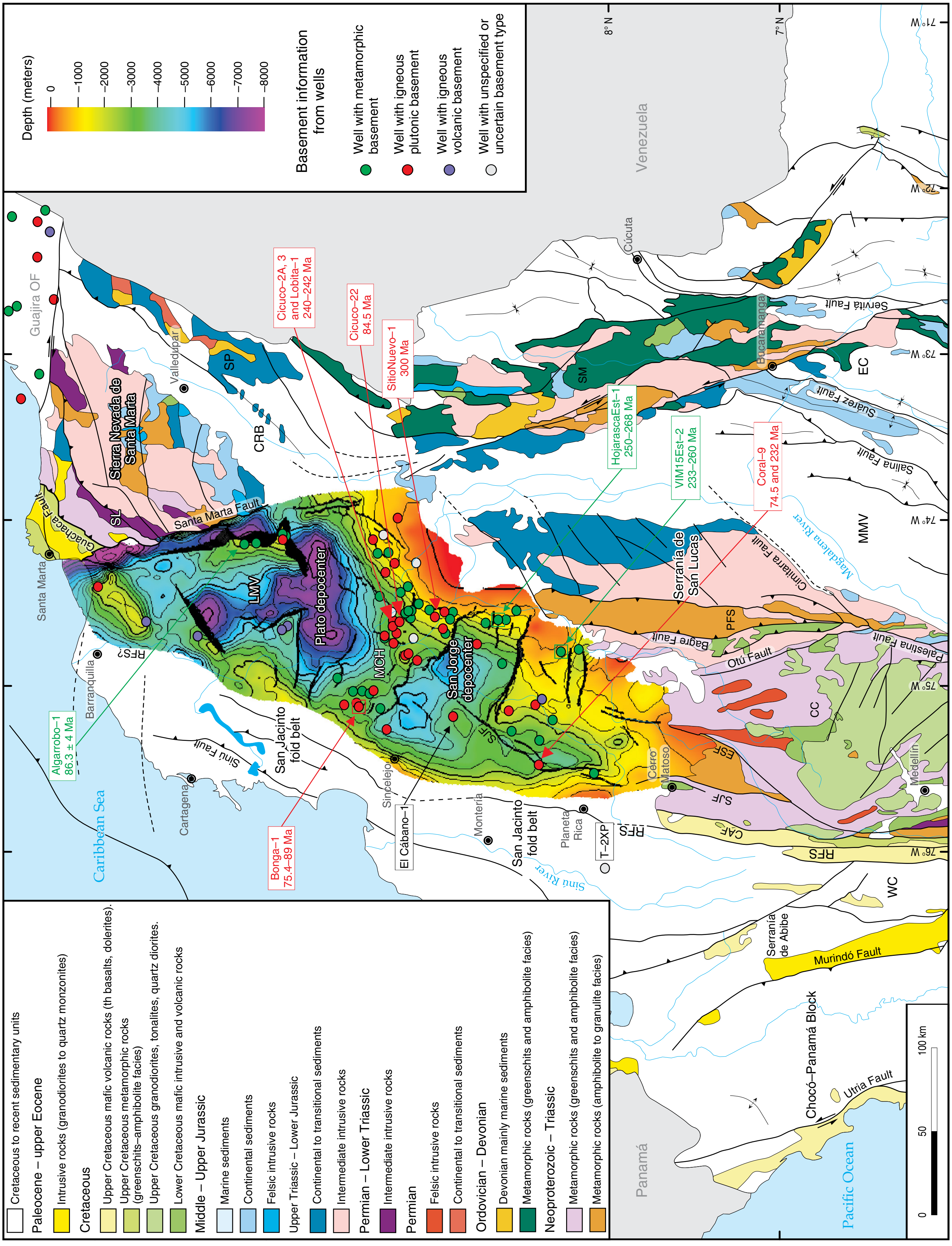
Depth (meters)
0
–1000
–2000
–3000
–4000
–5000
–6000
–7000
–8000
Basement information from wells
Well with metamorphic basement
Well with igneous plutonic basement
Well with igneous volcanic basement
Well with unspecified or uncertain basement type
Cretaceous to recent sedimentary units
Paleocene – upper Eocene
Intrusive rocks (granodiorites to quartz monzonites)
Cretaceous
Upper Cretaceous mafic volcanic rocks (th basalts, dolerites).
Upper Cretaceous metamorphic rocks (greenschits–amphibolite facies)
Upper Cretaceous granodiorites, tonalites, quartz diorites.
Lower Cretaceous mafic intrusive and volcanic rocks
Middle – Upper Jurassic
Marine sediments
Continental sediments
Felsic intrusive rocks
Upper Triassic – Lower Jurassic
Continental to transitional sediments
Intermediate intrusive rocks
Permian – Lower Triassic
Intermediate intrusive rocks
Permian
Felsic intrusive rocks
Continental to transitional sediments
Ordovician – Devonian
Devonian mainly marine sediments
Metamorphic rocks (greenschits and amphibolite facies)
Neoproterozoic – Triassic
Metamorphic rocks (greenschits and amphibolite facies)
Metamorphic rocks (amphibolite to granulite facies)
Caribbean Sea
Pacific Ocean
Panamá
Venezuela
Chocó–Panamá Block
Guajira OF
Santa Marta
Sierra Nevada de Santa Marta
Guachaca Fault
Santa Marta Fault
SL
SP
CRB
Valledupar
Barranquilla
RFS?
LMV
Plato depocenter
MCH
San Jorge depocenter
SJF
Cartagena
Sinú Fault
San Jacinto fold belt
Sincelejo
El Cábano–1
Montería
Planeta Rica
T–2XP
RFS
CAF
Sinú River
Cerro Matoso
ESF
SJF
Medellín
CC
Otú Fault
Bagre Fault
PFS
Palestina Fault
Serranía de San Lucas
Cimitarra Fault
Magdalena River
MMV
Salina Fault
Suárez Fault
EC
Bucaramanga
SM
Servitá Fault
Cúcuta
WC
Serranía de Abibe
Murindó Fault
Utría Fault
Algarrobo–1 86.3 ± 4 Ma
Bonga–1 75.4–89 Ma
Cicuco–2A, 3 and Lobita–1 240–242 Ma
Cicuco–22 84.5 Ma
SitioNuevo–1 300 Ma
HojarascaEst–1 250–268 Ma
VIM15Est–2 233–260 Ma
Coral–9 74.5 and 232 Ma
8° N
7° N
71° W
72° W
73° W
74° W
75° W
76° W
0
50
100 km

Figure 4. WNW–ESE–trending chronostratigraphic chart of the Sinú, San Jacinto, and Lower Magdalena areas, based on different sources (Guzmán, 2007; Hocol S.A., 1993; Instituto Colombiano del Petróleo, 2000) and adjusted with our recent analyses of well and outcrop samples. Biostratigraphy is based on numerous papers and industry reports by Duque–Caro (1979, 1984, 1991, 2000, 2001, 2010, 2014), tectonic events are after Villagómez et al. (2011), Parra et al. (2012), Saylor et al. (2012), Mora et al. (2013b), Caballero et al. (2013), Mora et al. (2015), De la Parra et al. (2015), while the eustatic curves are from Haq et al. (1987) and the climatic events from Zachos et al. (2001). Modified from Mora et al. (2017b).

been eroded in the southern part of the SJFB and is more preserved in the northern part (Figure 5). Sequence 4 is a locally preserved 2nd–order sequence comprising the siliciclastic San Jacinto unit and the calcareous Toluviejo unit (Figures 4 and 5), which according to biostratigraphic studies (Duque–Caro, 1979; Guzmán, 2007; Guzmán et al., 2004) are defined by the P.15 to P.20 planktonic foraminiferal zones of late Eocene to early Oligocene age.

4.6. Upper Oligocene to Recent Tectono–Stratigraphy and Paleo–Geography in the LMV and SJFB

Due to Pliocene to recent uplift and erosion in the SJFB, Oligocene to recent deposits are more preserved in the LMV. The general characteristics of the identified sequences are summarized in Table 2 of the Supplementary Information and in Mora et al. (2018). Since there is seismic and well data in the LMV, it was possible to reconstruct the Oligocene to recent paleo–geography of the LMV, which is depicted in Figures 8 to 10 for selected time windows. The detrital zircon U–Pb geochronology of Montes et al. (2015) was also integrated, to better constrain the sediment provenance.

The Oligocene to lower Miocene deposits are interpreted as a transgressive, 2nd–order sequence (Sequence 5), which filled from NW to SE the lowest paleo–topographic areas formed by the basement of the LMV (Figure 8a; Mora et al., 2018). This sequence, called "Lower Ciénaga de Oro", was associated to the planktonic zones P.20 to N.6 (M.3), equivalent to an early Oligocene to early Miocene age (Figure 4; Table 2 of the Supplementary Information). Seismic data shows that the Oligocene to lower Miocene shallow marine deposits gradually filled the proto–San Jorge and Plato depocenters from the W and NW and that the main structural basement features, such as the Sucre, Mojana, and Pivijay Faults, were actively extending (Figure 8a).

Sequence 6, deposited after a regional early Miocene tectonic event, records a major change in sedimentation in the basin. Biostratigraphic analyses indicate that it is a 3rd–order sequence of early to middle Miocene age (Burdigalian to Serravallian, zones N.7/M.4 to N.11/M.8) (Figure 4; Table 2 of the Supplementary Information; Mora et al., 2018). Deposition of this sequence, called "Upper Ciénaga de Oro" and "Lower Porquero", extends farther to the E and SE and begins with retrogradational, shallow marine, clastic sedimentation in low areas and carbonate deposition in high areas, which then changed to progradational deltaic sedimentation (Figures 8b and 9a).

Although Sequences 7 and 8 of middle to late Miocene age were partially eroded, they also continue to display a progradational pattern to the NW. These sequences represent 3rd–order cycles of middle to late Miocene age (Serravallian – Tortonian) and they are also limited by regional unconformities (Figure 4; Duque–Caro, 1979; Duque–Caro et al., 1996; Guzmán, 2007; Hocol S.A., 1993; Reyes–Harker et al., 2000). The sequences, called "Middle and Upper Porquero", exhibit mainly fine–grained facies with progradational stacking patterns, which are best preserved in the depocenters where erosion was less intense.

Sequence 9 is a 3rd–order sequence of late Miocene to early Pliocene age (zones N.17/M.14 to PL2 zones, Tortonian to Zanclean; Figure 4; Table 2 of the Supplementary Information). Reflection–seismic data shows that this sequence, which is better preserved in the Plato depocenter, is composed of low–angle (0.3–0.6°) and wide (100–200 km) sigmoidal clinoforms which advanced from SSE to NNW, representing the gradual advance of the proto–Magdalena River (Figure 9b).

Sequence 10 has been very poorly studied and comprises several higher order sequences, representing renewed subsidence in the southern LMV, focused in the San Jorge Graben where the thickest deposits occur (Figure 10). It is well preserved in the southern LMV, south of the Magangué–Cicuco High, where it is called "Corpa", while in the north it was mostly eroded. Taking into account the unconformities above the upper Miocene to lower Pliocene Tubará Sequence (9), and below the upper Pleistocene to recent deposits, we infer here a late Pliocene to early Pleistocene age for this sequence, spanning from 3 to 1.3 Ma (3rd– order cycle; Figure 4; Table 2 of the Supplementary Information). The expression of the Corpa Sequence in reflection–seismic data consists of low–angle clinoforms broadly prograding from south to north, which appear to represent the deposits of the paleo–Cauca drainage system, including fluvial channels, lakes, and swamps (Figure 10). The internal seismic–stratigraphic architecture of the Corpa Sequence reveals the time when the SJFB started to be uplifted (Mora et al., 2018), which appears to be close to the boundary between the Pliocene and Pleistocene.

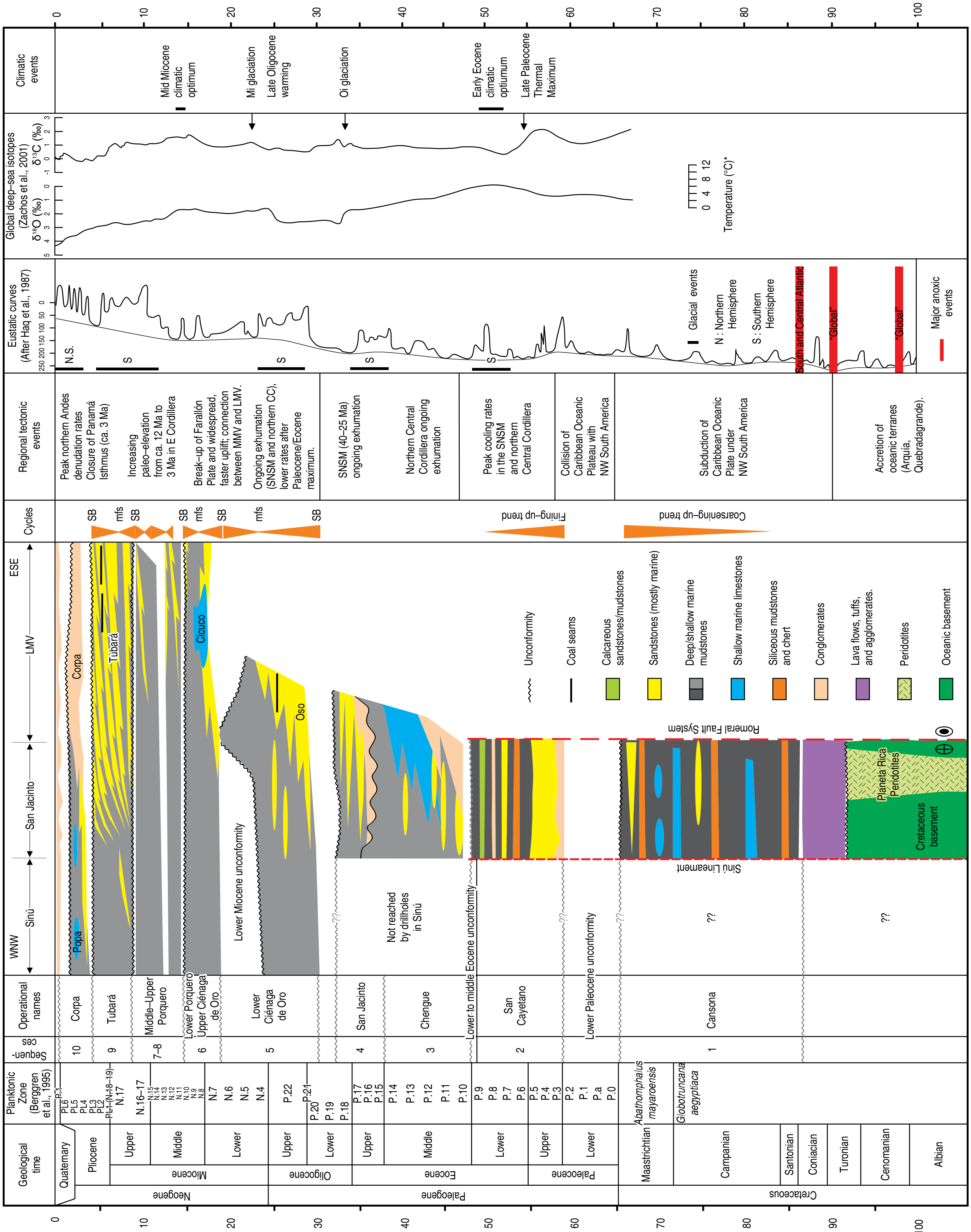
Geological time
Planktonic Zone (Berggren et al., 1995)
Sequences
Operational names
WNW
Sinú
San Jacinto
LMV
ESE
Cycles
Regional tectonic events
Eustatic curves (After Haq et al., 1987)
Global deep–sea isotopes (Zachos et al., 2001)
Climatic events
Mid Miocene climatic optimum
Mi glaciation
Late Oligocene warming
Oi glaciation
Early Eocene climatic optimum
Late Paleocene Thermal Maximum
Corpa
Tubará
Middle–Upper Porquero
Lower Porquero
Upper Ciénaga de Oro
Lower Ciénaga de Oro
San Jacinto
Chengue
San Cayetano
Cansona
Popa
Cicuco
Oso
Lower Miocene unconformity
Not reached by drillholes in Sinú
Lower to middle Eocene unconformity
Lower Paleocene unconformity
Sinú Lineament
Romeral Fault System
Planeta Rica Peridotites
Cretaceous basement
Fining–up trend
Coarsening–up trend
Unconformity
Coal seams
Calcareous sandstones/mudstones
Sandstones (mostly marine)
Deep/shallow marine mudstones
Shallow marine limestones
Siliceous mudstones and chert
Conglomerates
Lava flows, tuffs, and agglomerates.
Peridotites
Oceanic basement
Glacial events
N : Northern Hemisphere
S : Southern Hemisphere
Major anoxic events
Temperature (°C)*
Neogene
Paleogene
Cretaceous
Quaternary
Pliocene
Miocene
Oligocene
Eocene
Paleocene
Maastrichtian
Campanian
Santonian
Coniacian
Turonian
Cenomanian
Albian

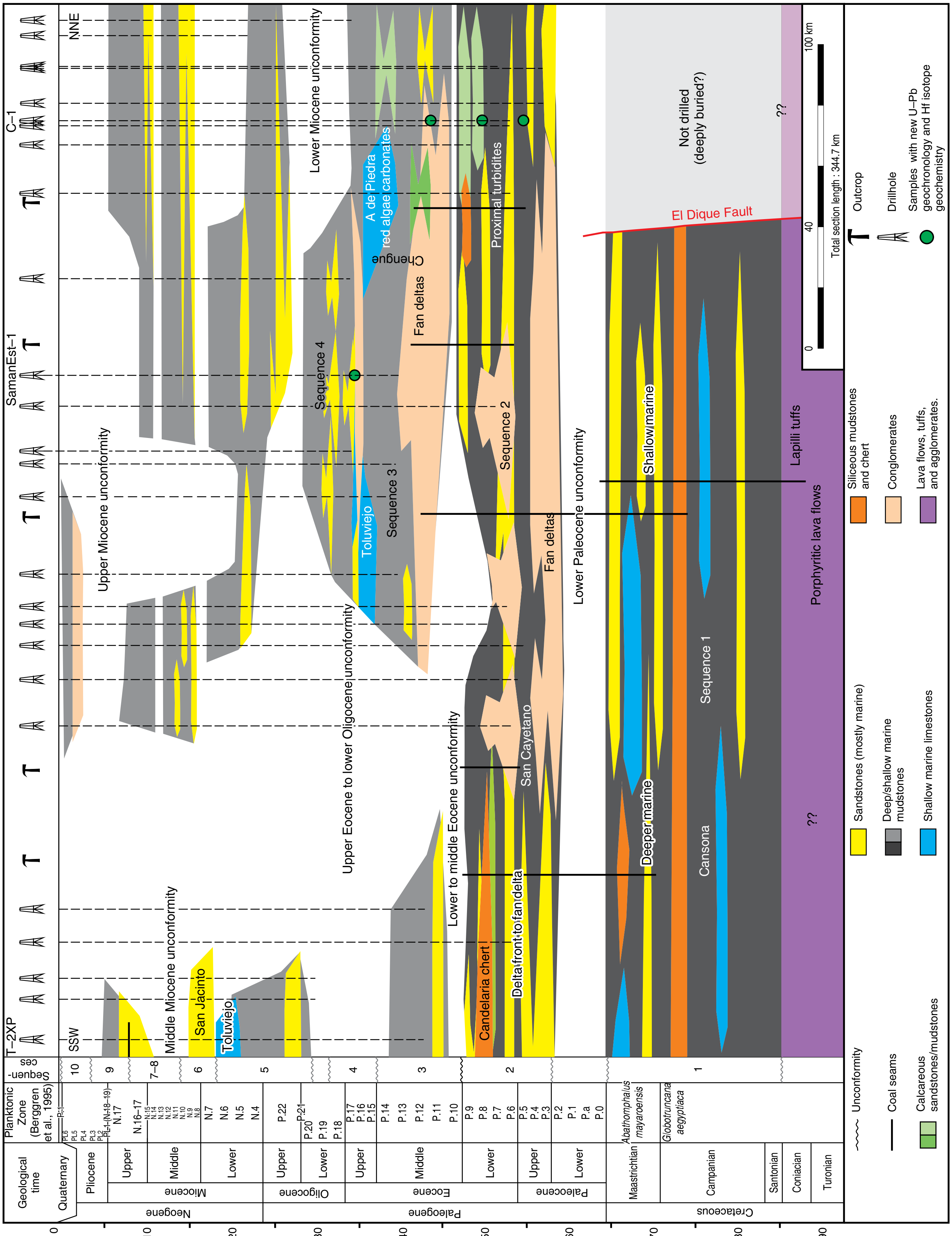

Geological time
Planktonic Zone (Berggren et al., 1995)
Sequences
Neogene
Paleogene
Cretaceous
Quaternary
Pliocene
Miocene
Oligocene
Eocene
Paleocene
Upper
Middle
Lower
Maastrichtian
Campanian
Santonian
Coniacian
Turonian
Abathomphalus mayaroensis
Globotruncana aegyptiaca
T–2XP
SamanEst–1
C–1
SSW
NNE
Middle Miocene unconformity
San Jacinto
Toluviejo
Upper Miocene unconformity
Lower Miocene unconformity
Upper Eocene to lower Oligocene unconformity
Lower to middle Eocene unconformity
Lower Paleocene unconformity
Candelaria chert
Delta front to fan delta
San Cayetano
Fan deltas
Sequence 1
Sequence 2
Sequence 3
Sequence 4
Cansona
Deeper marine
Shallow marine
Porphyritic lava flows
Lapilli tuffs
A de Piedra red algae carbonates
Chengue
Proximal turbidites
Not drilled (deeply buried?)
El Dique Fault
??
Total section length : 344.7 km
0
40
100 km
Outcrop
Drillhole
Samples with new U–Pb geochronology and Hf isotope geochemistry
Unconformity
Coal seams
Calcareous sandstones/mudstones
Sandstones (mostly marine)
Deep/shallow marine mudstones
Shallow marine limestones
Siliceous mudstones and chert
Conglomerates
Lava flows, tuffs, and agglomerates.

←

Figure 5. SSW–NNE–trending chronostratigraphic chart with wells and outcrops compiled along–strike (NE–SW) from the San Jacinto fold belt. Wells with new detrital zircon geochronological analyses are highlighted (green circles show approximate location of samples). Modified from Mora et al. (2017b).

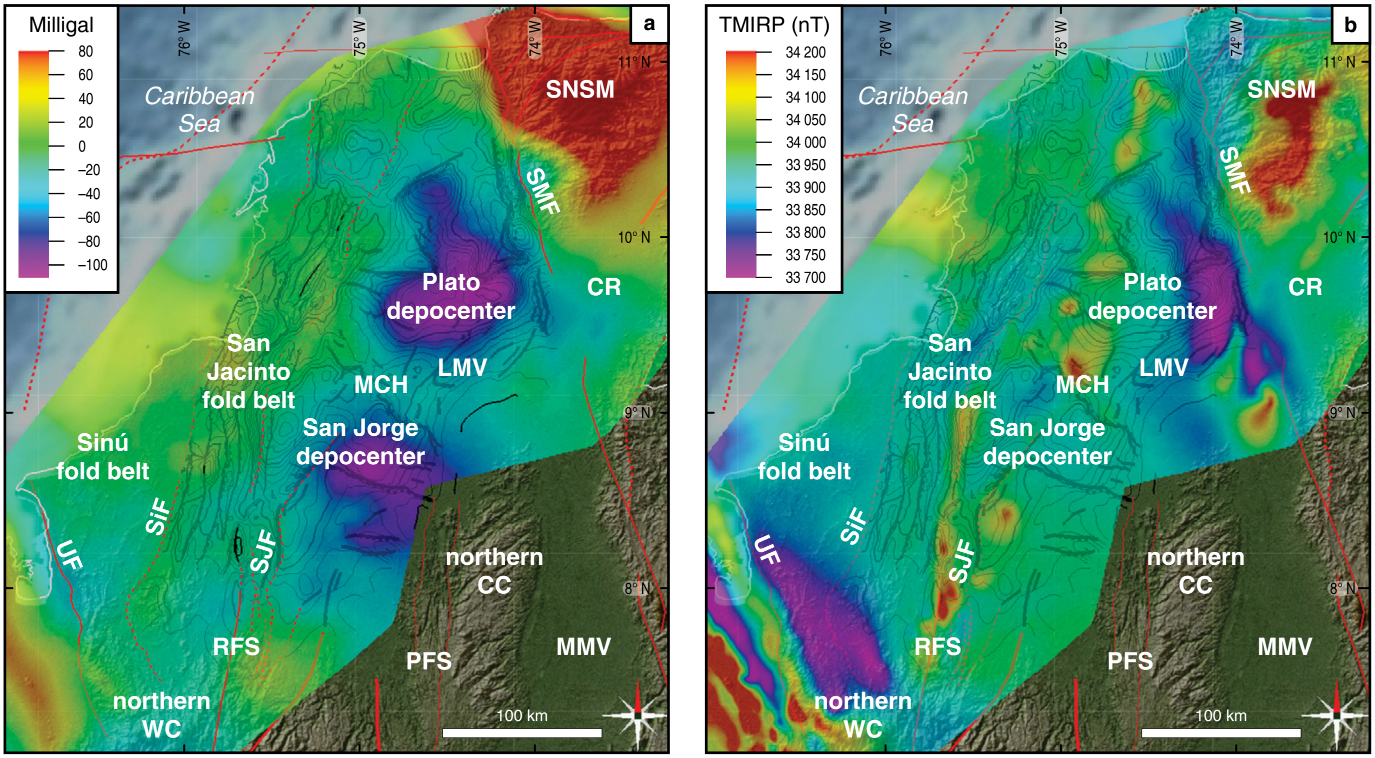

Figure 6. Airborne gravity and magnetics data from northern Colombia, acquired by Lithosphera Ltda. (2010) for Hocol S.A. and the Agencia Nacional de Hidrocarburos (ANH). **(a)** Total Bouguer anomaly, scale from –80 to 80 mGal. **(b)** Total magnetic intensity reduced to the pole (TMIRP) with scale from 33700 to 34200 nT. In the background we included the contours of the near top basement structural map in depth, after Mora et al. (2017a). (SNSM) Sierra Nevada de Santa Marta; (SMF) Santa Marta Fault; (CR) Cesar–Ranchería Basin; (MCH) Magangué–Cicuco High; (LMV) Lower Magdalena Valley Basin; (UF) Uramita Fault; (SiF) Sinú Fault; (SJF) San Jerónimo Fault; (CC) Central Cordillera; (RFS) Romeral Fault System; (PFS) Palestina Fault System; (MMV) Middle Magdalena Valley Basin; (WC) Western Cordillera. Modified after Mora et al. (2017a).

4.7. Seismicity Data and Present–Day Lithospheric Configuration of Northwestern Colombia

Using the publicly available seismicity data and data from previous research (e.g., Bezada et al., 2010b), the present–day geometry and configuration of the subduction zone of NW Colombia was studied by Mora et al. (2017a, 2017b). A depth map of the top of the subducted oceanic slab beneath South America and a cross–section depicting its geometry and the configuration of the subduction zone of NW Colombia were constructed (Figure 11). The study area is characterized by a low seismicity, with very few scattered, shallow (<70 km), and low magnitude (<4 Mw) events (Mora et al., 2017a), and there are no available focal mechanism solutions in the area of the San Jacinto fold belt.

According to Mora et al. (2017b), the Caribbean Plate subducted beneath NW South America appears to be formed by three different slab segments, separated by kinks or bends (Figure 11): a northwestern shallow and very flat slab segment, a central intermediate–depth and flat–slab segment (the "Caribbean" flat–slab of Syracuse et al., 2016), and a southeastern deep and very steep slab segment imaged by Bezada et al. (2010b). However, such segmented slab geometry of the subducted Caribbean Plate does not seem to continue to the north of the Oca–El Pilar–San Sebastian Fault System (OEPFS) and seismicity changes abruptly from the southern to the northern block of the OEPFS (see Figure S1 in Mora et al., 2017b).

Based on the steep descent of the Caribbean Plate under Maracaibo and the Mérida Andes, previous researchers have proposed that there should be a tear in the Caribbean Plate (Bezada et al., 2010b; Masy et al., 2011; Levander et al., 2015), which

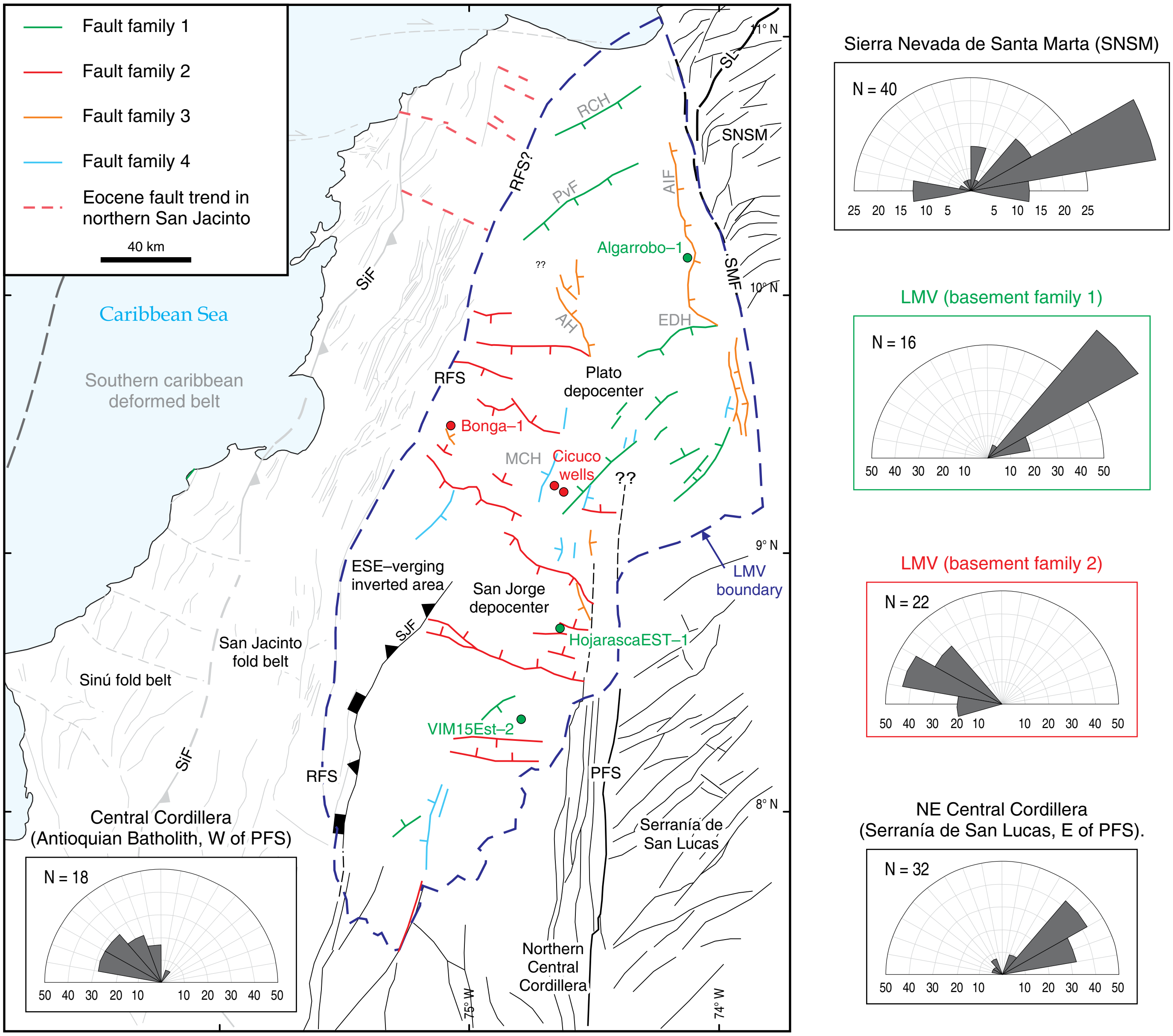

Figure 7. Fault families and structural fabric of the basement terranes in northwestern Colombia (northern CC, western SNSM, and LMV). Surface faults and lineaments were drawn from the Geological Map of Colombia (Gómez et al., 2007) and subsurface fault families were interpreted and drawn from our basement depth–models. In all rose diagrams, the bin size was set to 20 degrees. Light gray features drawn in the Sinú and San Jacinto fold belts are Neogene to recent structures. (SL) Sevilla Lineament; (RCH) Remolino–Ciénaga High; (RFS) Romeral Fault System; (SNSM) Sierra Nevada de Santa Marta; (SiF) Sinú Fault; (PvF) Pivijay Fault; (AlF) Algarrobo Fault; (SMF) Santa Marta Fault; (AH) Apure High; (EDH) El Difícil High; (MCH) Magangué–Cicuco High; (SJF) San Jerónimo Fault; (LMV) Lower Magdalena Valley; (PFS) Palestina Fault System. Modified from Mora et al. (2017a).

→

Figure 8. Interpreted late Oligocene **(a)** and early Miocene **(b)** paleogeography, based on seismic interpretation and well data, showing interpreted source areas (based on Mora et al., 2017a and others), active sedimentation areas, and proposed paleo–drainages in blue; thin red contours are thicknesses in meters of each sequence and the thick red contour represents the interpreted limit of deposition of each sequence. Detrital zircon U–Pb geochronology from Montes et al. (2015) is also plotted (purple circles with their respective histograms), and it shows a greater influence in the SE of Permian – Triassic and older basement sources (black bars in histograms), while Cretaceous sources in the Western and Central Cordilleras are more important in the NW (green bars in histograms). The development of local paleo–highs (e.g., Betulia and Cibarco) in the present–day SJFB, as interpreted from seismic data, is also shown. (SNSM) Sierra Nevada de Santa Marta; (PvF) Pivijay Fault; (CR) Cesar Ranchería; (MoF) Mojana Fault; (SuF) Sucre Fault; (CC) Central Cordillera; (MMV) Middle Magdalena Valley Basin.

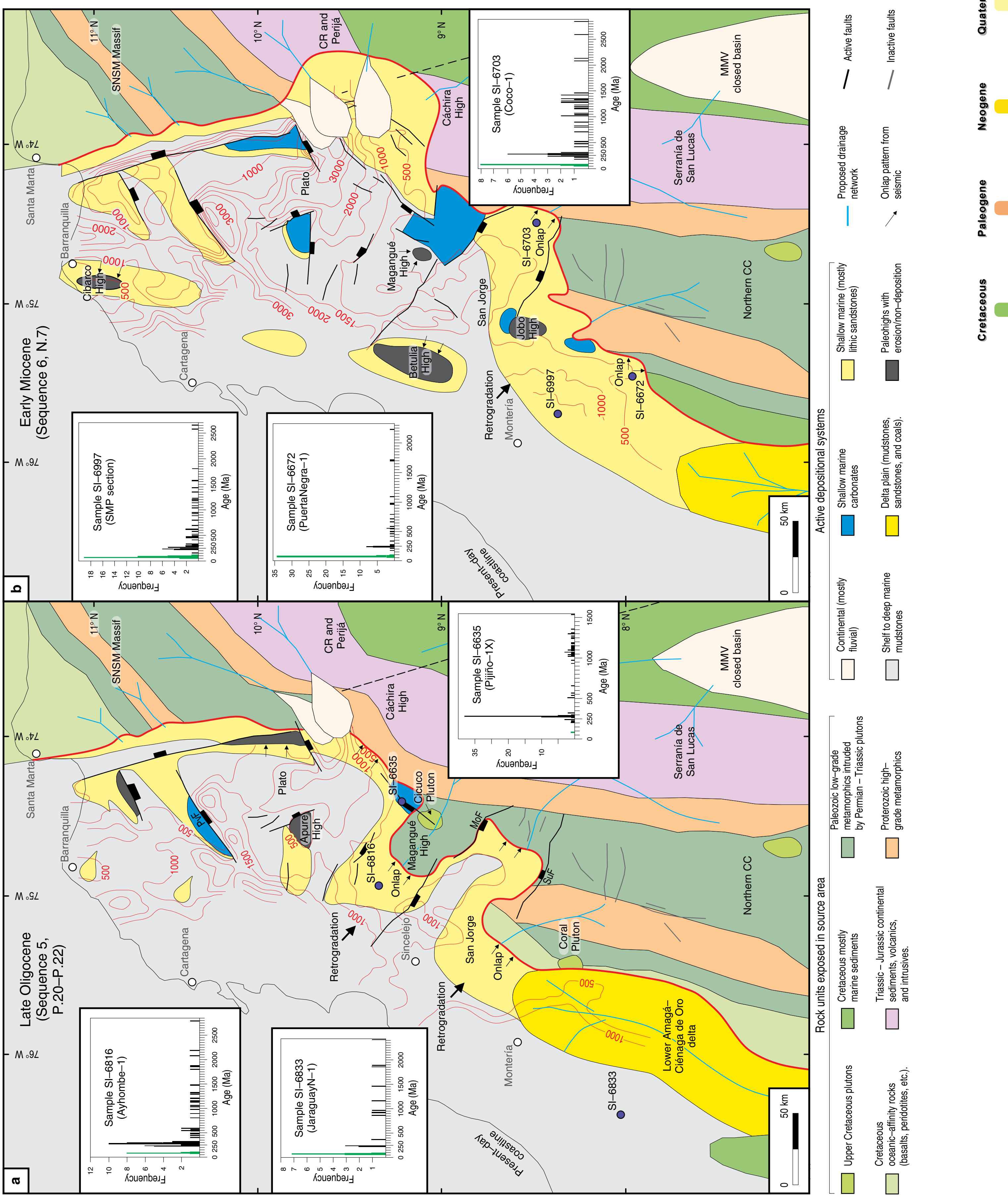
a
Late Oligocene
(Sequence 5, P.20–P.22)
Sample SI–6816
(Ayhombe–1)
Sample SI–6833
(JaraguayN–1)
Sample SI–6635
(Pijiño–1X)
Frequency
Age (Ma)
Santa Marta
Barranquilla
Cartagena
Sincelejo
Montería
SNSM Massif
Plato
Apure High
Magangué High
Cicuco Pluton
Cáchira High
CR and Perijá
MMV closed basin
Serranía de San Lucas
Northern CC
San Jorge
Coral Pluton
Lower Amagá–Ciénaga de Oro delta
Retrogradation
Onlap
PlF
MoF
SuF
SI–6816
SI–6635
SI–6833
Present–day coastline
50 km
b
Early Miocene
(Sequence 6, N.7)
Sample SI–6997
(SMP section)
Sample SI–6672
(PuertaNegra–1)
Sample SI–6703
(Coco–1)
Cibarco High
Magangué High
Betulia High
Jobo High
SI–6703
SI–6997
SI–6672
76° W
75° W
74° W
11° N
10° N
9° N
8° N
Rock units exposed in source area
Upper Cretaceous plutons
Cretaceous oceanic–affinity rocks (basalts, peridotites, etc.).
Cretaceous mostly marine sediments
Triassic – Jurassic continental sediments, volcanics, and intrusives.
Paleozoic low–grade metamorphics intruded by Permian – Triassic plutons
Proterozoic high–grade metamorphics
Active depositional systems
Continental (mostly fluvial)
Shelf to deep marine mudstones
Shallow marine carbonates
Delta plain (mudstones, sandstones, and coals).
Shallow marine (mostly lithic sandstones)
Paleohighs with erosion/non–deposition
Proposed drainage network
Onlap pattern from seismic
Active faults
Inactive faults
Cretaceous
Paleogene
Neogene
Quaternary

would be separating the steeper dipping Caribbean slabs, located to the south of the OEPFS, from the shallow Caribbean Plate that has been imaged north of the same fault system. Using data from previous research and our new depth map of the shallow subducted Caribbean oceanic segment under the San Jacinto fold belt, Lower Magdalena Valley Basin, and the serranía de Perijá (inset in Figure 11), Mora et al. (2017b) proposed a new interpretation of the three–dimensional plate tectonic configuration of northern Colombia and western Venezuela (Figure 12). This interpretation implies that the boundary between northern South America and the Caribbean Plate consists of two tears or subduction–transform edge propagator (STEP, Govers & Wortel, 2005) faults instead of only one. The Oca–San Sebastián–El Pilar dextral fault system would then be the surface expression of the tear fault that limits the Caribbean and South American/ Atlantic Plates at deeper crustal and mantle levels.

4.8. Cretaceous to Recent Paleo–Tectonic Reconstructions

Late Cretaceous to recent paleo–tectonic reconstructions were performed, using the free software package GPlates (Boyden et al., 2011) and two paleo–tectonic models available for this area (Boschman et al., 2014; Matthews et al., 2016, from the GPlates database) (Figure 13; Figures 1 and 2 of the Supplementary Information; Mora et al., 2017b, 2018). The reconstructions show the motion of the Caribbean Plate relative to a fixed South American Plate, but it is important to highlight that plate tectonic processes between the Caribbean and the Americas were driven by relatively fast, westward motion of North and South America, while the Caribbean Plate has remained nearly stationary since the Eocene (Müller et al., 1999). The constructed models were used to study the kinematic evolution of the tectonic plates, in order to relate them to the Upper Cretaceous to recent tectono–stratigraphy in the LMV and SJFB (Mora et al., 2017b, 2018).

Using average plate convergence velocities of the Caribbean Plate relative to South America over the last 45 Ma, Mora et al. (2017b) calculated for both models the geological time when each of the three subducted slab segments of the Caribbean Plate imaged along cross–section A–A' (Figure 11) entered the trench (Table 1). The age of entrance in the trench of the whole Caribbean slab (total length of 1065 ± 15 km) ranges from early Eocene (ca. 56 ± 2 Ma) to middle Eocene (ca. 43 ± 2 Ma) depending on the model used (Boschman et al., 2014 or Matthews et al., 2016, respectively). Kroehler et al. (2011) estimated the age of the initiation of subduction of the Venezuelan Basin at the southern Caribbean deformed belt based on the wedge–shaped asymmetrical thickness of the sediments in the trench adjacent to the thrust zones. The beginning of tectonic wedging appears in a middle Eocene megasequence in the west and is younger towards the east (Kroehler et al., 2011).

Equivalence of the obtained age of entrance in the trench of the Caribbean slab with the identified unconformities in the stratigraphic succession in the SJFB, and with the convergence velocities and obliquities, as shown in Figure 14, will be discussed in forthcoming sections.

4.9. Cross–Section Structure of the SJFB and LMV

The present–day SJFB is a west–verging and NNE–SSW–trending, fold and thrust belt that has been formed by Pliocene to recent contraction and inversion (Figure 15), but that experienced a complex pre–Oligocene tectonic history. Its structure has been influenced by the strike–slip activity of the Romeral Fault System (RFS), and by the contraction along the west–verging Sinú Fault (SiF), which appears to be related to the Sinú accretionary prism (Mora et al., 2017a, 2017b). Such complex deformation obscured the original Cretaceous to Eocene structural fabric, making seismic imaging very poor. However, Mora et al. (2017b) documented several areas in which pre–Oligocene sequences have preserved their original extensional structural fabric, exhibiting extensional rotated fault blocks which are forming two sets of extensional faults, one with a SSW–NNE orientation and the second one with a WNW–ESE orientation (Mora et al., 2013a). Sequences 1 and 2 are mostly restricted to the western side of the RFS (Figure 15), and would be limited to the east by the San Jerónimo Fault (SJF), while Sequences 3 and 4 extend farther to the east, into the western LMV. Interpreted seismic cross–sections also showed that the activity of the RFS considerably decreases from the south, close to the outcrops between the Central and Western Cordilleras, to the north. In fact, the RFS has been sealed by the lower to mid-

Figure 9. Interpreted middle Miocene **(a)** and late Miocene to early Pliocene **(b)** paleogeography, based on seismic interpretation and well data, showing interpreted source areas, active sedimentation areas, and interpreted paleo–drainages in blue. Thin red contours are thicknesses in meters of each sequence and the thick red contour represents the interpreted limit of deposition of each sequence. Detrital zircon U–Pb geochronology from Montes et al. (2015) is also plotted (purple circles with their respective histograms) in the left panel, showing a greater influence in the SE and north (Plato and Magangué–Cicuco High) of Permian – Triassic and older basement sources (black bars in histograms); Cretaceous (green bars) and Eocene to middle Miocene (yellow–orange bars) sources are more important in the SW, suggesting a much greater influence of the Western and Central Cordilleras as source areas in middle Miocene times. The development of paleo–highs, as interpreted from seismic data, is also shown. (SNSM) Sierra Nevada de Santa Marta; (CR) Cesar Ranchería; (LMV) Lower Magdalena Valley; (MMV) Middle Magdalena Valley; (CC) Central Cordillera.

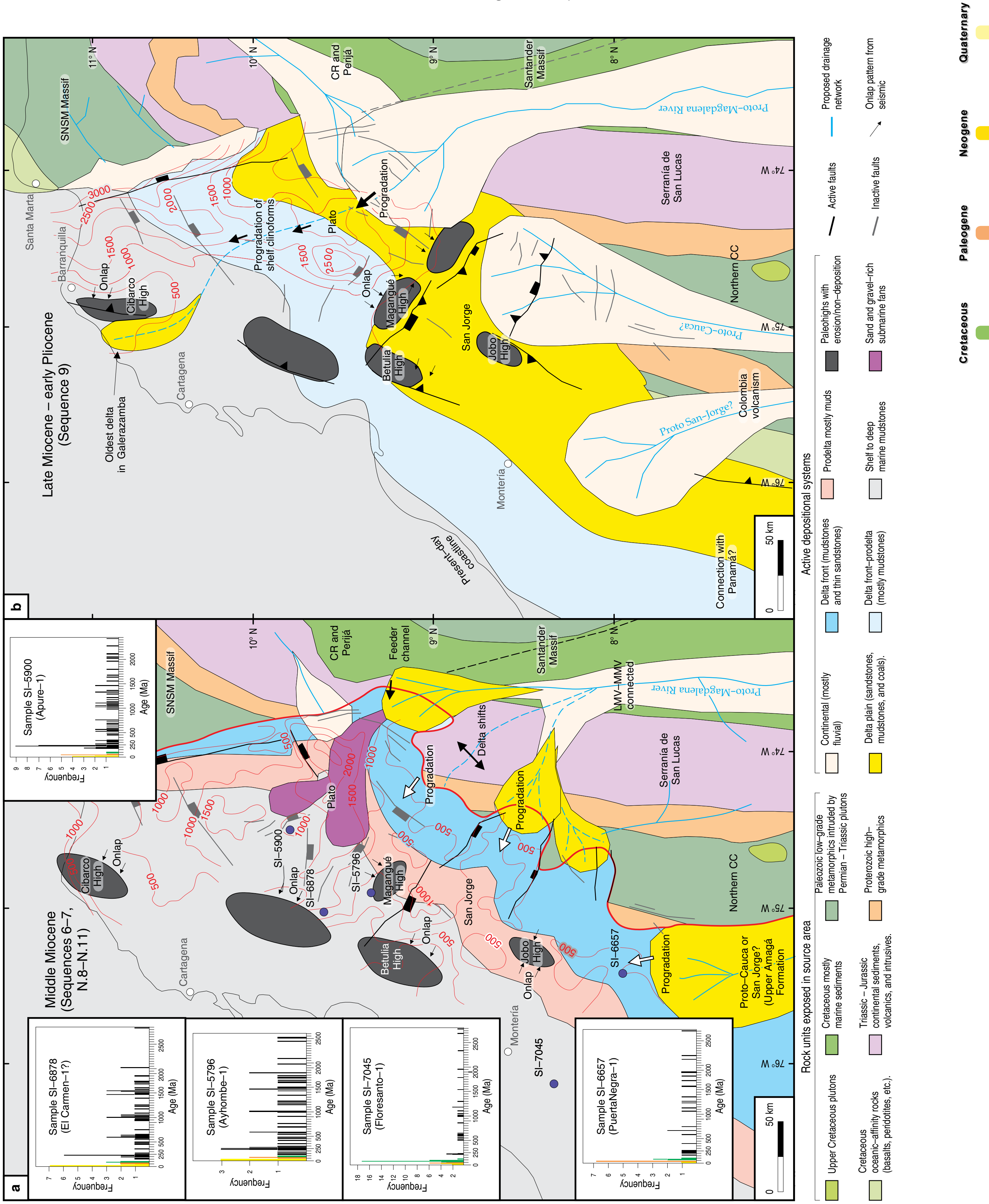
a
Middle Miocene
(Sequences 6–7, N.8–N.11)
Sample SI–6878
(El Carmen–1?)
Sample SI–5796
(Ayhombe–1)
Sample SI–7045
(Floresanto–1)
Sample SI–6657
(PuertaNegra–1)
Sample SI–5900
(Apure–1)
Frequency
Age (Ma)
SNSM Massif
CR and Perijá
Feeder channel
Santander Massif
LMV–MMV connected
Proto–Magdalena River
Serranía de San Lucas
Northern CC
Cibarco High
Betulia High
Magangué High
Jobo High
San Jorge
Plato
Cartagena
Montería
Onlap
Progradation
Delta shifts
Proto–Cauca or San Jorge? (Upper Amagá Formation
b
Late Miocene – early Pliocene
(Sequence 9)
Santa Marta
Barranquilla
Oldest delta in Galerazamba
Progradation of shelf clinoforms
Present-day coastline
Connection with Panamá?
Proto San-Jorge?
Proto–Cauca?
Colombia volcanism
Rock units exposed in source area
Upper Cretaceous plutons
Cretaceous oceanic–affinity rocks (basalts, peridotites, etc.).
Cretaceous mostly marine sediments
Triassic – Jurassic continental sediments, volcanics, and intrusives.
Paleozoic low-grade metamorphics intruded by Permian – Triassic plutons
Proterozoic high-grade metamorphics
Active depositional systems
Continental (mostly fluvial)
Delta plain (sandstones, mudstones, and coals).
Delta front (mudstones and thin sandstones)
Delta front–prodelta (mostly mudstones)
Prodelta mostly muds
Shelf to deep marine mudstones
Paleohighs with erosion/non-deposition
Sand and gravel–rich submarine fans
Active faults
Inactive faults
Proposed drainage network
Onlap pattern from seismic
Cretaceous
Paleogene
Neogene
Quaternary

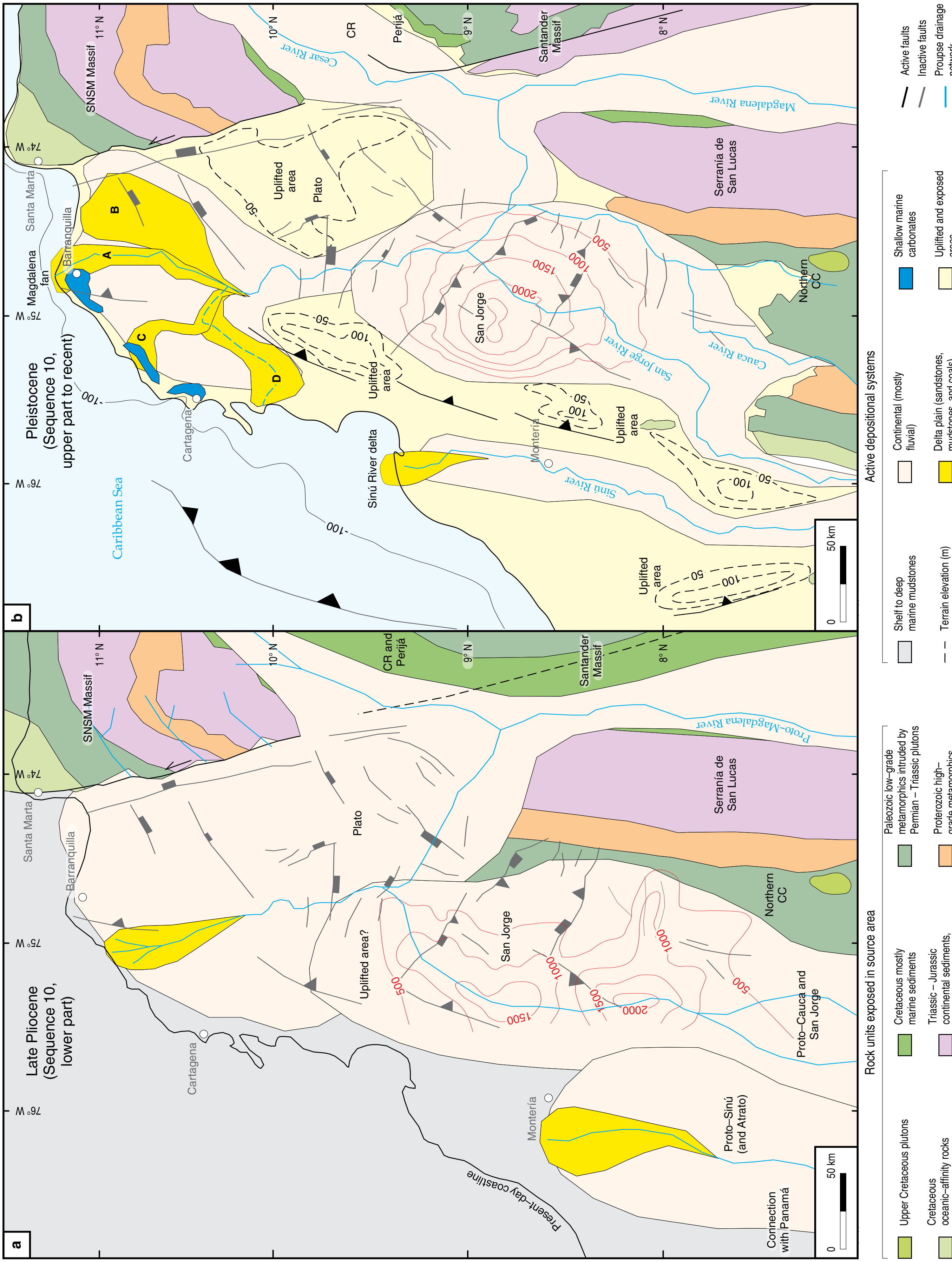
a
Late Pliocene (Sequence 10, lower part)
76° W
75° W
74° W
11° N
10° N
9° N
8° N
Santa Marta
Barranquilla
Cartagena
Montería
SNSM Massif
CR and Perijá
Santander Massif
Proto-Magdalena River
Plato
Uplifted area?
San Jorge
Serranía de San Lucas
Northern CC
Proto-Cauca and San Jorge
Proto-Sinú (and Atrato)
Connection with Panamá
Present-day coastline
500
1000
1500
2000
0
50 km
b
Pleistocene (Sequence 10, upper part to recent)
Caribbean Sea
Magdalena fan
A
B
C
D
Uplifted area
Plato
Cesar River
CR
Perijá
Santander Massif
Magdalena River
Serranía de San Lucas
San Jorge
San Jorge River
Cauca River
Northern CC
Sinú River delta
Sinú River
Uplifted area
-100
-50
100
50
0
50 km
Rock units exposed in source area
Upper Cretaceous plutons
Cretaceous oceanic-affinity rocks (basalts, peridotites, etc.).
Cretaceous mostly marine sediments
Triassic – Jurassic continental sediments, volcanics, and intrusives.
Paleozoic low-grade metamorphics intruded by Permian – Triassic plutons
Proterozoic high-grade metamorphics
Active depositional systems
Shelf to deep marine mudstones
Terrain elevation (m)
Continental (mostly fluvial)
Delta plain (sandstones, mudstones, and coals).
Shallow marine carbonates
Uplifted and exposed areas
Active faults
Inactive faults
Proupse drainage network

←

Figure 10. Interpreted late Pliocene **(a)** and Pleistocene **(b)** paleogeography, based on seismic interpretation and well data, showing interpreted source areas (based in Mora et al., 2017a and others), active sedimentation areas, and interpreted paleo–drainages in blue; thin red contours are thicknesses in meters of each sequence. In late Pliocene times, when the Magdalena River system reached the present–day coastline, the Plato depocenter was already overfilled, whereas sedimentation continued in the western San Jorge depocenter, which continued subsiding. In the Pleistocene, while the Magdalena River delta shifted its position, uplift of the San Jacinto fold belt and of the Plato depocenter created a round depocenter, which continues to subside today. Letters A to D represent positions of the Magdalena deltas (from Romero–Otero et al., 2015), with A representing the current position. (SNSM) Sierra Nevada de Santa Marta; (CR) Cesar Ranchería; (CC) Central Cordillera.

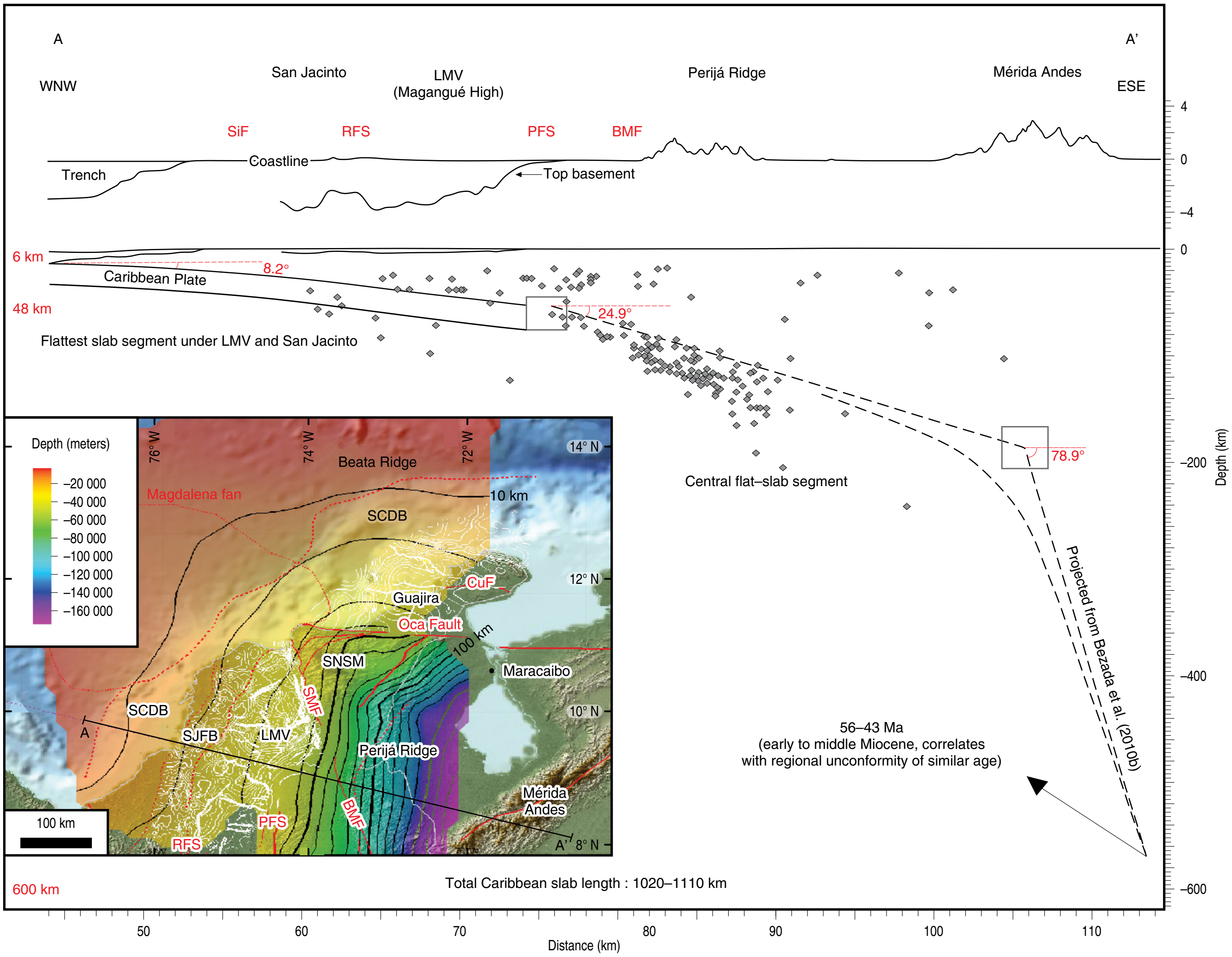

Figure 11. Regional WNW–ESE–trending cross–section showing the lithospheric configuration of the convergent margin of NW Colombia, as interpreted from reflection–seismic mapping for the shallowest part, intermediate–depth seismicity for the central, "Caribbean flat–slab" segment, and from published tomography data (Bezada et al., 2010b) for the deepest part of the cross–section. The top of the basement under the LMV from reflection–seismic mapping and the topography are also displayed. Gray squares represent the uncertainty in the horizontal and vertical measurements. Inset: Integrated depth map in meters of the top of the oceanic Caribbean Plate (in colors), which has been subducted under NW South America since middle Eocene times. Note the change in dip of the slab in the location of the Palestina Fault System (PFS) and how it changes its strike as it approaches the Oca Fault. The white contours are the depth structure of the basement below the LMV, SJFB, and Guajira Basins. (SiF) Sinú Fault; (RFS) Romeral Fault System; (LMV) Lower Magdalena Valley; (PFS) Palestina Fault System; (BMF) Bucaramanga Fault; (SCDB) South Caribbean deformed belt; (CuF) Cuisa Fault; (SNSM) Sierra Nevada de Santa Marta; (SMF) Santa Marta Fault; (SJFB) San Jacinto fold belt. Modified from Mora et al. (2017b).

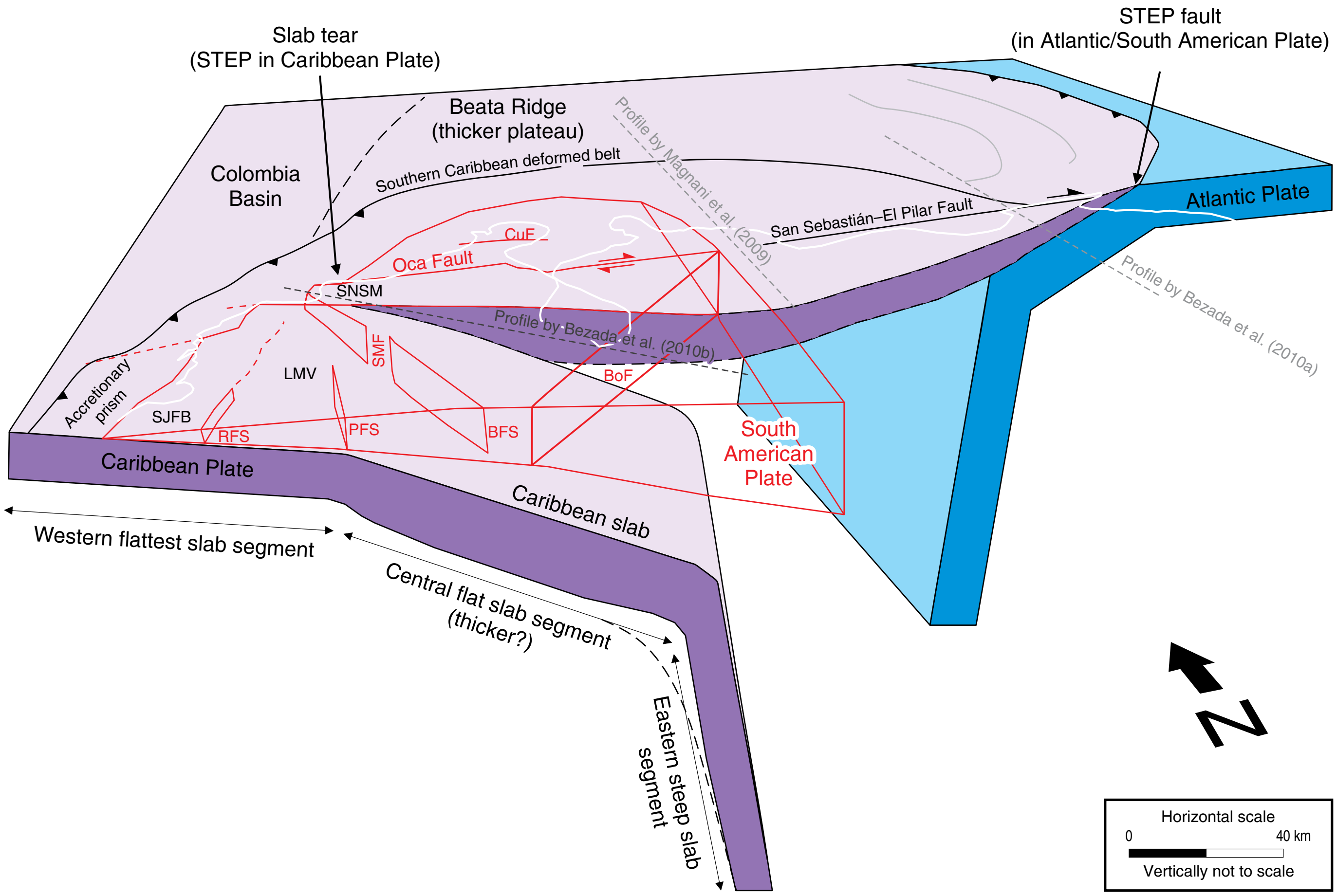

Figure 12. Proposed three–dimensional lithospheric configuration of NW South America, as interpreted from shallow reflection–seismic mapping, intermediate–depth seismicity, and deep tomographic imaging from previous studies (e.g., Bezada et al., 2010b); according to our interpretation, there would be a slab tear or STEP fault (subduction transform edge–propagator, Govers & Wortel, 2005) in the Caribbean Plate, probably represented in the upper crust by the western tip of the Oca–El Pilar–San Sebastián dextral fault system. (CuF) Cuisa Fault; (SNSM) Sierra Nevada de Santa Marta; (SJFB) San Jacinto fold belt; (RFS) Romeral Fault System; (LMV) Lower Magdalena Valley; (PFS) Palestina Fault System; (SMF) Santa Marta Fault; (BFS) Bucaramanga Fault System; (BoF) Boconó Fault. Modified from Mora et al. (2017b).

dle Eocene unconformity, except for local, later reactivations. The eastward tilting of the whole SJFB has been caused by a deeper and younger major fault that probably extends to the deformation front of the accretionary prism, located in offshore areas farther to the west.

The two main basement fault families defined by Mora et al. (2017a), trending ESE–WNW and ENE–WSW, are responsible for most of the extension in the LMV, and consist of nearly vertical extensional faults, which exhibit small heaves. Seismic–stratigraphic analyses show that deposition of the upper Oligocene to lower Miocene sequences (Ciénaga de Oro and Lower Porquero) had fault control, and that after the early Miocene, deposition was mainly due to sagging or non–fault related subsidence, giving rise to the classic Steer's Head model of basin geometry (Miall, 2000). This is evident in the regional cross–section in depth along the LMV (Figure 16), where the majority of the extensional faults are displacing the upper Oligocene to middle Miocene sequences, with related thickness changes across the major faults (Mora et al., 2018). By contrast, the upper Miocene to Pleistocene sequences filled broader depocenters in a uniform way, with only minor and localized fault displacements. The latest subsidence episode, which appears to continue active, is related to non–fault related subsidence of the San Jorge Graben that allowed the deposition of the very thick Pliocene to Pleistocene Sequence 10 (Corpa).

4.10. Sedimentation Rates and Subsidence in the LMV and San Jacinto Fold Belt

Thicknesses and ages from 32 wells drilled in the LMV and SJFB were compiled to calculate sedimentation rates and to carry out subsidence analyses of those provinces. Our analyses in the LMV indicate that after the lower Miocene unconformity there was an important increase in sedimentation and subsidence rates (Figure 17a, 17b). Though sedimentation rates were not corrected for compaction, the rates calculated for Sequence

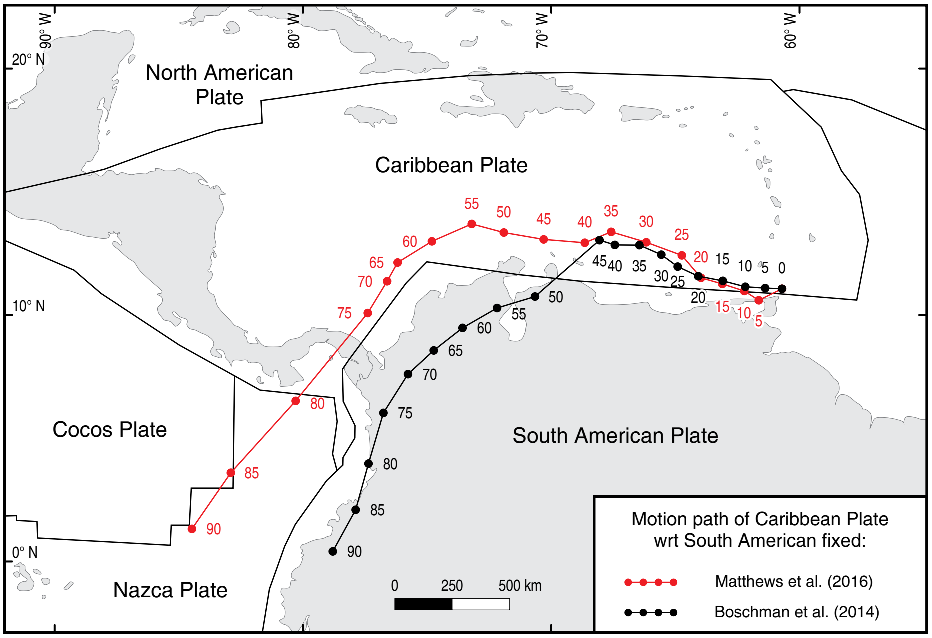

Figure 13. Displacement vectors of the Caribbean Plate relative to South America from the Cretaceous (90 Ma) to present day, shown in red according to the model of Matthews et al. (2016, GPlates database) and in black according to Boschman et al. (2014). Major changes in convergence velocity and obliquity are highlighted. Matthews et al. 's (2016) model shows a decrease in obliquity at 55 Ma (from 78 to 34° in average) and in velocity at 75 Ma (from 8.3 to 2.8 cm/y in average) and Boschman et al. 's (2014) model shows a decrease in obliquity (from 74 to 30° in average) and in velocity (from 4.3 to 1.9 cm/y in average) both at 45 Ma. Modified from Mora et al. (2017b).

Table 1. Compilation of the slab segment lengths, convergence velocities, and ages of entrance in the trench of each slab segment shown in Figure 11 (from Mora et al., 2017b).

	Slab segment length (km) (±15 km error)	Calculated age of slab entrance in the trench using mean plate velocities over the last 45 Ma	
		Boschman et al. (2014)	Matthews et al. (2016)
		19 mm/y	25 mm/y
Western flat slab segment under SJFB and LMV	278–308	14.6–16.2 Ma	11.1–12.3 Ma
Central intermediate–depth flat slab segment	341–371	18–19.5 Ma	13.6–14.8 Ma
Eastern deepest and steepest slab segment	401–431	21.1–22.7 Ma	16–17.2 Ma
Western plus central flat slab segments	619–679	32.6–35.7 Ma	24.8–27.2 Ma
All three slab segments	1020–1110	53.7–58.4 Ma (56 ± 2 Ma)	40.8–44.4 Ma (43 ± 2 Ma)
Slab length by van Benthem et al. (2013)*	900	47.4 Ma	36 Ma

Note: We calculated average velocities over the last 45 Ma according to each of the two available models (Boschman et al., 2014; Matthews et al., 2016). Using such velocities and the measured lengths of each slab segment, we could calculate the time at which each segment entered the trench. From these calculations, we found that the ca. 1000 km long Caribbean slab entered the trench in early to middle Eocene times, coinciding with regional unconformities identified in the San Jacinto fold belt.
* They interpret three slab segments, each one 300 km long.

6 (lower to middle Miocene) are generally above 60 m/my and locally exceed 300 m/my. In spite of being locally eroded, middle Miocene to Pliocene sequences (7 to 9) exhibit values close to 150 m/my, while Sequence 10 (Corpa, Pliocene to Pleistocene) displays high sedimentation rates, with an average of 530 m/my (Mora et al., 2018). A major increase in sedimentation rates after middle Miocene times is also seen in the Sinú fold belt and other offshore areas (Figure 18), where rates in excess of 2000 m/my were calculated.

Estimates of corrected total and tectonic subsidence show important variations depending on the geographic location (Figure 19a; Mora et al., 2018). The highest subsidence estimates were obtained in the southern Plato depocenter where 4.8 km of total subsidence and 2.1 km of tectonic subsidence were calcu-

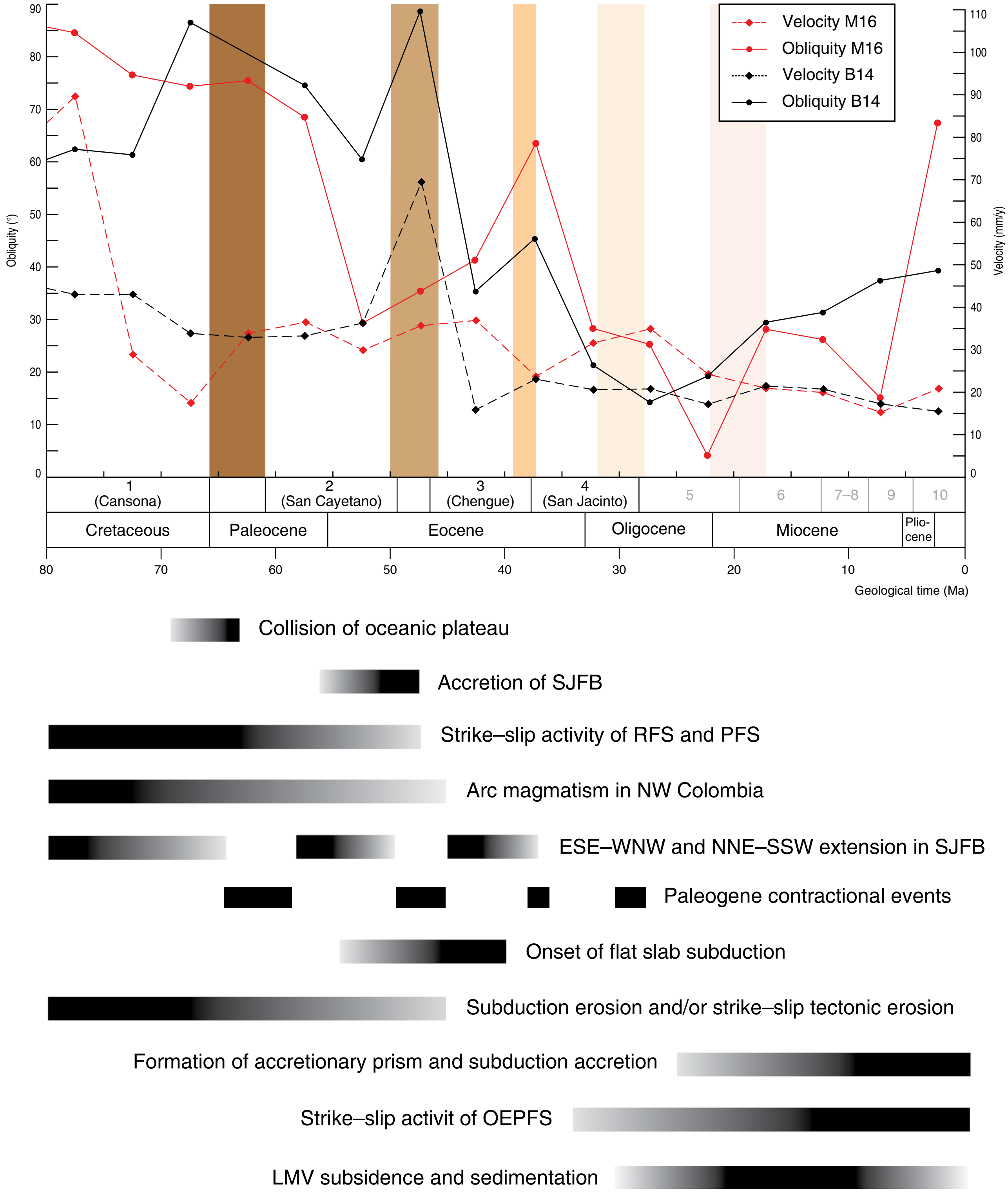

Figure 14. Evolution of Late Cretaceous to present–day tectonic plate convergence velocity and obliquity compared with major tectonic events and tectono–stratigraphic unconformities. The upper panel shows the changes in plate convergence velocity and obliquity with time for both models, compared with the pre–Oligocene tectono–stratigraphic sequences and unconformities (vertical bars of brown shades) and major tectonic events (black horizontal bars in the lower panel). We calculated velocities and obliquities in time–steps of 5 Ma, hence the points in the graph represent the middle of each time interval. The identified Paleogene unconformities correlate with major tectonic events such as the Late Cretaceous to early Paleocene collision of the Caribbean Plateau and the Eocene onset of Caribbean flat–slab subduction. Modified from Mora et al. (2017b). However, the best correlation is seen between the early to middle Eocene unconformity and the tectonic events listed in the lower part. (SJFB) San Jacinto fold belt; (RFS) Romeral Fault System; (PFS) Palestina Fault System; (OEPFS) Oca–El Pilar Fault System; (LMV) Lower Magdalena Valley.

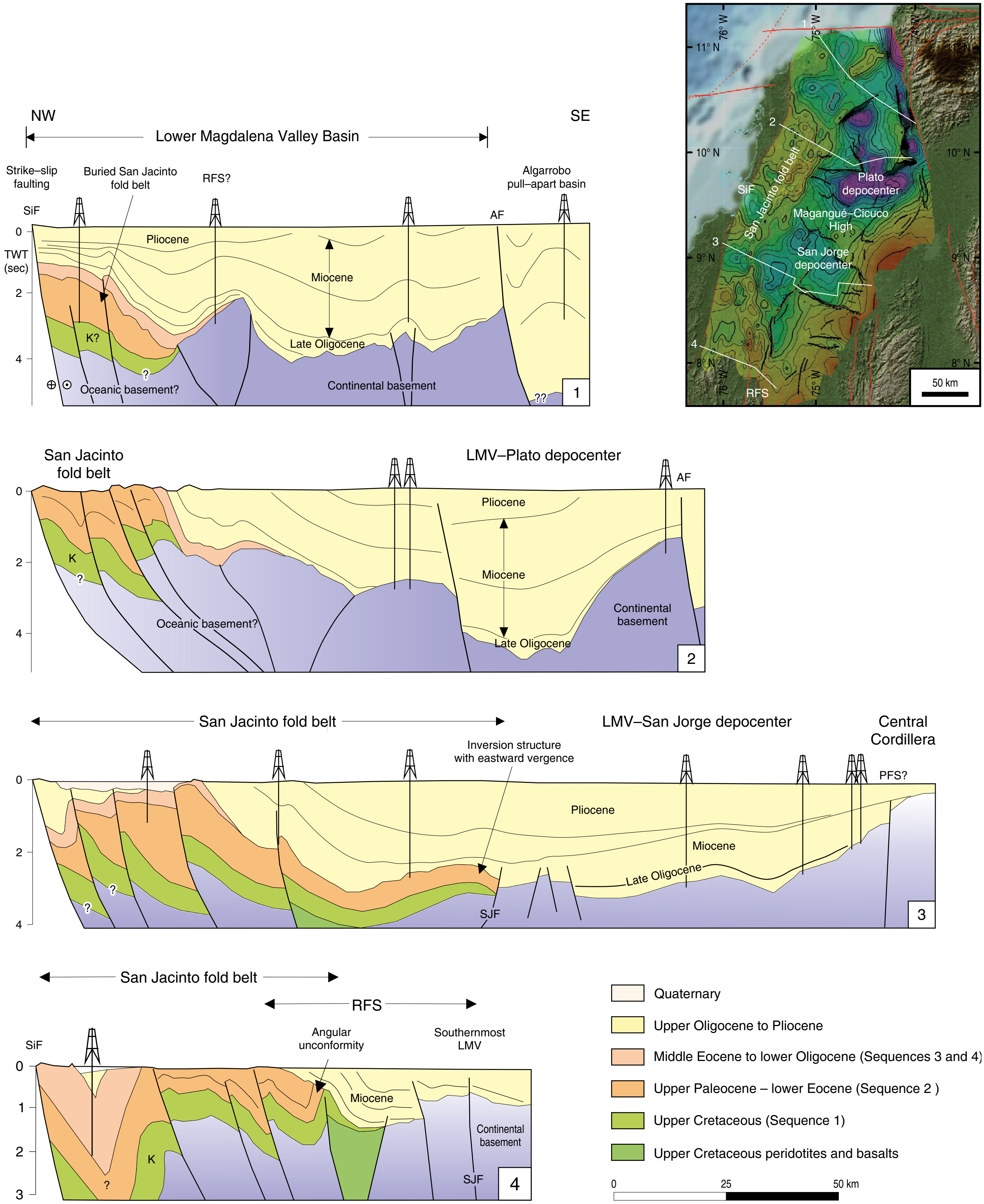

Figure 15. NW–SE–trending, interpreted, seismic cross–sections in two–way–time (TWT), showing the along strike variation in structure of the SJFB, LMV, and RFS, and highlighting tectono–stratigraphic relationships among the studied sequences (modified from Mora et al., 2017b). (SiF) Sinú Fault; (RFS) Romeral Fault System; (AF) Algarrobo Fault; (LMV) Lower Magdalena Valley; (PFS) Palestina Fault System; (SJF) San Jerónimo Fault System.

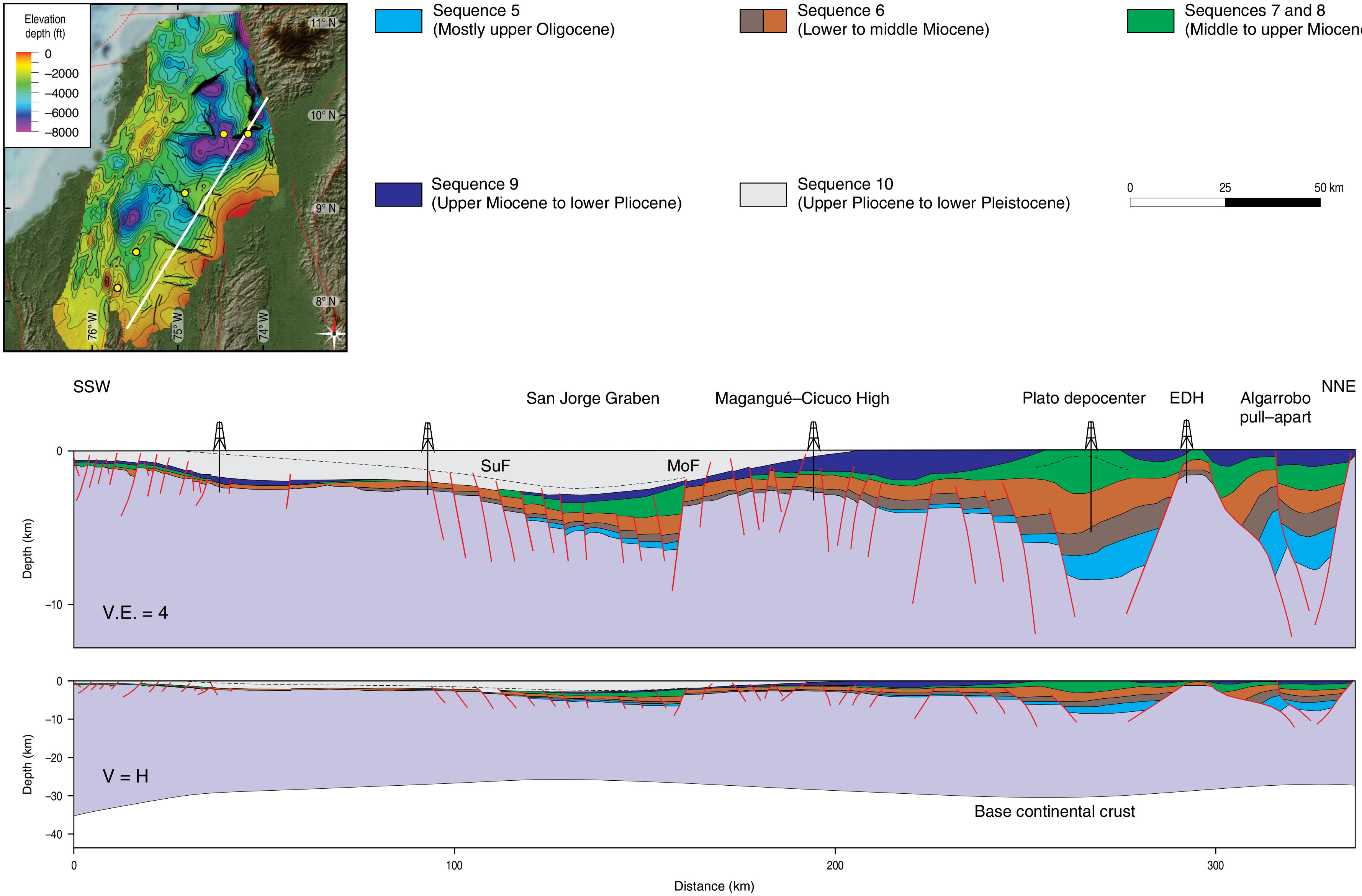

Figure 16. Regional structural cross–section in depth (meters), in two different scales to show the stratigraphic relationships, thicknesses and preservation of the studied Oligocene to Quaternary sequences. The lower section (scale 1:1), also shows the base of the continental crust, based on data by Poveda et al. (2015) and Bernal–Olaya et al. 2015a. Dashed line in Sequence 10 represents clinoform progradation to the north while dashed line in green unit (Sequences 7–8) represents thickening due to internal deformation. (SuF) Sucre Fault; (MoF) Mojana Fault; (EDH) El Difícil High.

lated. In the San Jorge Graben, 3.7 km of total subsidence and 1.8 km of tectonic subsidence were calculated. An increase in tectonic subsidence after 18 Ma is followed by a general decrease after 13 Ma, except for the wells located in the SW (La Esmeralda and Bonga), where there's an increase in tectonic and total subsidence after 3 Ma.

4.11. Extension in the LMV

The simple line–length calculation along the SSW–NNE transect (Figure 16) showed that the basement of the LMV has been extended 40.7 km, which represents 12.1% of extension or a stretching factor of 1.13 (Mora et al., 2018). However, the Algarrobo pull–apart would be accounting for 7% of the total extension in the LMV. According to the tectonic subsidence curves, β values oscillate between 1.1 and 2 in most of the LMV, while in deep parts of the Plato depocenter, β values range from 2 to 4, which are clearly overestimated. Compilation of the crustal thickness and Moho depth data from Poveda et al. (2015) and Bernal–Olaya et al. (2015a) showed that they range from 24 km in the northern LMV, to 50 km in the southeastern boundary of the basin against the northern Central Cordillera (Figure 19b–d). The basement beneath the LMV reaches depths of 8 km in the Plato depocenter and 6 to 7 km in the San Jorge Graben (Mora et al., 2017a). Removal of the sedimentary fill suggests that the crust is thinnest in the northwestern part of the basin and in the western San Jorge depocenter (ca. 20 km; Figure 19d).

Crustal thickness calculations in northern Colombia (Poveda et al., 2012) suggest that the continental crustal thickness in relatively undeformed areas such as the Middle Magdalena Valley Basin ranges from 40 to 45 km. Chulick et al. (2013) obtained a weighted average thickness of the continental South American of 38.17 km, while Assumpção et al. (2013) measured an average thickness of the crust in stable continental areas of Brasil of 39 ± 5 km and 35 km in sub–Andean foredeeps. Therefore, assuming an initial crustal thickness in the LMV area of 40 km and using the present–day crustal thickness map, crustal thinning would be >50% (β=2) in the Plato depocenter in the north, and around 50% in the Montería–San Jorge graben area, while in the rest of the basin there is much less crustal thinning (32–25 km, 20–38 % thinning). This means that the LMV experienced high extension in the two depocenters (Plato and San Jorge) and low extension in the rest of the basin. Table 2 summarizes our extension estimates using the three different approaches previously described and the previous extension calculations by Montes et al. (2010).

4.12. Oligocene to Recent Paleo–Geography and Kinematics of the LMV

In this section, we present the results of the integration and analysis of all our seismic, well and outcrop data, which are the basis for proposing an Oligocene to recent kinematic and paleogeographic evolution of the LMV. Such evolution is illustrated both in map view (Figures 8–10) and in cross–section view (Figures 20 and 21).

Seismic and well data shows that the LMV basin was initially filled by Oligocene, shallow–marine deposits of Sequence 5, which filled the paleo–topographic lows, as the sea transgressed from NW to SE (Figures 8a, 20, and 21). Fault–controlled subsidence observed in the seismic indicates that there was an extensional, NE–SW and SE–NE–trending reactivation of pre–existing basement faults. After a lower Miocene unconformity, basal deposits of Sequence 6 covered wider areas to the E, and correspond to shallow–marine clastic deposits in low areas and calcareous deposits in high areas (Figure 8b). Fault controlled subsidence continued, indicating similar extensional regime and trends as in the Oligocene. At least two important forearc highs (Betulia and Cibarco) are documented towards the western LMV, based on seismic onlap patterns. The upper part of the sequence starts displaying progradational patterns, which together with the occurrence of Cretaceous and Grenvillian detrital zircons in the eastern San Jorge depocenter, suggest the onset of drainages from the S or SE.

In middle Miocene times (Figures 9a, 20, and 21), seismic and well data show that deposition became strongly progradational to the NW and N. Though the upper part of Sequence 6 and Sequence 7 exhibit progradational patterns to the WNW (Figure 8), deep marine deposits prevail and the basin reached its maximum flooding at ca. 14 Ma, in agreement with a global sea–level rise (Figure 4). After such maximum flooding episode and in spite of continued basin subsidence and creation of accommodation space, progradational packages of Sequences 8 and 9 advance to the NW (Figure 9). We interpret the fact that progradation was able to overcome increasing subsidence and creation of accommodation space in middle to late Miocene times, as a clear indication of an increase in sediment supply from the SE.

Connection between the LMV and Middle Magdalena Valley (MMV) is probable, and correlates well with thick progradational packages filling the San Jorge depocenter in the south, and turbiditic and gravity–driven deposits filling the deep part of the Plato depocenter in the north. The main evidence for proposing a connection between the eastern LMV and the northern MMV comes from the seismic, well data, and facies models, all of which show that at middle Miocene times, there was progradation of marine stratigraphic packages from the northern MMV towards the NW. Furthermore, while the geochronology data of Montes et al. (2015) shows a Mesoproterozoic (Grenvillian) population of detrital zircons in samples from the eastern LMV, Gómez et al. (2005) and Caballero et al. (2013) proposed that a connection between the northern MMV and the northeastern LMV was established in earliest middle Miocene times, when the Colorado Formation covered the Cáchira Arch.

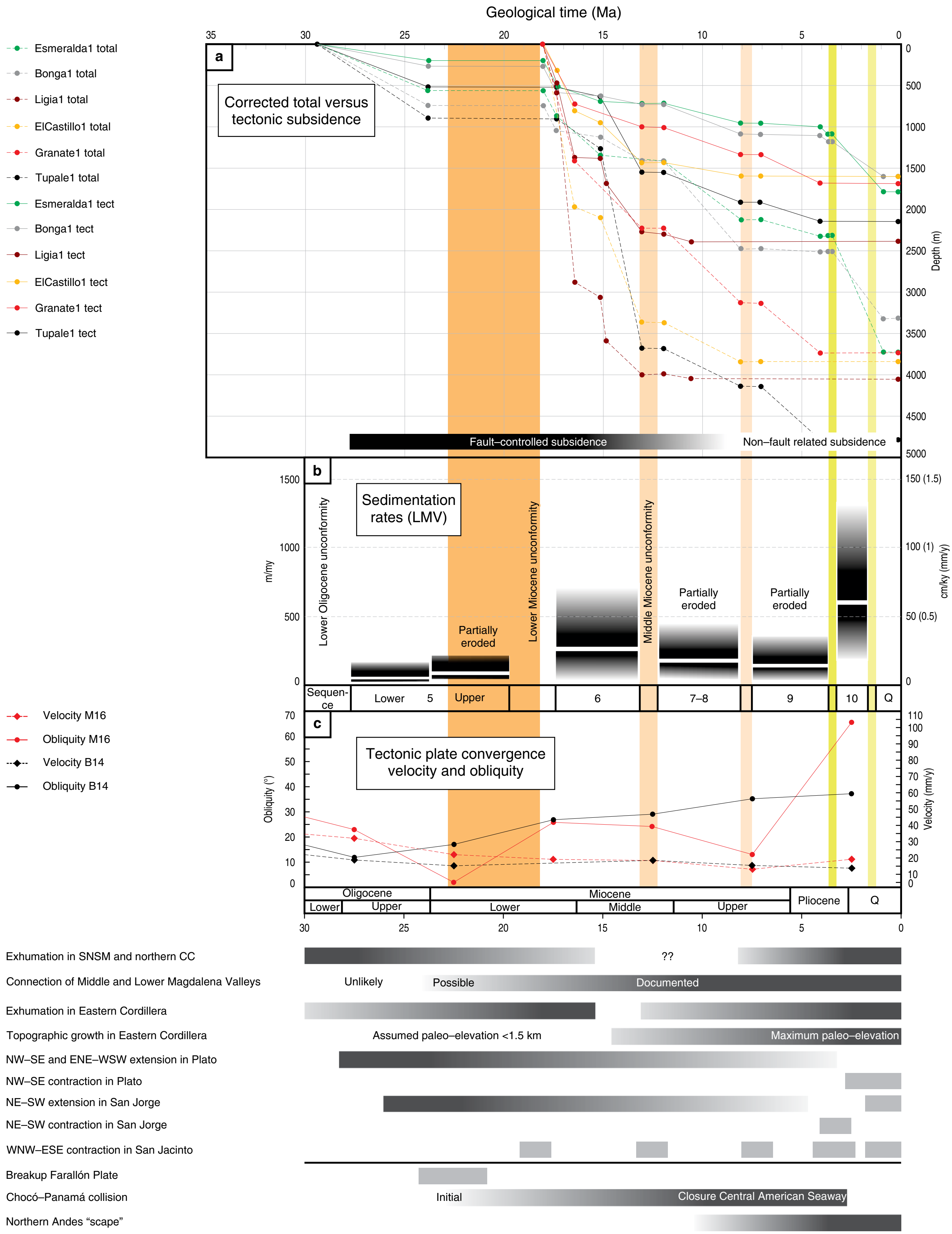
Geological time (Ma)
Esmeralda1 total
Bonga1 total
Ligia1 total
ElCastillo1 total
Granate1 total
Tupale1 total
Esmeralda1 tect
Bonga1 tect
Ligia1 tect
ElCastillo1 tect
Granate1 tect
Tupale1 tect
a
Corrected total versus tectonic subsidence
Depth (m)
Fault–controlled subsidence
Non–fault related subsidence
b
Sedimentation rates (LMV)
m/my
cm/ky (mm/y)
Lower Oligocene unconformity
Lower Miocene unconformity
Middle Miocene unconformity
Partially eroded
Sequence
Lower
5
Upper
6
7–8
9
10
Q
Velocity M16
Obliquity M16
Velocity B14
Obliquity B14
c
Tectonic plate convergence velocity and obliquity
Obliquity (°)
Velocity (mm/y)
Oligocene
Miocene
Pliocene
Lower
Upper
Middle
Exhumation in SNSM and northern CC
??
Connection of Middle and Lower Magdalena Valleys
Unlikely
Possible
Documented
Exhumation in Eastern Cordillera
Topographic growth in Eastern Cordillera
Assumed paleo–elevation <1.5 km
Maximum paleo–elevation
NW–SE and ENE–WSW extension in Plato
NW–SE contraction in Plato
NE–SW extension in San Jorge
NE–SW contraction in San Jorge
WNW–ESE contraction in San Jacinto
Breakup Farallón Plate
Chocó–Panamá collision
Initial
Closure Central American Seaway
Northern Andes "scape"

←

Figure 17. Integration of the subsidence (total vs. tectonic), sedimentation rate and Oligocene to present day, tectonic plate convergence velocity and obliquity, compared with major tectonic events and tectono–stratigraphic unconformities. Tectonic (continuous lines) and total (dashed lines) subsidence plots of representative wells in the LMV and San Jacinto are displayed in **(a)**, and sedimentation rates in **(b)**. **(c)** From top to bottom exhibits the changes in plate convergence velocity and obliquity with time, for two different paleo–tectonic models (Boschman et al., 2014 in black, B14; Matthews et al., 2016 in red, M16), compared with the Oligocene to Quaternary (Q) tectono–stratigraphic sequences and unconformities (vertical bars with diagonal lines) and major tectonic events (black to grey horizontal bars in the lower panel). We calculated velocities and obliquities in time–steps of 5 Ma, hence the points in the convergence velocity and obliquity graph represent the middle of each time interval. (LMV) Lower Magdalena Valley; (SNSM) Sierra Nevada de Santa Marta; (CC) Central Cordillera.

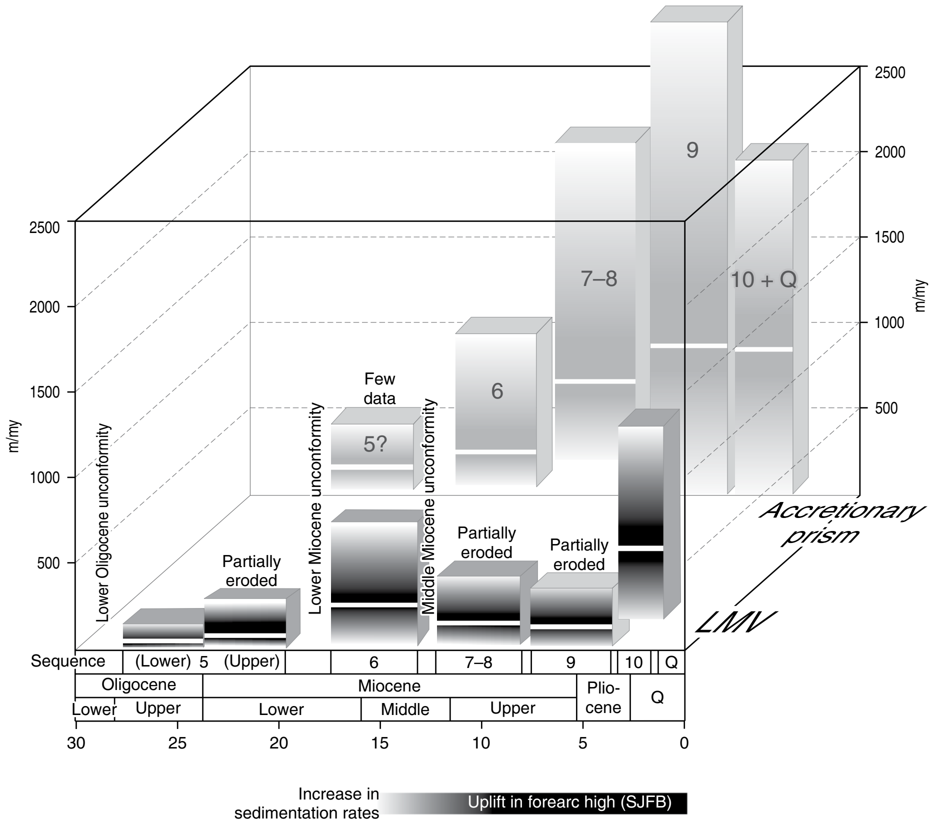

Figure 18. Comparison of Oligocene to recent, compacted sedimentation rates in the LMV and the accretionary prism (Sinú onshore and offshore) from well and seismic data. While there was partial erosion of middle and upper Miocene sequences in the LMV, very high sedimentation rates were measured in the accretionary prism for those sequences. The graph shows the proposed link between high sediment supply, sediment underplating, and uplift in San Jacinto with the formation of forearc highs. (LMV) Lower Magdalena Valley; (SJFB) San Jacinto fold belt.

In late Miocene to early Pliocene times (Sequence 9), the proto–Magdalena shelf clinoforms rapidly prograde to the NW and fill the Plato depocenter until they reach the current coastline, while the proto–Cauca and proto–San Jorge deposits also fill the southern LMV (Figures 9b, 20, and 21). Fault control ceased in the Plato depocenter, while the San Jorge Graben and the forearc highs experienced Pliocene, NE–SW and SE–NW–trending contraction, which was probably not coeval. Upper Pliocene deposits of Sequence 10 are poorly preserved in Plato, while they are well preserved in the San Jorge area, which is actively subsiding (Figure 10a). In the Pleistocene, the Plato area and the forearc highs are uplifted, while the San Jorge area continues to subside and accumulates thick fluvio–deltaic deposits in a round basin (Figures 10b and 20). Digital elevation models from the study area show that today, the northern LMV (Plato) and the San Jacinto fold belt are positive relief areas, while the southern LMV (San Jorge) continues subsiding. These patterns suggest that SE–NW–trending contraction and NE–SW–trending extension have been active since late Pliocene times, in agreement with the displacement vector of the Caribbean Plate relative to fixed South America.

Thickness analyses of each sequence allowed us to study the development and migration of depocenters since late Oli-

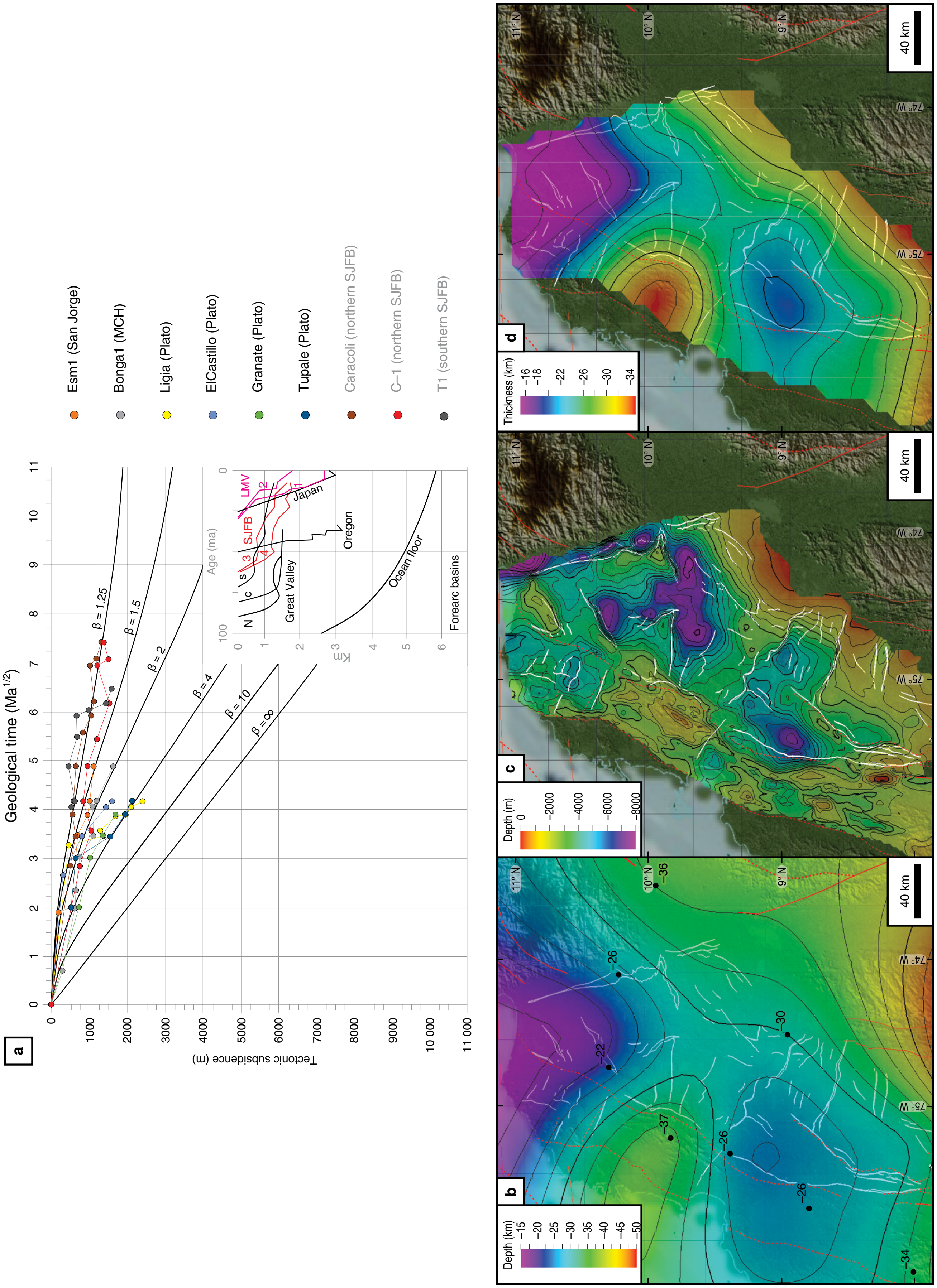
a
Geological time (Ma$^{1/2}$)
Tectonic subsidence (m)
β = 1.25
β = 1.5
β = 2
β = 4
β = 10
β = ∞
Age (ma)
km
LMV
SJFB
Japan
Oregon
Great Valley
Ocean floor
Forearc basins
Esm1 (San Jorge)
Bonga1 (MCH)
Ligia (Plato)
ElCastillo (Plato)
Granate (Plato)
Tupale (Plato)
Caracoli (northern SJFB)
C–1 (northern SJFB)
T1 (southern SJFB)
b
Depth (km)
c
Depth (m)
d
Thickness (km)
40 km
11° N
10° N
9° N
75° W
74° W

←

Figure 19. (a) Tectonic subsidence data plotted against the square root of the geological time (time since end of extension), in order to estimate stretching in the LMV (β–factor; McKenzie, 1978). Inset shows a comparison of our tectonic subsidence curves for the LMV and SJFB with data from other forearc basins compiled by Angevine et al. (1990), showing a good correlation with some basins. 1–Northern LMV (Plato); 2–Southern LMV (San Jorge); 3–Southern San Jacinto; 4–Northern San Jacinto. (b–d) Maps used to calculate extension in the LMV and SJFB. **(b)** Depth map of the Moho discontinuity, representing the crustal thickness, based on Poveda et al. (2015) and Bernal–Olaya et al. (2015a), showing that the crust thickness ranges from 22 km in the northern LMV to >30 km in the central and SW San Jacinto. Stations with measured values are depicted in black (values obtained from Bernal–Olaya et al. (2015a) were extrapolated as points from their regional gravity sections). **(c)** Basement map in depth (km) of the LMV, based on Mora et al. (2017a). **(d)** Crustal thickness map without sedimentary infill, obtained by subtracting the basement map in (c) from the crustal map in (b). It must be noted that the thinner crust (<20 km) in the NW of the LMV, where no thickness data is available, resulted from mapping extrapolation. (MCH) Magangué–Cicuco High; (SJFB) San Jacinto fold belt; (LMV) Lower Magdalena Valley.

Table 2. Compilation of extension calculations in previous (e.g., Montes et al., 2010) and this study, according to the different methods that were used. Further explanation in the text.

	Stretch factor	Extension in LMV	Comments
Line–length in cross–section	1.13	40.7 km (12.1%)	only the Algarrobo Fault System has been extended 26.7 km
Tectonic subsidence curves	β = 1.1 to 4		β values very high in depocenters (overestimated)
Crustal thickness measurements	β ≤ 2		maximum 50% in depocenters; 20–38 % elsewhere*
Montes et al. (2010)	β = 1.1 to >4	86 to 115 km	both extension calculations are overestimated

*Assuming initial crustal thickness of 40km.

gocene times. The detailed depocenter evolution and the possible reasons for depocenter migration are discussed in the following section.

5. Discussion

5.1. Structure and Age of the LMV Basement

5.1.1. Correlations with Outcropping Basement Terranes

The integration of potential methods, reflection seismic, and detrital zircon U–Pb geochronology and Hf isotope geochemistry allowed Mora et al. (2017a) to propose more robust correlations between the basement terranes in the surrounding massifs and the basement terranes identified in the LMV basement. These authors confirmed the extension of the Tahamí–Panzenú Terrane to the north into the LMV and proposed that an oceanic terrane, which could correspond to the Quebradagrande Complex or to a younger Late Cretaceous, allochthonous intra–oceanic arc, also extends in the western LMV, while the San Lucas (Chibcha) Terrane terminates against the northeastern LMV (Figure 22a; Mora et al., 2017a).

The data obtained from the Cicuco–22 well (Silva–Arias et al., 2016) and the new Coniacian – Campanian crystallization ages from the Bonga–1 granitoid confirmed the continuity to the north of the Late Cretaceous magmatic arc in the northern CC, which includes important plutons like the Antioquian Batholith (88–83 Ma, Ibañez–Mejia et al., 2007 and 93–87 Ma, Villagómez et al., 2011). Geochemical analyses of the Upper Cretaceous Cicuco intrusive suggested that this granitoid is related to a subduction environment and corresponds to calc–alkaline magmas, interpreted to be emplaced in a continental Andean–type crust (Silva–Arias et al., 2016). However, the new Bonga Hf isotopic data indicate a clear juvenile component, with limited evidence for significant contamination with older continental crust. Furthermore, the highly positive Bonga εHf values obtained are in contrast with the less radiogenic values obtained for the Upper Cretaceous granitoids of the northern CC such as the Antioquian Batholith (Restrepo et al., 2007). Considering these observations, and taking into account the proximity of the Bonga granitoid to the Romeral Fault System, Mora et al. (2017a) considered that the Bonga Pluton intruded a previously accreted oceanic terrane possibly located within the Romeral System, which may correspond to the northern continuation of the Quebradagrande Complex (Nivia et al., 2006). The Quebradagrande Terrane was accreted to South America along the San Jerónimo Fault in Albian times (115 to 105 Ma, Villagómez & Spikings, 2013).

An alternative possibility contemplates that the Bonga Pluton formed within an allochthonous intra–oceanic arc, which collided against the Permian – Triassic continental margin in latest Cretaceous to early Paleocene times (Bayona et al., 2011; Cardona et al., 2012). According to this interpretation, this pluton would correspond to the Great Arc of the Caribbean (Al-

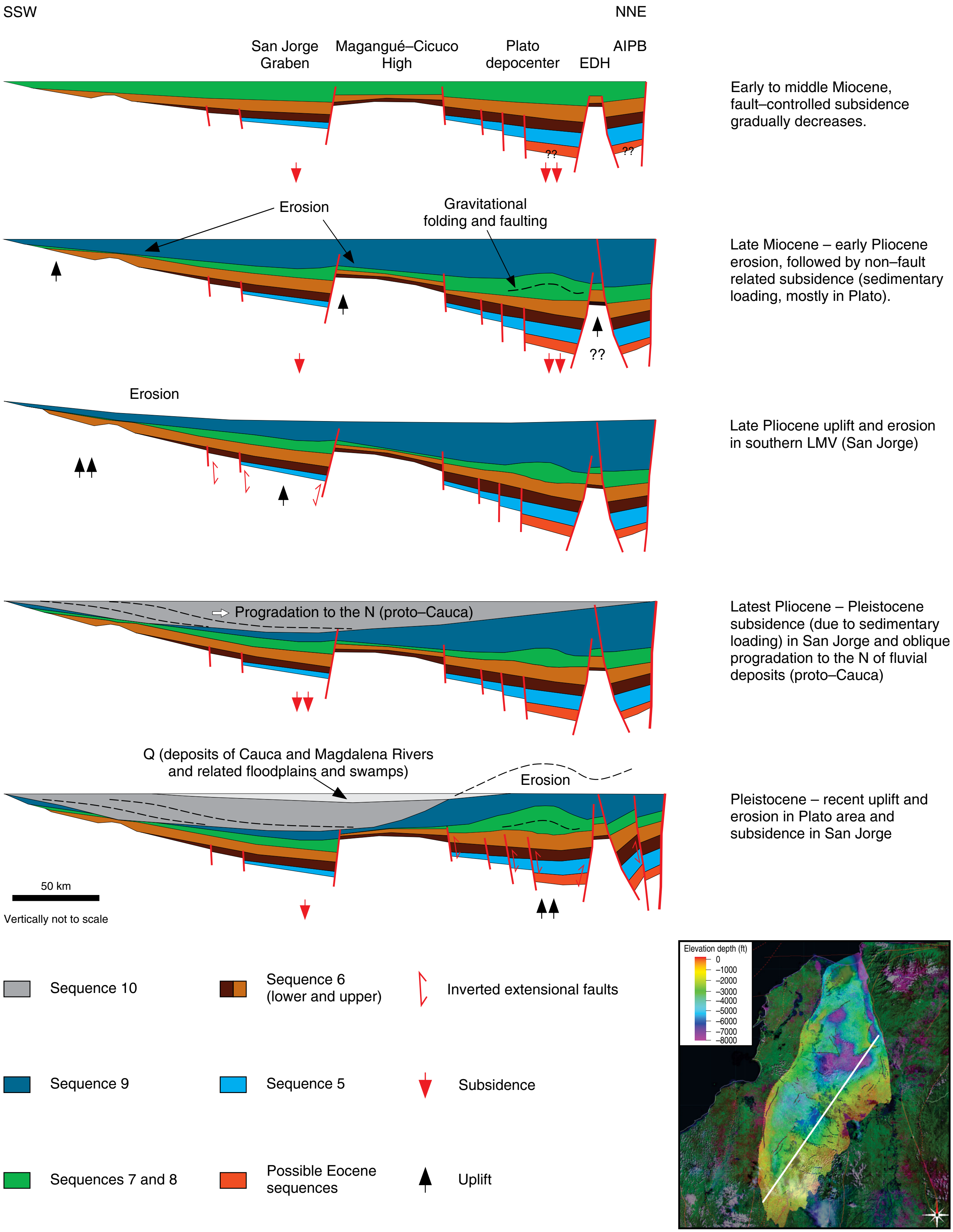
SSW
NNE
San Jorge Graben
Magangué–Cicuco High
Plato depocenter
EDH
AIPB
??
??
Early to middle Miocene, fault–controlled subsidence gradually decreases.
Erosion
Gravitational folding and faulting
??
Late Miocene – early Pliocene erosion, followed by non–fault related subsidence (sedimentary loading, mostly in Plato).
Erosion
Late Pliocene uplift and erosion in southern LMV (San Jorge)
Progradation to the N (proto–Cauca)
Latest Pliocene – Pleistocene subsidence (due to sedimentary loading) in San Jorge and oblique progradation to the N of fluvial deposits (proto–Cauca)
Q (deposits of Cauca and Magdalena Rivers and related floodplains and swamps)
Erosion
Pleistocene – recent uplift and erosion in Plato area and subsidence in San Jorge
50 km
Vertically not to scale
Sequence 10
Sequence 9
Sequences 7 and 8
Sequence 6 (lower and upper)
Sequence 5
Possible Eocene sequences
Inverted extensional faults
Subsidence
Uplift
Elevation depth (ft)
0
−1000
−2000
−3000
−4000
−5000
−6000
−7000
−8000

←

Figure 20. Simplified Oligocene to recent evolution of the LMV, shown in a NNE–SSW–trending regional section. Oligocene to middle Miocene fault–controlled subsidence, which affected Sequences 5 to 7, was replaced by non–fault related subsidence (sagging) during deposition of Sequences 8 to 10. After the middle Miocene, the two depocenters (Plato and San Jorge) started to experience different subsidence and uplift phases. Figure vertically not to scale. (EDH) El Difícil High; (AIPB) Algarrobo pull–apart basin.

tamira & Burke, 2015; Burke, 1988; Escalona & Mann, 2011; Kroehler et al., 2011; Villagómez & Spikings, 2013), a regional arc that appears to extend from Ecuador to the Lesser Antilles.

5.1.2. Formation of LMV Basement Fabric and Late Cretaceous Geodynamic Setting

The basement architecture of northwestern Colombia was built from Cretaceous to middle Eocene times and resulted in the formation of two major suture zones, the Romeral and the Palestina Fault Systems (Cediel et al., 2003; Restrepo & Toussaint, 1988). Based on previous studies and recent data and interpretations, Mora et al. (2017a) proposed that the basement fabric in the LMV and San Jacinto fold belt was formed by two main, regional tectonic processes (Figure 22b): (i) Jurassic rifting and (ii) Late Cretaceous to middle Eocene oblique convergence of the Caribbean and South American Plates, producing large–scale, dextral strike–slip displacement, arc–parallel extension due to displacement partitioning, and clockwise block rotation. The inherited pre–Oligocene basement fabric was later reactivated during the late Oligocene and early Miocene, allowing the formation and infill of the LMV. The new results allowed the reconstruction of the Late Cretaceous geodynamic setting of the LMV and San Jacinto, consisting of an east–dipping subduction of the "normal" thickness oceanic plate beneath South America, generating intracontinental arc magmatism of the Bonga and Cicuco Plutons. The current proximity of the Bonga Pluton to the trench suggests that significant erosion of the older forearc occurred by subduction erosion (Clift & Vannucchi, 2004) and/or by dextral strike–slip. However, there is also the possibility of formation of the Bonga Pluton in an intraoceanic arc, such as the Great Arc of the Caribbean (Altamira & Burke, 2015; Burke, 1988), which collided with northwestern South America in Late Cretaceous times (ca. 70 Ma, Luzieux et al., 2006).

5.2. San Jacinto: An Late Cretaceous to Early Eocene Marine Forearc Basin Formed in an Oblique Convergence Tectonic Setting

5.2.1. San Jacinto Late Cretaceous to Early Eocene Forearc Evolution

From the available information, it appears that during Late Cretaceous (Coniacian to Campanian) times, a forearc basin existed SW of the study area, with an intra–continental, magmatic arc to the east, formed by the east–dipping subduction of a "normal" thickness, Caribbean oceanic plate under South America (Mora et al., 2017a). Magmatism affected both continental and accreted oceanic crust (the Quebradagrande Terrane or a younger, allochthonous intra–oceanic arc) and supplied abundant mafic and felsic, volcaniclastic material to the proximal parts of the basin. Abundant outcrop and the very few available well data show that sedimentation in the area of the present–day SJFB occurred in a marine shelf in which proximal marine environments occurred in the central area (San Jacinto) while deeper marine environments occurred in the south.

The absence of lower Paleocene deposits in northwestern Colombia (planktonic zones P.0 to P.2., 65 to 61 Ma) and the unconformity that has been reported in outcrops between Sequence 1 (Cansona) and Sequence 2 (San Cayetano) are the expression of a regional shortening event which took place in latest Cretaceous to early Paleocene times, and which would be related to a collision episode of the Caribbean Plateau. The abrupt decrease in convergence velocity between 75 and 70 Ma, according to Matthews et al. (2016) could be related to this collision event (Figure 14). After the early Paleocene shortening episode, forearc extension, subsidence, and marine sedimentation resumed. New U–Pb geochronology and Hf isotope geochemistry results (Mora et al., 2017b) suggest that the upper Paleocene – lower Eocene sedimentites of Sequence 2 were mainly sourced from Upper Cretaceous plutons of both oceanic (e.g., Bonga, Mora et al., 2017a) and continental affinity (Magangué Arc, Silva–Arias et al., 2016; Antioquian Batholith), and from the Permian – Triassic igneous–metamorphic terranes in the LMV and northern CC (Cochrane et al., 2014; Mora et al., 2017a). Paleo–tectonic reconstructions (Mora et al., 2017b) show that after a considerable (ca. 1077 km) northwestward displacement of the Caribbean oceanic terranes in Late Cretaceous times, such terranes including San Jacinto, had almost reached their current position, thus supporting the previously mentioned provenance considerations. These data also support a forearc basin setting in which both the oceanic and continental affinity, Late Cretaceous to Paleocene magmatic arcs were being eroded and providing sediment for the marine basin to the northwest.

5.2.2. The Lower to Middle Eocene Unconformity and the Onset of Flat Subduction

The prominent lower to middle Eocene angular unconformity that marks the top of Sequence 2 (San Cayetano) is the most im-

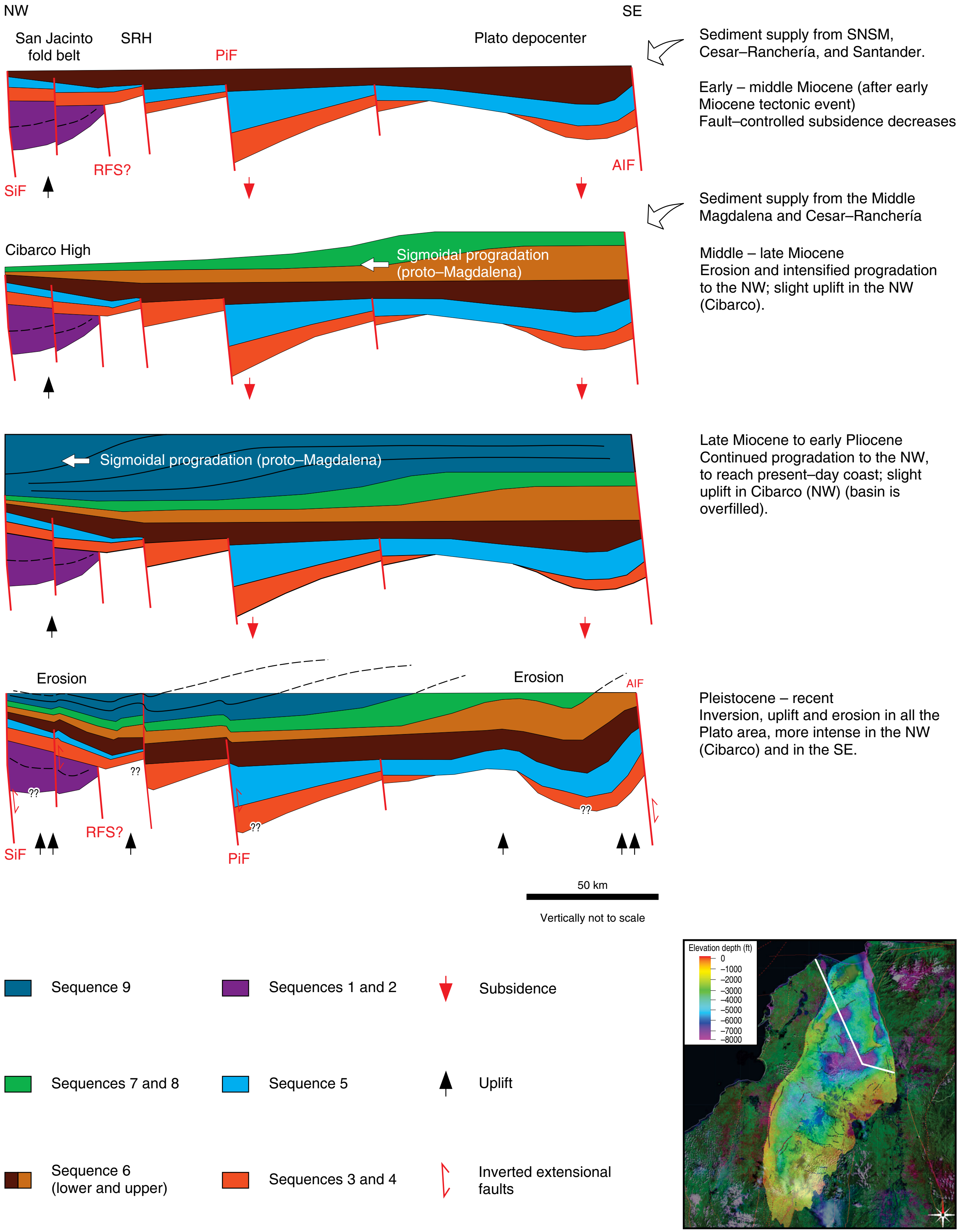
NW
SE
San Jacinto fold belt
SRH
PiF
Plato depocenter
Sediment supply from SNSM, Cesar–Ranchería, and Santander.
Early – middle Miocene (after early Miocene tectonic event)
Fault–controlled subsidence decreases
RFS?
AIF
SiF
Sediment supply from the Middle Magdalena and Cesar–Ranchería
Cibarco High
Sigmoidal progradation (proto–Magdalena)
Middle – late Miocene
Erosion and intensified progradation to the NW; slight uplift in the NW (Cibarco).
Sigmoidal progradation (proto–Magdalena)
Late Miocene to early Pliocene
Continued progradation to the NW, to reach present–day coast; slight uplift in Cibarco (NW) (basin is overfilled).
Erosion
Erosion
AIF
??
??
??
??
Pleistocene – recent
Inversion, uplift and erosion in all the Plato area, more intense in the NW (Cibarco) and in the SE.
SiF
RFS?
PiF
50 km
Vertically not to scale
Sequence 9
Sequences 1 and 2
Subsidence
Sequences 7 and 8
Sequence 5
Uplift
Sequence 6 (lower and upper)
Sequences 3 and 4
Inverted extensional faults
Elevation depth (ft)
0
–1000
–2000
–3000
–4000
–5000
–6000
–7000
–8000

←

Figure 21. Simplified Oligocene to recent evolution of the LMV, shown in a SE–NW–trending regional section. After Eocene to middle Miocene, fault–controlled extension, connection with the Middle Magdalena caused sigmoidal progradation to the NW of Sequences 7 to 9 in the Plato depocenter, until it became overfilled. Pleistocene to recent shortening was responsible for the inversion of previous extensional faults and intense erosion towards the area of the Algarrobo Fault (AlF). Figure vertically not to scale. (SiF) Sinú Fault; (RFS) Romeral Fault System; (SRH) Santa Rita High; (PiF) Pivijay Fault; (AlF) Algarrobo (Arjona) Fault; (SNSM) Sierra Nevada de Santa Marta; (AF) Algarrobo Fault.

portant evidence of the final episode of activity of the Romeral Fault System and of a major shortening event in northern Colombia. Seismic data shows that this event also marks the end and fossilization of the San Jacinto Forearc Basin and the birth of a new basin of middle Eocene to recent age (Lower Magdalena, Mora et al., 2017b). Taking into account the present–day lithospheric and mantle geometry, as interpreted in Figure 11, the onset of subduction of the Caribbean Plate occurred in early to middle Eocene times, 56 to 43 Ma ago (Table 1; Mora et al., 2017b). Interestingly, this calculated time of onset of subduction of the Caribbean Plateau coincides with the time of plate tectonic readjustment between the Caribbean and the Americas (Figure 14), with the estimated age of the lower to middle Eocene unconformity in the San Jacinto fold belt (planktonic foram zones P.9 to P.10, 50.4 to 45.8 Ma) and with the time of cessation of magmatism in northern Colombia (50–45 Ma; Bayona et al., 2012). Therefore, it appears that a major early to middle Eocene plate–tectonic readjustment, consisting of an abrupt decrease in both convergence velocity and obliquity in early to middle Eocene times, seems to be the most likely cause of: (i) the onset of flat–slab subduction in northwestern Colombia, (ii) the cessation of magmatism in northern Colombia in the middle Eocene, (iii) a major shortening event with the exhumation and partial erosion of the Late Cretaceous to early Eocene San Jacinto Forearc Basin, (iv) the end of the tectonic activity of major Cretaceous fault systems such as Romeral and Palestina, and (v) the later onset of right–lateral strike–slip displacement along the newly formed Oca–El Pilar Fault System (Boschman et al., 2014; Müller et al., 1999; Pindell & Kennan, 2009).

The imprint of such tectonic readjustment in the stratigraphic record of the San Jacinto fold belt is the lower to middle Eocene unconformity, though the upper Eocene unconformity could also be related. These unconformities could also be the result of the early to middle Eocene, collision episode of the Great Arc of the Caribbean with South America, which caused a subduction polarity reversal (Escalona & Mann, 2011; Kroehler et al., 2011), as seen in other areas of active, arc–continent collision. According to this interpretation, the previously described events would be collisional effects.

After the early to middle Eocene plate tectonic readjustment (or collision with polarity reversal, according to Kroehler et al., 2011) and the onset of flat subduction, the San Jacinto area experienced renewed forearc extension, subsidence, and sedimentation which comprised coarse–grained clastics and shallow marine carbonates of Sequences 3 and 4 (Chengue and San Jacinto). U–Pb geochronology and Hf isotope geochemistry results (Mora et al., 2017b) show the same Late Cretaceous and Permian – Triassic peaks as seen in samples from the sequence below (San Cayetano), hence sediment supply was mostly coming from the northern CC and SNSM in the SE and NE respectively. Figure 17c clearly shows that the Caribbean–NW South America convergent margin became relatively stable since Oligocene times, exhibiting low convergence velocities and obliquities. The margin probably evolved from a highly oblique convergent margin, possibly exhibiting subduction erosion (Clift & Vannucchi, 2004) in Late Cretaceous to Eocene times, to a more orthogonal convergent margin, exhibiting subduction accretion since early Miocene times, when the accretionary prism probably started forming.

5.3. Lower Magdalena Valley: A Middle Eocene to Recent Amagmatic Forearc Basin, Formed in a Nearly–Orthogonal, Flat Subduction Tectonic Setting

5.3.1. Formation of the LMV

We consider that the formation of the LMV is related to the cooling of the Cretaceous to early Eocene, intra–continental magmatic arc of NW Colombia, and to the fault–controlled subsidence at the initial subduction stages (Figure 23). Cooling caused the extensional reactivation of the main pre–Oligocene basement features such as the Mojana and Sucre Faults that limit the San Jorge Graben, and the Pivijay, Apure, Pijiño, and other faults of the Plato depocenter. Extensional reactivation of the main pre–Oligocene basement structures was crucial for the tectonic segmentation of the basin and for the formation of its two depocenters (Plato and San Jorge). However, it is also possible that initial subsidence could have been caused by crustal thinning due to possible Cretaceous to Eocene subduction erosion (Clift & Vannucchi, 2004), as suggested by Mora et al. (2017a, 2017b). Tectonic clockwise block rotation caused by Paleogene oblique convergence, and older than previously proposed block rotations (e.g., Montes et al., 2010; Reyes–Harker et al.), could have also influenced the formation of the LMV. Bernal–Olaya et al. (2015c) proposed that the extension in the

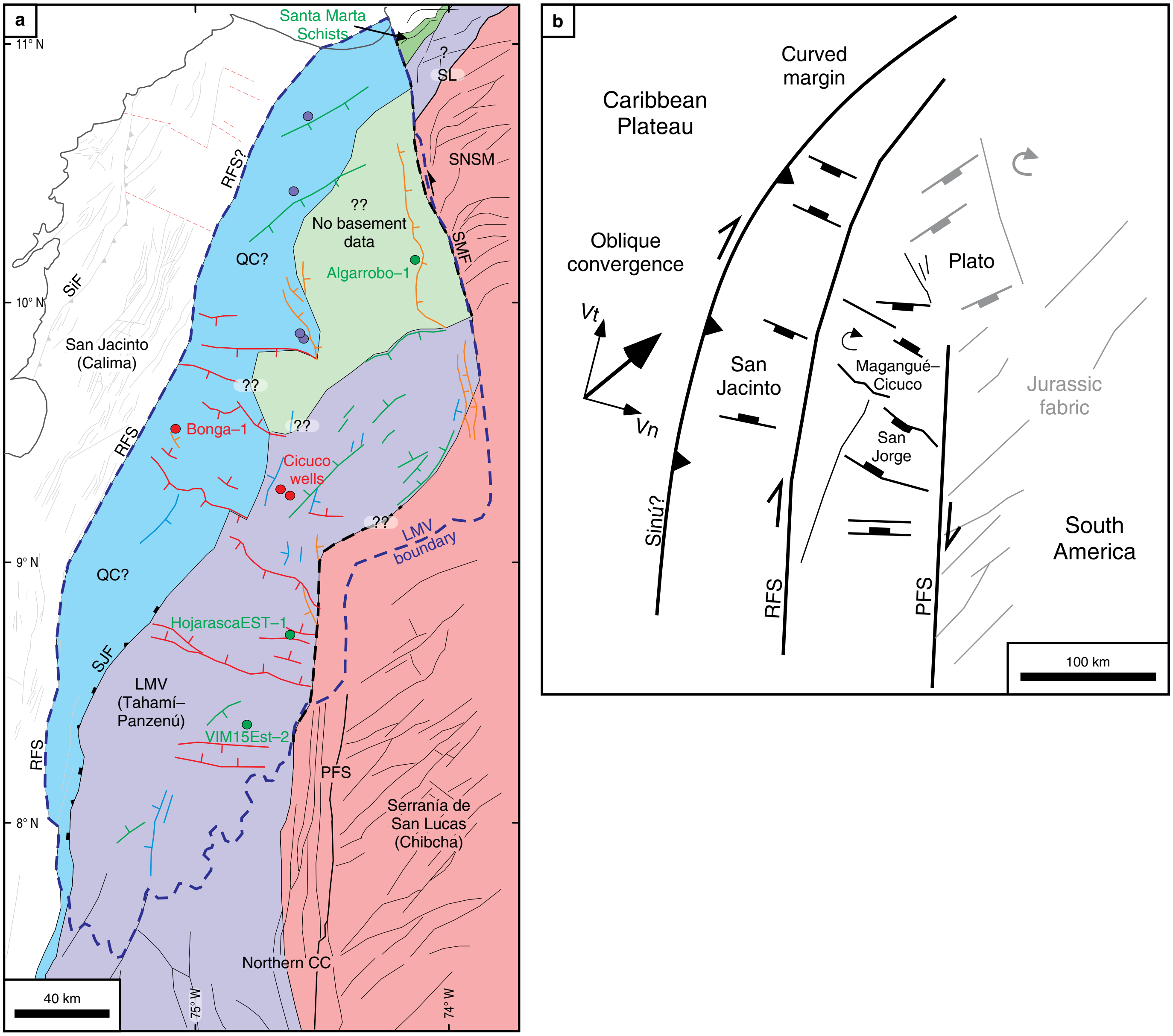

Figure 22. (a) Interpreted basement terranes in the LMV and surrounding massifs (after Mora et al., 2017a). Chibcha Terrane is in pink, Tahamí–Panzenú in lavender, Quebradagrande Complex (QC) in blue, and Calima is white. Upper Cretaceous, low–grade metamorphic terranes in LMV (El Difícil and Algarrobo) and in the northwestern SNSM are colored in green. Correlation of the Tahamí–Panzenú Terrane towards the N (SNSM) is being revised to include new data from Piraquive (2017). Modified from Mora et al. (2017a). **(b)** Sketch illustrating the proposed mechanisms of formation of the basement architecture in the LMV and San Jacinto areas of northernwestern Colombia, which acted during Late Cretaceous to middle Eocene times. Modified from Mora et al. (2017a). (SL) Sevilla Lineament; (RFS) Romeral Fault System; (SNSM) Sierra Nevada de Santa Marta; (SiF) Sinú Fault; (SMF) Santa Marta Fault; (LMV) Lower Magdalena Valley; (SJF) San Jerónimo Fault; (PFS) Palestina Fault System; (CC) Central Cordillera; (Vt) displacement vector component parallel to the margin; (Vn) displacement vector component normal to the plate margin.

LMV and formation of the two depocenters was related to the curvature of the margin. This could also be valid considering the oblique convergence model presented in Figure 22b, displaying a curved margin.

Recent estimates of extension in the LMV (Table 2; Mora et al., 2018) show that the basin has been moderately extended (stretching factor from 1.1 to 1.5), except for local areas where the crust has been considerably thinned (western San Jorge depocenter and northern LMV). The LMV thus appears to have a relatively thin crust, with thicknesses varying from 18 to 28 km, whereas a thicker crust would occur in the central SJFB (30–34 km; Figure 19d). A relatively thin crust could be related to the location of the LMV close to the plate margin, and/or to the proposed pre–Oligocene subduction erosion (Mora et al.,

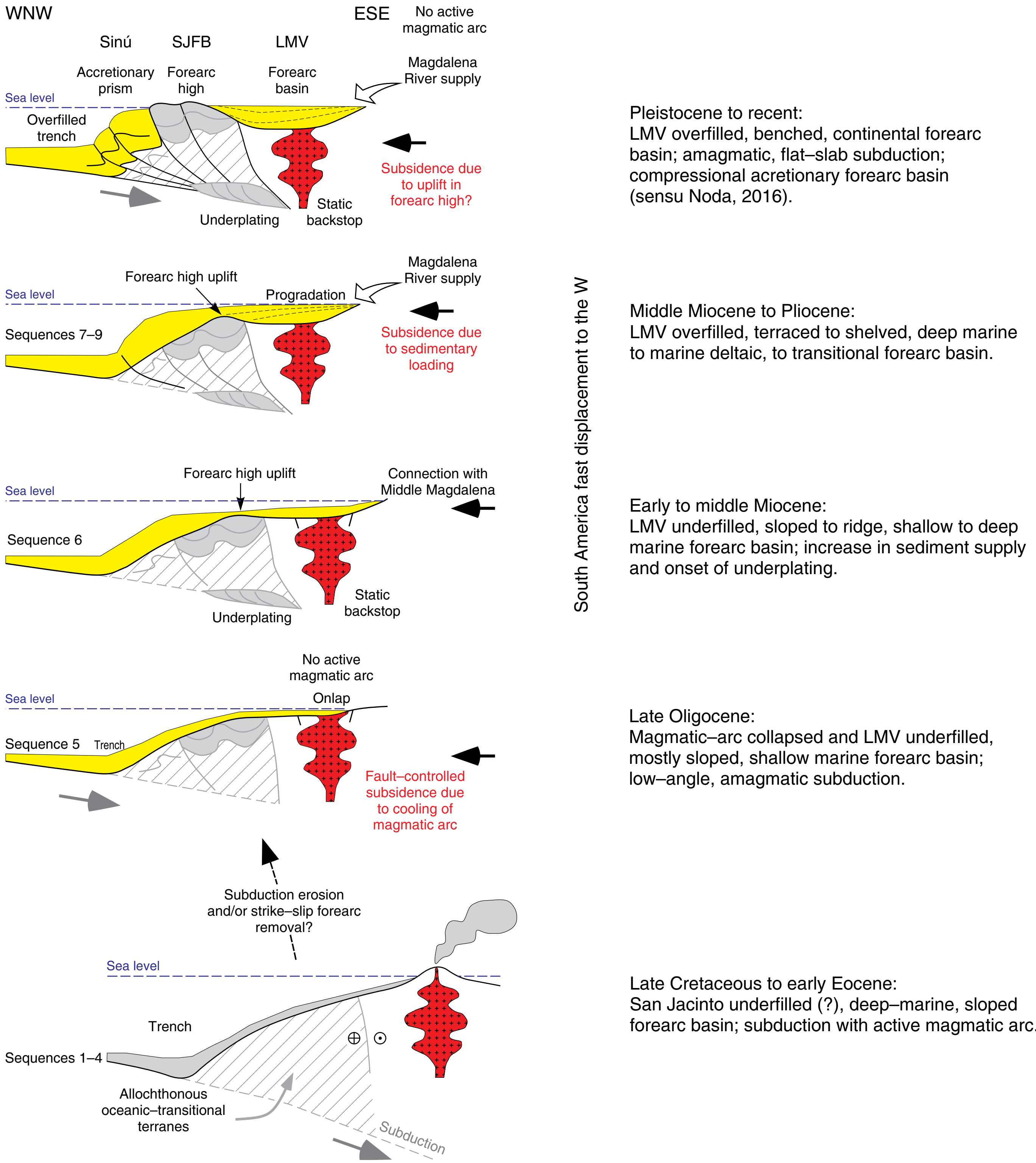

Figure 23. Interpreted cross section evolution of the morphology of the Lower Magdalena Valley (LMV) and San Jacinto fold belt (SJFB), from an Upper Cretaceous to Eocene underfilled, sloped forearc basin (sensu Dickinson, 1995) with an active magmatic arc, to the current amagmatic and overfilled, benched continental forearc basin. Increased Miocene sediment flux, the inherited basement structure, and flat–slab subduction were the main controls on Oligocene to recent forearc basin evolution.

2017b). Such thinned crust would have made easier an extensional reactivation of pre–existing features.

5.3.2. Oligocene to Recent Forearc Evolution

Eocene deposits are mostly preserved in the SJFB, though they could also be preserved at great depths in the footwall of extensional faults in the LMV. According to paleo–tectonic reconstructions (Boschman et al., 2014; Müller et al., 1999; Pindell & Kennan, 2009) and to reconstructions using the GPlates software (Figure 13; Figures 1 and 2 of the Supplementary Information), the last 30 Ma were characterized by low convergence obliquities and relatively low velocities, which do not appear to show abrupt changes in their trend (Figure 17c), making difficult clear correlations with reported tectonic events such as subsidence or uplift pulses. In spite of the relative stability of the Oligocene to recent convergence between the Caribbean Plate and NW South America, the analyses carried out by Mora et al. (2018) indicate that after the early Miocene tectonic event, there was an increase in subsidence and sedimentation in the LMV, possibly related to the formation of the Magdalena fluvial system, when the eastern LMV was connected to the Middle Magdalena Valley (Anderson et al., 2016; Hoorn et al., 2010; Reyes–Harker et al., 2015).

Second–order processes such as flat–slab subduction of a buoyant oceanic plateau substantially modify the tectonic configuration of the upper plate and produce modified forearc basins (Ridgway et al., 2012). This could be the case of the LMV, which according to Mora et al. (2017b), was formed during low–angle subduction of the Caribbean oceanic plateau beneath South America. Fault–controlled subsidence took place in the LMV from Oligocene to middle Miocene times (29–13 Ma), spanning for 16 my, and then it was replaced by non–fault related subsidence (Mora et al., 2018). However, in the SW (San Jorge depocenter, Bonga and Esmeralda wells), there is an increase in tectonic subsidence after 3 Ma, related to the deposition of Sequence 10.

A dramatic increase in sedimentation at ca. 17 Ma, after an lower Miocene regional unconformity, would have influenced the change of fault–controlled subsidence to non–fault related subsidence, implying that sedimentary loading became the main subsidence mechanism since late Miocene times. A relatively thin and not very strong crust in the LMV would have made easier for sedimentary loading to become the main subsidence mechanism since middle Miocene times. The increased sediment supply also strongly influenced the plate interface, by lubricating the subduction channel, thus affecting the transmission of stresses to the upper plate and producing underplating. Crustal thickening by tectonic underplating of subducted materials has been proposed as a cause of uplift in forearc coastal terranes such as the Chile Forearc (e.g., Clift & Hartley, 2007; Glodny et al., 2005), the Aleutians (Moore et al., 1991), the Hikurangi margin (Scherwath et al., 2010), and the Cascadia subduction zone (Calvert et al., 2011). In the Aleutians (Moore et al., 1991), layered reflectors beneath the Kodiak accretionary complex were interpreted as the result of underplating and may represent an antiformal stack of thrust sheets, such as those interpreted by Mora et al. (2017a, their Figure S1), based on deep seismic imaging. Therefore, uplift in the forearc high in the SJFB as seen in the western LMV and current San Jacinto fold belt, may be related to tectonic underplating. The occurrence of a deformed outer high to the W (San Jacinto fold belt) and an undeformed forearc basin behind it, to the E (LMV), is explained if the continental basement beneath the LMV acted as a static backstop, with geologically reasonable contrasts in mechanical properties compared to the sediments just trenchward of it (Byrne et al., 1993; Mantilla–Pimiento et al., 2009).

5.3.3. A Comment about the Connection of Panamá with the LMV

Based on a few U–Pb detrital zircon geochronology analyses in localized wells in the LMV, Montes et al. (2015) proposed a mixed provenance for middle Miocene strata including material derived from the old northwestern South American orogens and from the Panamá Arc. For such proposal they suggest the existence of fluvial channels flowing from the Panamá Arc in the SW to the NE, along more than 300 km, to reach areas such as the Apure High in the Plato depocenter (BH3 in Montes et al., 2015). Our regional study, which includes thousands of kilometers of reflection–seismic data, hundreds of boreholes and outcrop data, does not support such interpretation: while seismic data allowed the mapping of the stratigraphic features (e.g., clinoforms) clearly prograding to the WNW in early Miocene to Pliocene times (Mora et al. 2018), data from hundreds of wells indicate that middle to upper Miocene units (Sequences 6 to 8) consist of fine–grained, distal deltaic, shelf and even turbiditic deposits and that unambiguous fluvial facies only appear in Sequences 9 and 10, after 7 Ma (late Miocene to Pliocene). Furthermore, the middle Miocene to recent forearc highs in the area of the present–day SJFB, proposed by Bernal–Olaya et al. (2015c) and Mora et al. (2018), would have acted as a barrier, making very difficult a sedimentary connection with the distant Panamá Arc in the SW. Such results show that the northern LMV was clearly not sourced from the Panamá Arc in Miocene times. We thus consider that geochronological analyses must be taken with extreme caution; they must be integrated with other types of methods and all the data together must be interpreted within a robust regional tectono–stratigraphic framework. In addition, researchers dealing with mixed provenance results should always propose several possible interpretations instead of assuming a single, unique interpretation.

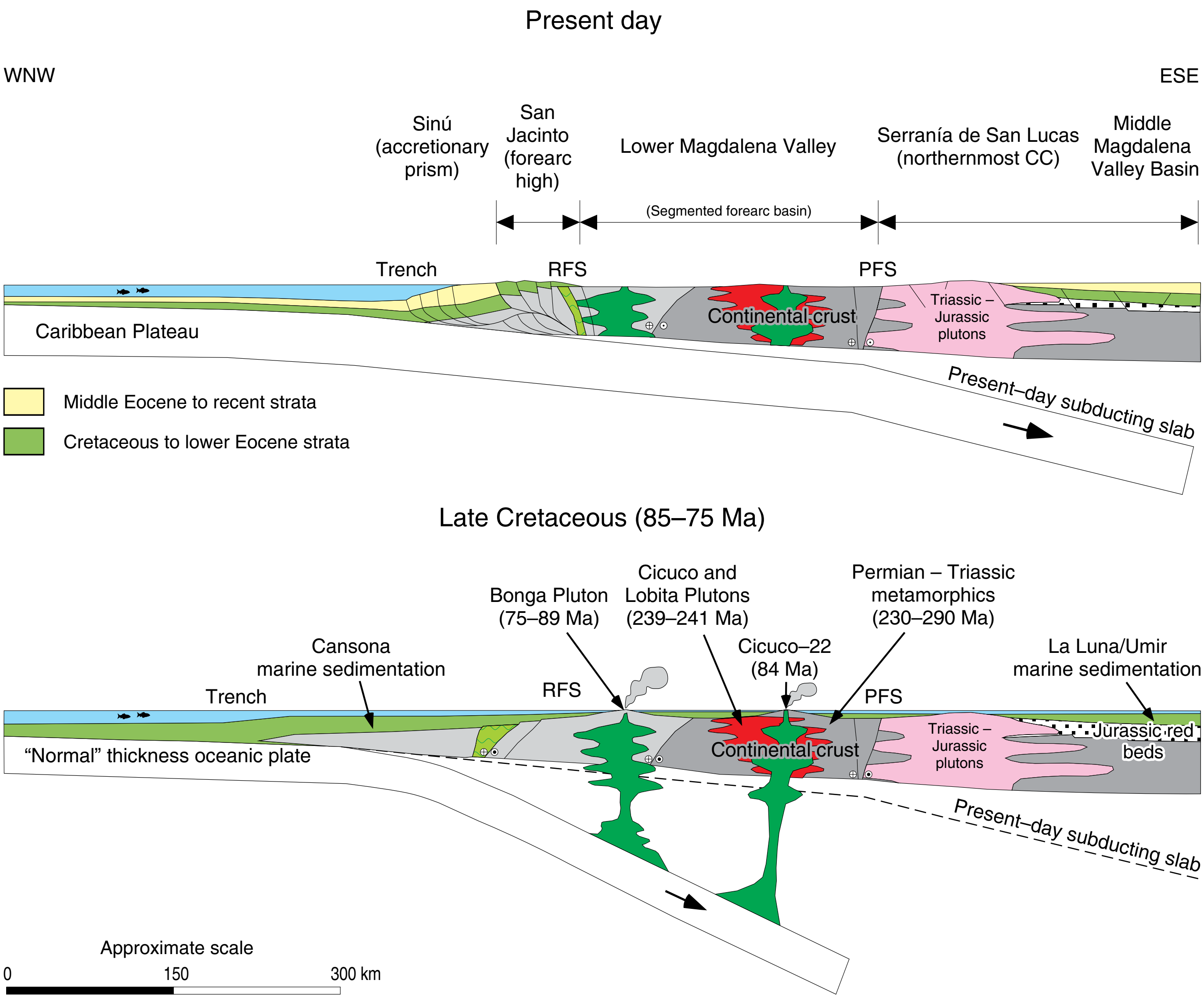

Figure 24. In the lower part we show a hypothetical cross section with the interpreted geodynamic setting at the Magangué–Cicuco High, in Late Cretaceous times (modified from Mora et al., 2017a). In the upper part, the interpreted present–day geodynamic and basin configuration of the Lower Magdalena Valley (LMV) and San Jacinto fold belt (SJFB). Though the present–day trench shown in the figure appears to be located farther to the east than the Cretaceous trench, it should really be located farther to the west in a mantle reference frame, considering that plate tectonic processes between the Caribbean and the Americas have been driven by relatively fast, westward motion of North and South America (Müller et al., 1999). In Late Cretaceous times, subduction was probably of a "normal" thickness plate while today, an oceanic plateau is being subducted. (RFS) Romeral Fault System; (PFS) Palestina Fault System; (CC) Central Cordillera.

5.3.4. Tectonic Segmentation and Depocenter Evolution in the LMV

Based on the measured thicknesses of the tectono–stratigraphic sequences, the Oligocene to recent depocenter evolution in the LMV was studied, and it was found that there was a depocenter landward migration and shifting from north to south. Landward migration of depocenters is a distinctive feature of compressional accretionary forearc basins (sensu Noda, 2016), whereas the depocenter shifting from north to south indicates tectonic segmentation into differentially subsiding zones. Forearc basin segmentation has also been related to continental forearc basins formed in flat–slab subduction settings (Ridgway et al., 2012), where marked along–strike changes in basin configuration were related to insertion of wide fragments of thick crust. However, our results suggest that the pre–Oligocene basement fabric in the LMV, which is different beneath each depocenter (Figure 7), was the main cause of the tectonic segmentation of the basin, especially after 10 Ma, due to the differential response of each fault family to the stress regime. Uplift pulses in the forearc high could have also influenced depocenter migration.

5.3.5. LMV Subsidence History and Trends

Global studies of basin subsidence history (Xie & Heller, 2009) concluded that subsidence curves from forearc basins, as a group, have a diverse range of shapes, indicating that a variety of factors may contribute to basin subsidence. According to Dickinson (1995), there are four subsidence mechanisms in forearc basins: negative buoyancy of the descending slab, loading by the subduction (accretionary) complex, sediment or volcanic loading, and thermal subsidence of the arc massif. Results obtained by Mora et al. (2018) suggest that in the LMV, fault–controlled subsidence probably due to cooling of a pre–Oligocene arc was more important initially (late Oligocene to middle Miocene), and then it was replaced by sedimentary loading as the main subsidence mechanism in the basin during the late Miocene. An exception would be an increase in tectonic subsidence in the SW at 3 Ma (Figure 17a), probably related to uplift in forearc highs to the west.

Comparison with subsidence curves from other forearc basins in the world shows a fair match (Angevine et al., 1990, inset in Figure 19a). However, as previously noted, the LMV curves show the opposite pattern compared to the passive rift basins considered in the stretching model of McKenzie (1978); therefore, they show that LMV is not suitable for applying the uniform stretching methodology by McKenzie (1978) and that extension using this methodology is overestimated in this basin, as previously shown by Montes et al. (2010) (Table 2). Data from the few wells in the northern SJFB show that the area experienced lower but constant subsidence rates compared to the LMV, and the SJFB curves show a similar trend to other forerarc basins in the world. The high sedimentation rates in the LMV, especially in the Miocene, suggest that there was an important influence of sediment load in the total basin subsidence. Tectonic segmentation of both the LMV and the SJFB is also evident from the subsidence curves (inset in Figure 19a).

5.3.6. Proposed Mechanisms that Controlled LMV Evolution

Among all the mechanisms that control the evolution of forearc basins, Mora et al. (2018) suggest that three mechanisms strongly controlled the evolution of the LMV. Such mechanisms are: sediment flux due to uplift and drainage evolution in hinterland areas, pre–existing basement fabric, and configuration of the subducting plate. The reconstruction of the extension, subsidence, sedimentation, and paleogeographic history suggests that sediment flux in the LMV was the most important mechanism in controlling basin evolution because, (i) it supplied sediment to the trench and as a consequence, triggered underplating and uplift in forearc high areas, (ii) it rapidly filled the basin, providing sedimentary loads which kept the depocenters subsiding, as previous subsidence mechanisms became less effective, and (iii) it defined the type and geometry of the basin. Due to the sediment flux, the LMV evolved from an underfilled, sloped, marine forearc basin to an overfilled, benched, terrestrial forearc basin (sensu Dickinson, 1995, Figure 23). Considering the classification by Noda (2016), the whole margin evolved from an Oligocene extensional non–accretionary type to the present–day compressional accretionary type forearc basin, and such evolution was strongly controlled by changes in sediment flux.

The pre–existing basement fabric underneath the LMV was fundamental for the evolution of this basin and its tectonic segmentation, because the different fault families identified under the two depocenters (Mora et al., 2017a), were probably reactivated in different ways, according to the regional stress fields. Basement fabric and tectonic segmentation also controlled the distribution of sedimentary environments and facies.

Concerning the configuration of the subducting plate, the LMV evolution has also been controlled by the low–angle subduction of an irregular Caribbean oceanic plateau, which would have influenced the along–strike tectonic segmentation and stratigraphic variations observed in the LMV, as observed in other similar basins (Ridgway et al., 2012). The variations in geometry of the subducted Caribbean Plateau under the LMV, described by Mora et al. (2017b) could represent irregularities, such as the Beata Ridge which separates the Colombian Basin from the Venezuelan Basin, at the top of the plateau (Duque–Caro, 1979). Flat–slab subduction would also be responsible for the lack of a magmatic arc in the LMV, a condition that would otherwise have formed a completely different forearc basin.

The results of the studies by Mora et al. (2017a, 2017b, 2018) allow the comparison of the geometry and configuration of the convergent margin of NW Colombia in Late Cretaceous times with the present–day geometry (Figure 24). The LMV basement and the SJFB where formed in a Late Cretaceous "normal" subduction margin, due to oblique convergence of the Caribbean relative to South America, with active dextral strike–slip displacement and possible subduction erosion. The onset of more orthogonal, low–angle subduction of the oceanic Caribbean Plateau after Eocene times resulted in a major change in the convergent margin, causing the cessation of magmatism and the formation of an accretionary, tectonically segmented forearc basin in the LMV, and forearc highs in the SJFB (Figures 23 and 24). However, it is also possible that if the lower to middle Eocene unconformity is related to the collision of the Caribbean Arc, causing a subduction polarity reversal as proposed by Kroehler et al. (2011). Nevertheless, this is only one of the many issues that remains to be solved and that make necessary that we continue doing research in these basins of NW South America.

6. Conclusions

Using a regional geological and geophysical dataset, the formation and evolution of the Lower Magdalena Valley Basin (LMV) and San Jacinto fold belt (SJFB) of NW Colombia has been illustrated. Detailed interpretations of reflection seismic data and new geochronological analyses revealed that the basement of the LMV is the northward continuation of the basement terranes of the northern Central Cordillera, and that it consists of Permian – Triassic metasedimentary rocks, which were subsequently intruded by Upper Cretaceous granitoids. Structural analyses suggest that the NE–SW trend of basement faults in the northeastern LMV is inherited from a Jurassic rifting event, while the ESE–WNW trend in the western LMV is inherited from a Late Cretaceous to Eocene strike–slip and extension episode. The Upper Cretaceous to lower Eocene sedimentites preserved in the present–day SJFB were deposited in a forearc marine basin formed by the oblique convergence between the Caribbean Plateau and the South American Plate, with a related intracontinental magmatic arc. A lower to middle Eocene angular unconformity at the top of the San Cayetano Sequence, the termination of the activity of the Romeral Fault System and the cessation of arc magmatism are interpreted to indicate the onset of low–angle orthogonal subduction of the Caribbean Plateau beneath South America, which occurred between 56 and 43 Ma. Flat subduction of the plateau has continued to the present and would be the main cause of amagmatic post–Eocene deposition and formation of the LMV. After the collapse of a pre–Oligocene magmatic arc, late Oligocene to early Miocene fault–controlled subsidence allowed initial infill of the LMV. Extensional reactivation of inherited, pre–Oligocene basement faults allowed tectonic segmentation and the formation of the two basin depocenters (Plato and San Jorge). Oligocene to early Miocene uplift of Andean terranes made possible the connection of the Lower and Middle Magdalena Valleys, and the formation of the most important Colombian drainage system (Magdalena River system). The proto–Magdalena River in the north and the proto–Cauca River in the south both started delivering enormous amounts of sediment in middle Miocene times, as fault controlled subsidence was gradually replaced by non–fault related subsidence, due to increased sedimentary load. Such dramatic increase in sedimentation delivered huge amounts of sediments to the trench, causing the formation of an accretionary prism farther west of San Jacinto. This probably weakened the plate interface and caused underplating, with the development of forearc highs in the San Jacinto area. A stronger backstop under the Lower Magdalena would explain shortening in the forearc high and accretionary wedge areas to the W, while the Lower Magdalena remained essentially unaffected. Our results highlight the fundamental role of plate kinematics, inherited basement structure, and sediment flux on the evolution of forearc basins such as San Jacinto and the Lower Magdalena.

Acknowledgments

This work is part of the PhD thesis by Josué Alejandro MORA–BOHÓRQUEZ at the Freie Universität Berlin and at the German Research Centre for Geosciences (GFZ) in Potsdam, Germany. This research was entirely supported by Hocol S.A. Josué Alejandro MORA–BOHÓRQUEZ thanks Hocol S.A. for permission to publish this study and all the exploration staff for fruitful discussions and suggestions. Elsa JAIMES, Exploration Vicepresident of Hocol S.A., is acknowledged for permission to present this research, for supporting this project, and for providing the time to prepare it. We also thank Jorge GÓMEZ TAPIAS and the Servicio Geológico Colombiano for inviting us to participate in this important project and for all their help during the manuscript preparation. We are also grateful to Hernán CARVAJAL and Jaime LÓPEZ (Hocol S.A.) for their help in preparing most of the figures. We thank reviewers Mauricio PARRA and Paul MANN whose comments greatly improved the quality of this manuscript.

References

Allen, P.A. & Allen, J.R. 2005. Basin analysis: Principles and applications, 2nd edition. Blackwell Publishing Ltd., 549 p. Singapore.

Altamira, A. & Burke, K. 2015. The Ribbon continent of South America in Ecuador, Colombia, and Venezuela. In: Bartolini, C. & Mann, P. (editors), Petroleum geology and potential of the Colombian Caribbean margin. American Association of Petroleum Geologists, Memoir 108, p. 39–84. https://doi.org/10.1306/13531931M108846

Anderson, V.J., Horton, B.K., Saylor, J.E., Mora, A., Tesón, E., Breecker, D.O. & Ketcham, R.A. 2016. Andean topographic growth and basement uplift in southern Colombia: Implications for the evolution of the Magdalena, Orinoco, and Amazon River systems. Geosphere, 12(4): 1235–1256. https://doi.org/10.1130/GES01294.1

Angevine, C.L., Heller, P.L. & Paola, C. 1990. Quantitative sedimentary basin modeling. American Association of Petroleum Geologists Continuing Education Course, Note Series 32, 133 p.

Assumpção, M., Bianchi, M., Julia, J., Dias, F., Sand Franca, G., Nascimento, R., Drouet, S., Garcia Pavão, C., Farrapo, D. & Lopes, A. 2013. Crustal Thickness map of Brazil: Data compilation and main features. Journal of South American Earth Sciences, 43: 74–85. http://dx.doi.org/10.1016/j.jsames.2012.12.009

Barrero, D., Álvarez, J. & Kassem, T. 1969. Actividad ígnea y tectónica en la cordillera Central durante el Meso–Cenozoico. Boletín Geológico, 17(1–3): 145–173.

Bayona, G., Montes, C., Cardona, A., Jaramillo, C.A., Ojeda, G., Valencia, V. & Ayala–Calvo, C. 2011. Intraplate subsidence and basin filling adjacent to an oceanic arc–continent collision: A case from the southern Caribbean–South America plate margin. Basin Research, 23(4): 403–422. https://doi.org/10.1111/j.1365-2117.2010.00495.x

Bayona, G., Cardona, A., Jaramillo, C., Mora, A., Montes, C., Valencia, V., Ayala, C., Montenegro, O. & Ibañez–Mejia, M. 2012. Early Paleogene magmatism in the northern Andes: Insights on the effects of oceanic plateau–continent convergence. Earth and Planetary Science Letters, 331–332: 97–111. https://doi.org/10.1016/j.epsl.2012.03.015

Berggren, W.A., Kent, D.V., Swisher III, C.C. & Aubry, M.P. 1995. A revised Cenozoic geochronology and chronostratigraphy. In: Berggren, W.A., Kent, D.V., Swisher III, C.C., Aubry, M.P. & Hardenbol, J. (editors), Geochronology, Time Scales and Global Stratigraphic Correlation. Society of Economic Paleontologists and Mineralogists, Special Publication 54, p. 129–212. https://doi.org/10.2110/pec.95.04.0129

Bernal–Olaya, R., Mann, P. & Vargas, C.A. 2015a. Earthquake, tomographic, seismic reflection, and gravity evidence for a shallowly dipping subduction zone beneath the Caribbean margin of northwestern Colombia. In: Bartolini, C. & Mann, P. (editors), Petroleum geology and potential of the Colombian Caribbean margin. American Association of Petroleum Geologists, Memoir 108, p. 247–269. https://doi.org/10.1306/13531939M1083642

Bernal–Olaya, R., Sánchez, J., Mann, P. & Murphy, M. 2015b. Along–strike crustal thickness variations of the subducting Caribbean Plate produces two distinctive styles of thrusting in the offshore South Caribbean deformed belt, Colombia. In: Bartolini, C. & Mann, P. (editors), Petroleum geology and potential of the Colombian Caribbean margin. American Association of Petroleum Geologists, Memoir 108, p. 295–322. https://doi.org/10.1306/13531941M1083645

Bernal–Olaya, R., Mann, P. & Escalona, A. 2015c. Cenozoic tectonostratigraphic evolution of the Lower Magdalena Basin, Colombia: An example of an under– to overfilled forearc basin. In: Bartolini, C. & Mann, P. (editors), Petroleum geology and potential of the Colombian Caribbean margin. American Association of Petroleum Geologists, Memoir 108, p. 345–397. https://doi.org/10.1306/13531943M1083645

Bezada, M., Magnani, M., Zelt, C., Schmitz, M. & Levander, A. 2010a. The Caribbean–South American plate boundary at 65°W: Results from wide–angle seismic data. Journal of Geophysical Research: Solid Earth, 115(B08): 1–17.

Bezada, M.J., Levander, A. & Schmandt, B. 2010b. Subduction in the southern Caribbean: Images from finite–frequency P wave tomography. Journal of Geophysical Research: Solid Earth, 115(B12): 1–19. https://doi.org/10.1029/2010JB007682

Blow, W.H. 1969. Late middle Eocene to recent planktonic foraminiferal biostratigraphy. In: Bronnimann, P. & Renz, H.H. (editors), Proceedings of the First International Conference on Planktonic Microfossils, 1, p. 199–422. Geneva, Switzerland.

Boschman, L.M., van Hinsbergen, D.J.J., Torsvik, T.H., Spakman, W. & Pindell, J.L. 2014. Kinematic reconstruction of the Caribbean region since the Early Jurassic. Earth–Science Reviews, 138: 102–136. https://doi.org/10.1016/j.earscirev.2014.08.007

Boyden, J.A., Müller, R.D., Gurnis, M., Torsvik, T.H., Clark, J.A., Turner, M., Ivey–Law, H., Watson, R.J. & Cannon, J.S. 2011. Next–generation plate–tectonic reconstructions using GPlates. In: Keller, R. & Baru, C. (editors), Geoinformatics: Cyberinfrastructure for the solid earth sciences. Cambridge University Press, p. 95–114. https://doi.org/10.1017/CBO9780511976308.008

Burke, K. 1988. Tectonic evolution of the Caribbean. Annual Review of Earth and Planetary Sciences, 16: 201–230. https://doi.org/10.1146/annurev.ea.16.050188.001221

Byrne, D.E., Wang, W.H. & Davis, D.M. 1993. Mechanical role of backstops in the growth of forearcs. Tectonics, 12(1): 123–144. https://doi.org/10.1029/92TC00618

Caballero, V., Mora, A., Quintero, I., Blanco, V., Parra, M., Rojas, L.E., López, C., Sánchez, N., Horton, B.K., Stockli, D. & Duddy, I. 2013. Tectonic controls on sedimentation in an intermontane hinterland basin adjacent to inversion structures: The Nuevo Mundo Syncline, Middle Magdalena Valley, Colombia. In: Nemčok, M., Mora, A. & Cosgrove, J.W. (editors), Thick–skin–dominated orogens: From initial inversion to full accretion. Geological Society of London, Special Publication 377, p. 315–342. https://doi.org/10.1144/SP377.12

Calvert, A.J., Preston, L.A. & Farahbod, A.M. 2011. Sedimentary underplating at the Cascadia mantle–wedge corner revealed by seismic imaging. Nature Geoscience, 4: 545–548. https://doi.org/10.1038/ngeo1195

Cardona, A., Montes, C., Ayala, C., Bustamante, C., Hoyos, N., Montenegro, O., Ojeda, C., Niño, H., Ramírez, V., Valencia, V., Rincón, D., Vervoort, J. & Zapata, S. 2012. From arc–continent collision to continuous convergence, clues from Paleogene conglomerates along the southern Caribbean–South America plate boundary. Tectonophysics, 580: 58–87. https://doi.org/10.1016/j.tecto.2012.08.039

Case, J.E. & MacDonald, W.D. 1973. Regional gravity anomalies and crustal structure in northern Colombia. Geological Society of America Bulletin, 84(9): 2905–2916. https://doi.org/10.1130/0016-7606(1973)84<2905:RGAACS>2.0.CO;2

Catuneanu, O., Abreu, V., Bhattacharya, J.P., Blum, M.D., Dalrymple, R.W., Eriksson, P.G., Fielding, C.R., Fisher, W.L., Galloway, W.E., Gibling, M.R., Giles, K.A., Holbrook, J.M., Jordan, R., Kendall, C.G.St.C., Macurda, B., Martinsen, O.J., Miall, A.D., Neal, J.E., Nummedal, D., Pomar, L., Posamentier, H.W., Pratt, B.R., Sarg, J.F., Shanley, K.W., Steel, R.J., Strasser, A., Tucker, M.E. & Winker, C. 2009. Towards the standardization of sequence stratigraphy. Earth–Science Reviews, 92(1–2): 1–33. https://doi.org/10.1016/j.earscirev.2008.10.003

Cediel, F., Shaw, R.P. & Cáceres, C. 2003. Tectonic assembly of the northern Andean block. In: Bartolini, C., Buffler, R.T. & Blickwede, J. (editors), The circum–Gulf of Mexico and the Caribbean: Hydrocarbon habitats, basin formation, and plate tectonics. American Association of Petroleum Geologists, Memoir 79, p. 815–848. Tulsa, USA.

Cerón, J.F., Kellogg, J.N. & Ojeda, G.Y. 2007. Basement configuration of the northwestern South America–Caribbean margin from recent geophysical data. Ciencia, Tecnología y Futuro, 3(3): 25–49.

Chulick, G., Detweiler, Sh. & Mooney, W. 2013. Seismic structure of the crust and uppermost mantle of South America and surrounding oceanic basins. Journal of South American Earth Sciences, 42: 260–276. http://dx.doi.org/10.1016/j.jsames.2012.06.002

Clift, P.D. & Hartley, A.J. 2007. Slow rates of subduction erosion and coastal underplating along the Andean margin of Chile and Perú. Geology, 35(6): 503–506. https://doi.org/10.1130/G23584A.1

Clift, P. & Vannucchi, P. 2004. Controls on tectonic accretion versus erosion in subduction zones: Implications for the origin and recycling of the continental crust. Reviews of Geophysics, 42(2), p. 1–31. https://doi.org/10.1029/2003RG000127

Cochrane, R., Spikings, R., Gerdes, A., Ulianov, A., Mora, A., Villagómez, D., Putlitz, B. & Chiaradia, M. 2014. Permo–Triassic anatexis, continental rifting and the disassembly of western Pangaea. Lithos, 190–191: 383–402. https://doi.org/10.1016/j.lithos.2013.12.020

De la Parra, F., Mora, A., Rueda, M. & Quintero, I. 2015. Temporal and spatial distribution of tectonic events as deduced from reworked palynomorphs in the eastern northern Andes. American Association of Petroleum Geologists Bulletin, 99(8): 1455–1472. https://doi.org/10.1306/02241511153

Dhuime, B., Hawkesworth, C. & Cawood, P. 2011. When continents formed. Science, 331(6014): 154–155. https://doi.org/10.1126/science.1201245

Dickinson, W. 1995. Forearc basins. In: Busby, C.J. & Ingersoll, R.V. (editors), Tectonics of sedimentary basins. Blackwell Science, p. 221–261. Cambridge, USA.

Dickinson, W.R. & Gehrels, G.E. 2009. Use of U–Pb ages of detrital zircons to infer maximum depositional ages of strata: A test against a Colorado Plateau Mesozoic database. Earth and Planetary Science Letters, 288(1–2): 115–125. https://doi.org/10.1016/j.epsl.2009.09.013

Duque–Caro, H. 1979. Major structural elements and evolution of northwestern Colombia. In: Watkins, J.S., Montadert, L. & Wood–Dickerson, P. (editors), Geological and geophysical investigations of continental margins. American Association of Petroleum Geologists, Memoir 29, p. 329–351. Tulsa, USA.

Duque–Caro, H. 1984. Structural style, diapirism, and accretionary episodes of the Sinú–San Jacinto Terrane, southwestern Caribbean borderland. In: Bonini, W.E., Hargraves, R.B. & Shagam, R. (editors), The Caribbean–South American plate boundary and regional tectonics. Geological Society of America, Memoir 162, p. 303–316. https://doi.org/10.1130/MEM162-p303

Duque–Caro, H. 1991. Contributions to the geology of the Pacific and the Caribbean coastal areas of northwestern Colombia and South America. Doctoral thesis, Princeton University, 132 p. Princeton, USA.

Duque–Caro, H. 2000. Análisis bioestratigráficos de 400 muestras de 34 pozos y 16 muestras de superficie de las cuencas de San Jorge, Sinú, Plato y Barranquilla en el Valle Inferior del Magdalena. Ecopetrol, unpublished report, 403 p. Bogotá.

Duque–Caro, H. 2001. Análisis bioestratigráficos de 250 muestras de 5 pozos de las cuencas de San Jorge, Sinú, Plato y Barranquilla en el Valle Inferior del Magdalena. Ecopetrol, unpublished report, 293 p. Bogotá.

Duque–Caro, H. 2010. Análisis microestratigráficos de 36 muestras del pozo Saman Norte–1. Hocol, unpublished report, 4 p. Bogotá.

Duque–Caro, H. 2014. Microstratigraphic analyses of 39 samples from the Well Calipso–1, Barranquilla Province. Hocol, unpublished report, 47 p. Bogotá.

Duque–Caro, H., Guzmán–Ospitia, G. & Hernández, R. 1996. Memoria explicativa: Mapa geológico de la plancha 38 Carmen de Bolívar. Scale 1:100 000. Ingeominas, 83 p. Bogotá.

Escalona, A. & Mann, P. 2011. Tectonics, basin subsidence mechanisms, and paleogeography of the Caribbean–South American plate boundary zone. Marine and Petroleum Geology, 28(1): 8–39. https://doi.org/10.1016/j.marpetgeo.2010.01.016

Etayo–Serna, F., Barrero, D., Lozano, H., Espinosa, A., González, H., Orrego, A., Ballesteros, I., Forero, H., Ramírez, C., Zambrano–Ortiz, F., Duque–Caro, H., Vargas, R., Núñez, A., Álvarez, J., Ropaín, C., Cardozo, E., Galvis, N., Sarmiento, L., Alberts, J.P., Case, J.E., Singer, D.A., Bowen, R.W., Berger, B.R., Cox, D.P. & Hodges, C.A. 1983. Mapa de terrenos geológicos de Colombia. Publicaciones Geológicas Especiales del Ingeominas, 14 (I), 235 p. Bogotá.

Flinch, J.F. 2003. Structural evolution of the Sinu–Lower Magdalena area (northern Colombia). In: Bartolini, C., Buffler, R.T. & Blickwede, J. (editors), The circum–Gulf of Mexico and the Caribbean: Hydrocarbon habitats, basin formation, and plate tectonics. American Association of Petroleum Geologists, Memoir 79, p. 776–796.

Glodny, J., Lohrmann, J., Echtler, H., Gräfe, K., Seifert, W., Collao, S. & Figueroa, O. 2005. Internal dynamics of a paleoaccretionary wedge: Insights from combined isotope tectonochronology and sandbox modelling of the South–Central Chilean forearc. Earth and Planetary Science Letters, 231(1–2): 23–39. https://doi.org/10.1016/j.epsl.2004.12.014

Gómez, E., Jordan, T.E., Allmendinger, R.W., Hegarty, K. & Kelley, S. 2005. Syntectonic Cenozoic sedimentation in the northern Middle Magdalena Valley Basin of Colombia and implications for exhumation of the northern Andes. Geological Society of America Bulletin, 117(5–6): 547–569. https://doi.org/10.1130/B25454.1

Gómez, J., Nivia, Á., Montes, N.E., Tejada, M.L., Jiménez, D.M., Sepúlveda, M.J., Osorio, J.A., Gaona, T., Diederix, H., Uribe,

H. & Mora, M., compilers. 2007. Geological Map of Colombia 2007. Scale 1:1 000 000. Ingeominas, 2 sheets. Bogotá.

Gómez, J., Montes, N.E., Nivia, Á. & Diederix, H., compilers. 2015. Geological Map of Colombia 2015. Scale 1:1 000 000. Servicio Geológico Colombiano, 2 sheets. Bogotá. https://doi.org/10.32685/10.143.2015.936

Govers, R. & Wortel, M.J.R. 2005. Lithosphere tearing at STEP faults: Response to edges of subduction zones. Earth and Planetary Science Letters, 236(1–2): 505–523. https://doi.org/10.1016/j.epsl.2005.03.022

Guzmán, G. 2007. Stratigraphy and sedimentary environment and implications in the Plato Basin and the San Jacinto Belt northwestern Colombia. Doctoral thesis, Université de Liège, 275 p. Liège, Belgium.

Guzmán, G., Gómez–Londoño, E. & Serrano–Suárez, B.E. 2004. Geología de los cinturones del Sinú, San Jacinto y borde occidental del Valle Inferior del Magdalena, Caribe Colombiano. Ingeominas, unpublished report, 134 p. Bogotá.

Haq, B.U., Hardenbol, J. & Vail, P.R. 1987. Chronology of fluctuating sea levels since the Triassic. Science, 235: 1156–1167.

Hocol S.A. 1993. Lower Magdalena Valley technical evaluation agreement. Phase I. Unpublished report, 200 p. Cartagena.

Hoorn, C., Wesselingh, F.P., ter Steege, H., Bermúdez, M.A., Mora, A., Sevink, J., Sanmartin, I., Sánchez–Meseguer, A., Anderson, C.L., Figueiredo, J.P., Jaramillo, C., Riff, D., Negri, F.R., Hooghiemstra, H., Lundberg, J., Stadler, T., Särkinen, T. & Antonelli, A. 2010. Amazonia through time: Andean uplift, climate change, landscape evolution, and biodiversity. Science, 330(6006): 927–931. https://doi.org/10.1126/science.1194585

Ibañez–Mejia, M., Tassinari, C.C.G. & Jaramillo–Mejía, J.M. 2007. U–Pb zircon ages of the "Antioquian Batholith": Geochronological constraints of late Cretaceous magmatism in the central Andes of Colombia. XI Congreso Colombiano de Geología. Memoirs. 11p. Bucaramanga.

Instituto Colombiano del Petróleo. 2000. Evaluación regional integrada cuenca Valle Inferior del Magdalena. Unpublished report, 360 p. Piedecuesta, Colombia.

Kroehler, M.E., Mann, P., Escalona, A. & Christeson, G.L. 2011. Late Cretaceous – Miocene diachronous onset of back thrusting along the South Caribbean deformed belt and its importance for understanding processes of arc collision and crustal growth. Tectonics, 30(6): 31 p. https://doi.org/10.1029/2011TC002918

Levander, A., Bezada, M.J., Niu, F. & Schmitz, M. 2015. The two subduction zones of the southern Caribbean: Lithosphere tearing and continental margin recycling in the east, flat slab subduction and Laramide–style uplifts in the west. American Geophysical Union, Fall Meeting. Abstracts, 1 p. San Francisco, USA.

Lithosphera Ltda. 2010. Interpretación gravimétrica cuantitativa, región Sinú–San Jacinto y Valle Inferior del Magdalena. Unpublished report, 21 p. Bogotá.

Luzieux, L.D.A., Heller, F., Spikings, R., Vallejo, C.F. & Winkler, W. 2006. Origin and Cretaceous tectonic history of the coastal Ecuadorian forearc between 1° N and 3° S: Paleomagnetic, radiometric and fossil evidence. Earth and Planetary Science Letters, 249(3–4): 400–414. https://doi.org/10.1016/j.epsl.2006.07.008

Magnani, M.B., Zelt, C.A., Levander, A. & Schmitz, M. 2009. Crustal structure of the South American–Caribbean plate boundary at 67°W from controlled source seismic data. Journal of Geophysics Research, 114: B02312.

Mantilla–Pimiento, A.M. 2007. Crustal structure of the southwestern Colombian Caribbean margin: Geological interpretation of geophysical data. Doctoral thesis, Friedrich–Schiller–Universität Jena, 98 p. Jena, Germany.

Mantilla–Pimiento, A.M., Jentszsch, G., Kley, J. & Alfonso–Pava, C. 2009. Configuration of the Colombian Caribbean margin: Constraints from 2D seismic reflection data and potential fields interpretation. In: Lallemand, S. & Funiciello, F. (editors), Subduction zone geodynamics. Frontiers in Earth Sciences. Springer, p. 247–272. Berlin, Heidelberg. https://doi.org/10.1007/978-3-540-87974-9_13

Masy, J., Niu, F., Levander, A. & Schmitz, M. 2011. Mantle flow beneath northwestern Venezuela: Seismic evidence for a deep origin of the Mérida Andes. Earth and Planetary Science Letters, 305(3–4): 396–404. https://doi.org/10.1016/j.epsl.2011.03.024

Matthews, K.J., Maloney, K.T., Zahirovic, S., Williams, S.E., Seton, M. & Muller, D. 2016. Global plate boundary evolution and kinematics since the late Paleozoic. Global and Planetary Change, 146: 226–250. https://doi.org/10.1016/j.gloplacha.2016.10.002

McKenzie, D. 1978. Some remarks on the development of sedimentary basins. Earth and Planetary Science Letters, 40(1): 25–32. https://doi.org/10.1016/0012-821X(78)90071-7

Miall, A.D. 2000. Principles of sedimentary basin analysis, 3rd edition. Springer–Verlag, 616 p. Berlin–Heidelberg. https://doi.org/10.1007/978-3-662-03999-1

Montes, C., Guzmán, G., Bayona, G., Cardona, A., Valencia, V. & Jaramillo, C. 2010. Clockwise rotation of the Santa Marta Massif and simultaneous Paleogene to Neogene deformation of the Plato–San Jorge and Cesar–Ranchería Basins. Journal of South American Earth Sciences, 29(4): 832–848. https://doi.org/10.1016/j.jsames.2009.07.010

Montes, C., Cardona, A., Jaramillo, C., Pardo, A., Silva, J.C., Valencia, V., Ayala, C., Pérez–Ángel, L.C., Rodríguez–Parra, L.A., Ramírez, V. & Niño, H. 2015. Middle Miocene closure of the Central American Seaway. Science, 348(6231): 226–229. https://doi.org/10.1126/science.aaa2815

Moore, J.C., Diebold, J., Fisher, M.A., Sample, J., Brocher, T., Talwani, M., Ewing, J., von Huene, R., Rowe, C., Stone, D., Stevens, C. & Sawyer, D. 1991. EDGE deep seismic reflection transect of the eastern Aleutian arc–trench layered lower crust reveals underplating and continental growth. Geology, 19(5): 420–424. https://doi.org/10.1130/0091-7613(1991)019<0420:EDSRTO>2.3.CO;2

Mora, A., De Freitas, M. & Vélez, V. 2013a. Cenozoic tectonostratigraphy of the northern San Jacinto fold belt, northwestern

Colombia. American Association of Petroleum Geologists International Convention and Exhibition. Poster. Cartagena.

Mora, A., Reyes–Harker, A., Rodríguez, G., Tesón, E., Ramírez–Arias, J.C., Parra, M., Caballero, V., Mora, J.P., Quintero, I., Valencia, V., Ibañez–Mejia, M., Horton, B.K. & Stockli, D.F. 2013b. Inversion tectonics under increasing rates of shortening and sedimentation: Cenozoic example from the Eastern Cordillera of Colombia. In: Nemčok, M., Mora, A. & Cosgrove, J.W. (editors), Thick–skin–dominated orogens: From initial inversion to full accretion. Geological Society of London, Special Publication 377, p. 411–442. https://doi.org/10.1144/SP377.6

Mora, A., Parra, M., Rodríguez–Forero, G., Blanco, V., Moreno, N., Caballero, V., Stockli, D., Duddy, I. & Ghorbal, B. 2015. What drives orogenic asymmetry in the northern Andes?: A case study from the apex of the northern Andean orocline. In: Bartolini, C. & Mann, P. (editors), Petroleum geology and potential of the Colombian Caribbean margin. American Association of Petroleum Geologists, Memoir 108, p. 547–586. https://doi.org/10.1306/13531949M1083652

Mora, J.A., Ibañez–Mejia, M., Oncken, O., De Freitas, M., Vélez, V., Mesa, A. & Serna, L. 2017a. Structure and age of the Lower Magdalena Valley Basin basement, northern Colombia: New reflection–seismic and U–Pb–Hf insights into the termination of the central Andes against the Caribbean Basin. Journal of South American Earth Sciences, 74: 1–26. https://doi.org/10.1016/j.jsames.2017.01.001

Mora, J.A., Oncken, O., Le Breton, E., Ibañez–Mejia, M., Faccenna, C., Veloza, G., Vélez, V., De Freitas, M. & Mesa, A. 2017b. Linking Late Cretaceous to Eocene tectono–stratigraphy of the San Jacinto fold belt of NW Colombia with Caribbean plateau collision and flat subduction. Tectonics, 36(11): 2599–2629. https://doi.org/10.1002/2017TC004612

Mora, J.A., Oncken, O., Le Breton, E., Mora, A., Veloza, G., Vélez, V. & De Freitas, M. 2018. Controls on forearc basin formation and evolution: Insights from Oligocene to recent tectono–stratigraphy of the Lower Magdalena Valley basin of northwest Colombia. Marine and Petroleum Geology, 97: 288–310. https://doi.org/10.1016/j.marpetgeo.2018.06.032

Müller, R.D., Royer, J.Y., Cande, S.C., Roest, W.R. & Maschenkov, S. 1999. New constraints on the Late Cretaceous/Tertiary plate tectonic evolution of the Caribbean. Sedimentary Basins of the World, 4: 33–59. https://doi.org/10.1016/S1874-5997(99)80036-7

Nivia, A., Marriner, G.F., Kerr, A.C. & Tarney, J. 2006. The Quebradagrande Complex: A Lower Cretaceous ensialic marginal basin in the Central Cordillera of the Colombian Andes. Journal of South American Earth Sciences, 21(4): 423–436. https://doi.org/10.1016/j.jsames.2006.07.002

Noda, A. 2016. Forearc basins: Types, geometries, and relationships to subduction zone dynamics. Geological Society of America Bulletin, 128(5–6): 879–895. https://doi.org/10.1130/B31345.1

Parra, M., Mora, A., López, C., Rojas, L.E. & Horton, B.K. 2012. Detecting earliest shortening and deformation advance in thrust belt hinterlands: Example from the Colombian Andes. Geology, 40(2): 175–178. https://doi.org/10.1130/G32519.1

Petters, V. & Sarmiento, R. 1956. Oligocene and lower Miocene biostratigraphy of the Carmen–Zambraon area, Colombia. Micropaleontology, 2(1): 7–35. https://doi.org/10.2307/1484490

Pindell, J.L. & Kennan, L. 2009. Tectonic evolution of the Gulf of Mexico, Caribbean and northern South America in the mantle reference frame: An update. In: James, K.H., Lorente, M.A. & Pindell, J.L. (editors), The origin and evolution of the Caribbean Plate. Geological Society of London, Special Publication 328, p. 1–55. https://doi.org/10.1144/SP328.1

Piraquive, A. 2017. Structural framework, deformation and exhumation of the Santa Marta Schists: Accretion and deformational history of the Caribbean Terrane at the north of the Sierra Nevada de Santa Marta. Doctoral thesis, Université Grenoble Alpes, 237 p. Grenoble, France.

Poveda, E., Monsalve, G. & Vargas, C.A. 2012. Crustal thickness estimation beneath the northern Andes (Colombia) from teleseismic receiver functions. American Geophysical Union, Fall Meeting. Poster. San Francisco, USA.

Poveda, E., Monsalve, G. & Vargas, C.A. 2015. Receiver functions and crustal structure of the northwestern Andean region, Colombia. Journal of Geophysical Research: Solid Earth, 120(4): 2408–2425. https://doi.org/10.1002/2014JB011304

Restrepo, J.J. & Toussaint, J.F. 1988. Terranes and continental accretion in the Colombian Andes. Episodes, 11(3): 189–193. https://doi.org/10.18814/epiiugs/1988/v11i3/006

Restrepo, S., Foster, D.A. & Kamenov, G.D. 2007. Formation age and magma sources for the Antioqueño Batholith derived from LA–ICP–MS uranium–lead dating and hafnium–isotope analysis of zircon grains. Geological Society of America Annual Meeting, Abstracts, p. 181. Denver, USA.

Reyes–Harker, A., Montenegro–Buitrago, G. & Gómez–Gutiérrez, P.D. 2000. Evolución tectonoestratigráfica del Valle Inferior del Magdalena, Colombia. VIII Simposio Bolivariano–Exploración Petrolera en las Cuencas Subandinas. Memoir, p. 293–309. Caracas.

Reyes–Harker, A., Ruiz–Valdivieso, C.F., Mora, A., Ramírez–Arias, J.C., Rodríguez, G., De la Parra, F., Caballero, V., Parra, M., Moreno, N., Horton, B.K., Saylor, J.E., Silva, A., Valencia, V., Stockli, D. & Blanco, V. 2015. Cenozoic paleogeography of the Andean foreland and retroarc hinterland of Colombia. American Association of Petroleum Geologists Bulletin, 99(8): 1407–1453. https://doi.org/10.1306/06181411110

Ridgway, K.D., Trop, J.M. & Finzel, E.S. 2012. Modification of continental forearc basins by flat–slab subduction processes: A case study from southern Alaska. In: Busby, C. & Azor, A. (editors), Tectonics of sedimentary basins: Recent advances, first edition, P. 327–346. Blackwell Publishing Ltd. https://doi.org/10.1002/9781444347166.ch16

Romero–Otero, G.A., Slatt, R.M. & Pirmez, C. 2015. Evolution of the Magdalena deepwater fan in a tectonically active setting, offshore Colombia. In: Bartolini, C. & Mann, P. (editors), Petroleum geology and potential of the Colombian Caribbean margin. American Association of Petroleum Geologists, Memoir 108, p. 675–708. https://doi.org/10.1306/M1081307

Rosello, E. & Cossey, S. 2012. What is the evidence for subduction in the Caribbean margin of Colombia? XI Simposio Bolivariano: Petroleum Exploration in Subandean Basins, Memoirs, p. 1–7. Cartagena de Indias, Colombia.

Saylor, J.E., Horton, B.K., Stockli, D.F., Mora, A. & Corredor, J. 2012. Structural and thermochronological evidence for Paleogene basement–involved shortening in the axial Eastern Cordillera, Colombia. Journal of South American Earth Sciences, 39: 202–215. https://doi.org/10.1016/j.jsames.2012.04.009

Scherwath, M., Kopp, H., Flueh, E.R., Henrys, S.A., Sutherland, R., Stagpoole, V.M., Barker, H.N., Reyners, M.E., Bassett, D.G., Planert, L. & Dannowski, P.A. 2010. Fore–arc deformation and underplating at the northern Hikurangi margin, New Zealand. Journal of Geophysical Research, 115(B6): 23 P. https://doi.org/10.1029/2009JB006645

Silva–Arias, A., Páez–Acuña, L.A., Rincón–Martínez, D., Tamara–Guevara, J.A., Gómez–Gutiérrez, P.D., López–Ramos, E., Restrepo–Acevedo, S.M., Mantilla–Figueroa, L.C. & Valencia, V. 2016. Basement characteristics in the Lower Magdalena Valley and the Sinú and San Jacinto fold belts: Evidence of a Late Cretaceous magmatic arc at the South of the Colombian Caribbean. Ciencia, Tecnología y Futuro, 6(4): 5–36.

Steckler, M.S. & Watts, A.B. 1978. Subsidence of the Atlantic–type continental margin off New York. Earth and Planetary Science Letters, 41(1): 1–13. https://doi.org/10.1016/0012-821X(78)90036-5

Symithe, S., Calais, E., De Chabalier, J.B., Robertson, R. & Higgins, M. 2015. Current block motions and strain accumulation on active faults in the Caribbean. Journal of Geophysical Research: Solid Earth, 120(5): 3748–3774. https://doi.org/10.1002/2014JB011779

Syracuse, E.M., Maceira, M., Prieto, G.A., Zhang, H. & Ammon, C.J. 2016. Multiple plates subducting beneath Colombia, as illuminated by seismicity and velocity from the joint inversion of seismic and gravity data. Earth and Planetary Science Letters, 444: 139–149. https://doi.org/10.1016/j.epsl.2016.03.050

Toussaint, J.F. & Restrepo, J.J. 1994. The Colombian Andes during Cretaceous times. In: Salfity, J.A. (editor), Cretaceous tectonics of the Andes. Earth Evolution Series. Vieweg and Teubner Verlag, Wiesbaden, p. 61–100. https://doi.org/10.1007/978-3-322-85472-8_2

Trenkamp, R., Kellogg, J.N., Freymueller, J.T. & Mora, H. 2002. Wide plate margin deformation, southern Central America and northwestern South America, CASA GPS observations. Journal of South American Earth Sciences, 15(2): 157–171. https://doi.org/10.1016/S0895-9811(02)00018-4

van Benthem, S., Govers, R., Spakman, W. & Wortel, R. 2013. Tectonic evolution and mantle structure of the Caribbean. Journal of Geophysical Research, 118: 3019–3036.

Vervoort, J.D. & Blichert–Toft, J. 1999. Evolution of the depleted mantle: Hf isotope evidence from juvenile rocks through time. Geochimica et Cosmochimica Acta, 63(3–4): 533–556. https://doi.org/10.1016/S0016-7037(98)00274-9

Villagómez, D. & Spikings, R. 2013. Thermochronology and tectonics of the Central and Western Cordilleras of Colombia: Early Cretaceous – Tertiary evolution of the northern Andes. Lithos, 160–161: 228–249. https://doi.org/10.1016/j.lithos.2012.12.008

Villagómez, D., Spikings, R., Magna, T., Kammer, A., Winkler, W. & Beltrán, A. 2011. Geochronology, geochemistry and tectonic evolution of the Western and Central Cordilleras of Colombia. Lithos, 125(3–4): 875–896. https://doi.org/10.1016/j.lithos.2011.05.003

Watts, A.B. & Ryan, W.B.F. 1976. Flexure of the lithosphere and continental margin basins. Tectonophysics, 36(1–3): 25–44. https://doi.org/10.1016/0040-1951(76)90004-4

Xie, X. & Heller, P.L. 2009. Plate tectonics and basin subsidence history. Geological Society of America Bulletin, 121(1–2): 55–64. https://doi.org/10.1130/B26398.1

Zachos, J.C., Pagani, M., Sloan, L., Thomas, E. & Billups, K. 2001. Trends, rhythms, and aberrations in global climate 65 Ma to present. Science, 292(5517): 686–693. https://doi.org/10.1126/science.1059412

Explanation of Acronyms, Abbreviations, and Symbols:

CC	Central Cordillera
LMV	Lower Magdalena Valley Basin
MCH	Magangué–Cicuco High
MMV	Middle Magdalena Valley
OEPFS	Oca–El Pilar–San Sebastian Fault System
PFS	Palestina Fault System
RFS	Romeral Fault System
SiF	Sinú Fault
SJF	San Jerónimo Fault
SJFB	San Jacinto fold belt
SMF	Santa Marta Fault
SNSM	Sierra Nevada de Santa Marta
STEP	Subduction–transform edge propagator
TWT	Two–way–time

Authors' Biographical Notes

Josué Alejandro MORA–BOHÓRQUEZ graduated as a geologist from the Universidad Nacional de Colombia, Bogotá, in 1998, then obtained a MS degree in basin evolution and dynamics at Royal Holloway, University of London, United Kingdom, in 2001 and a PhD degree at the Freie Universität Berlin/GFZ Potsdam, Germany in 2018 (magna cum laude). He works as senior exploration geologist for Hocol S.A. since 2006. Prior to working for Hocol S.A., he was an exploration geologist at Petrobras Colombia doing regional studies of the Upper and Middle Magdalena Valley Basins from 2002 to 2004, and then he worked in coalbed methane and conventional hydrocarbon exploration for Drummond Ltd. Colombia, from 2004 to 2006. His research interests are tectonics and sedimentation, basin analysis, petroleum exploration, and hydrocarbon systems.

Onno ONCKEN is a full professor at the Department of Earth Sciences of the Freie Universität Berlin and is the head of Department 4–"Geomaterials" and of section 4.1–"Lithosphere Dynamics" of the German Research Centre for Geosciences (GFZ) at Potsdam, Germany. He has published widely and received several awards such as Leibniz Price in 1998. His research interests are tectonics of plate margins and orogens, deformation analysis, and analogue modelling.

Eline LE BRETON obtained her Masters and PhD degrees in geology from the University of Rennes 1, France. Since 2012, she is postdoctoral research associate and lecturer at the Department of Earth Sciences of the Freie Universität Berlin. She has several publications and her research interests are plate tectonics and kinematic reconstructions, geodynamics, and structural geology.

Mauricio IBAÑEZ–MEJIA graduated as a geologist from the Universidad Nacional de Colombia, Bogotá, in 2007. He obtained MS (2010) and PhD (2014) degrees in petrology and geochemistry from the University of Arizona, USA, followed by two years as a W.O. Crosby postdoctoral fellow in the Massachusetts Institute of Technology in Cambridge, USA, and four years as an assistant professor in the Department of Earth and Environmental Sciences at University of Rochester, USA. He is currently an assistant professor in the Department of Geosciences at the University of Arizona, USA. His main research interests are in the fields of isotope geochemistry, geochronology, petrology, and crustal evolution.

Gabriel VELOZA obtained his Bachelor degree in geology in 2005 from the Universidad Nacional de Colombia, Bogotá and after working for the oil industry with Hocol S.A., Emerald Energy and Maurel et Prom, he moved to the University of Kansas, USA, where he obtained his Masters degree in 2012. While at the U.S., he also worked as a development geologist with the California Resources Corporation and in 2015, he returned to Colombia and joined Hocol S.A., where he is currently working as a senior exploration geologist. He is also pursuing a PhD at the University of Kansas. His research interests are tectonics and sedimentation, hydrocarbon exploration, and reservoir characterization.

Andrés MORA is the technical leader of onshore Colombia and foothills exploration at Ecopetrol. He received his BS in geology from the Universidad Nacional de Colombia and PhD from the Institut für Geowissenschaften, Universität Potsdam. His research interests include structural geology, petroleum exploration, and petroleum geology.

Vickye VÉLEZ obtained her bachelor's degree in geology from the Universidad Nacional de Colombia in 1990 and her Master of Science degree focused on structural geology from the University of Texas at Austin, U.S.A. in 2000. She worked for 14 years as senior exploration geologist and technical leader in the Llanos Foothills and Middle Magdalena Valley for Ecopetrol and then joined Hocol S.A. in 2006. She is currently exploration manager of the northern Colombia team of Hocol S.A. Her research interests are structural geology and hydrocarbon exploration.

Mario DE FREITAS obtained his bachelor's degree in earth sciences from the Universidade de São Paulo, Brasil in 1983. He joined Petrobras International in 1985 and worked primarily in projects in Brasil, UK, Norway, and Colombia. In 2002 he joined Hocol S.A. as senior geophysicist, then as exploration vice president from 2006 to 2015. He was responsible for a large diversification of Hocol's portfolio, including incursions into the Llanos, where several oil discoveries were made, the Lower Magdalena Valley Basin and San Jacinto fold belt of NW Colombia, where the company also made gas discoveries. His research interests are structural geology, hydrocarbon exploration, and regional basin studies.